CHARACTERIZATION OF CHEMOKINE AND DENDRITIC CELL POPULATIONS IN PULMONARY GRANULOMAS FROM CYNOMOLGUS MACAQUES INFECTED WITH *MYCOBACTERIUM TUBERCULOSIS*

by

Craig Lee Fuller

BS, Baylor University, 1993

MS, Baylor University, 1996

MS, University of Pittsburgh, 2001

Submitted to the Graduate Faculty of

Graduate School of Public Health in partial fulfillment

of the requirements for the degree of

Doctor of Philosophy

University of Pittsburgh

2004

UNIVERSITY OF PITTSBURGH

GRADUATE SCHOOL OF PUBLIC HEALTH

This dissertation was presented

by

Craig Lee Fuller

It was defended on

August 9, 2004

and approved by

Todd A. Reinhart, Sc.D.
Graduate Advisor, Associate Professor
Department of Infectious Diseases and Microbiology
Graduate School of Public Health
University of Pittsburgh

Phalguni Gupta, Ph.D.
Committee Member, Professor
Department of Infectious Diseases and Microbiology
Graduate School of Public Health
University of Pittsburgh

Simon Barratt-Boyes, Ph.D., B.V.Sc.
Committee Member, Assistant Professor
Department of Infectious Diseases and Microbiology
Graduate School of Public Health
University of Pittsburgh

JoAnne L. Flynn, Ph.D.
Committee Member, Associate Professor
Department of Molecular Genetics and Biochemistry
School of Medicine
University of Pittsburgh

Todd A. Reinhart, Sc.D.

CHARACTERIZATION OF CHEMOKINE AND DENDRITIC CELL POPULATIONS IN PULMONARY GRANULOMAS FROM CYNOMOLGUS MACAQUES INFECTED WITH *MYCOBACTERIUM TUBERCULOSIS*

Craig Lee Fuller, Ph.D.

University of Pittsburgh, 2004

One-third of the world's population is infected with *Mycobacterium tuberculosis*, which causes over 2 million deaths annually. *M. tuberculosis* typically infects humans through the inhalation of aerosolized microorganisms and the host's immune system controls the infection by developing a granuloma, which consists predominantly of macrophages and lymphocytes. The factors initiating the formation and maintenance of these granulomas are not well understood, but immune cells are likely recruited to the site of inflammation to maintain immune control of the infection. Chemokines and cytokines play important roles in cell trafficking and migration of immune cells, and DC initiate an adaptive immune response. My hypothesis is that DC (in conjunction with macrophages) recruit immune cells to the granulomatous site by the expression of IFN-γ-inducible chemokines, which are expressed due to mycobacterial antigen stimulation. To determine local cytokine- and chemokine-specific and DC-associated mRNA expression patterns in granulomatous lesions, I performed *in situ* hybridization (ISH) on paraformaldehyde-fixed, cryopreserved lung tissue sections obtained from cynomolgus macaques (*Macaca fascicularis*) infected with a low dose of virulent *M. tuberculosis*. In addition, we evaluated the presence of mycobacterial 16S rRNA to determine the distribution of the mycobacteria and the mycobacterial burden within the granulomas. To model the immune environment in the

pulmonary granulomas, I infected human monocyte-derived DC with *M. tuberculosis* in the presence of IFN-γ. Although I found an abundant expression of the IFN-γ-inducible chemokines and numerous DC-associated genes within the granulomas, the IFN-γ-inducible chemokine expression was predominantly produced by macrophages. The presence of DC in the granuloma may serve to skew the immune response to a type I environment, but our data do not suggest a direct role in the production of IFN-γ-inducible chemokines. These studies provide further information on the potential roles for chemokines and DC in granuloma formation and maintenance as well as the composition of local DC populations. These studies further illustrate the complex microenvironment of granulomas, which are important in the control of tuberculosis infection. Further understanding of granuloma formation and maintenance could lead to the development of therapeutic treatments needed to reduce this public health epidemic.

ACKNOWLEDGMENTS

I would like to thank Dr. Todd Reinhart for all of his support and encouragement through the last 5 ½ years. He has encouraged me to continually pursue excellence in science and has provided me with an amazing foundation to proceed in the field of science. I also would like to thank my committee members, Drs. Phalguni Gupta, Simon Barratt-Boyes and JoAnne Flynn. This committee has continually impressed upon me the importance of quality science and the necessity for clear, concise reasoning within this project.

My deepest appreciation is extended to my co-workers, who were not just my labmates, but also my friends. These individuals have provided me with an enormous amount of support, encouragement, laughter, frustration, and most of all, friendship. These wonderful people are Dr. Todd Schaefer, Beth A. Fallert, Dr. Ian Bell, Mimi Ghosh, Melanie Pfeifer and Cheryl Austin. I will greatly miss these individuals and wish them all of the success in the world.

I would also like to thank my dearest friends, who have always stood by me in good times and bad. These individuals have provided me with more love and support than I have ever known. Thank you, Dr. Denise Croix, Dr. Jamie Mc Minn, Paul Semapongpan, and Kim Nguyen. Thank you for being so influential in my life.

Finally, I would like to thank my family. My family has always supported this thirty-something individual that has never had a "real" job. With all of their love, laughter and support, my family has helped me achieve this and all of my accomplishments. My wonderful family consists of Dad, Mom, Wes, Patti, Barry, Brenda, Hayden, Harrison, Hattie, Angela, Christina and Michael. Thank you all, but most of all, thank you Mom and Dad. I love you both.

TABLE OF CONTENTS

LIST OF TABLES

LIST OF FIGURES

I.

INTRODUCTION

Tuberculosis (TB) is a life-threatening disease in which one-third of the world's population is currently infected with *Mycobacterium tuberculosis* and 2.2 million deaths occur annually (1). In humans, infection by *M. tuberculosis* typically occurs by inhalation of aerosolized microorganisms into the lungs, which serve as the primary site of infection. *M. tuberculosis* is a slow-growing, acid-fast, rod-shaped bacillus, which preferentially infects macrophages and is capable of residing in macrophages in a state that is resistant to immune responses. Infected macrophages release cytokines, which increase local inflammation and result in the development of a granulomatous lesion (2). This microenvironment within a granulomatous lesion restricts the bacterium from dissemination and allows the intimate interaction of immune cells and infected macrophages. The acquired immune response and these granulomatous structures are an effective prevention of active disease in approximately 90% of all *M. tuberculosis* infections (2,3).

Granulomas: histological characteristic of tuberculosis

Granulomas are histological hallmarks of several chronic infectious diseases, such as tuberculosis, brucellosis, and schistosomiasis, and also develop due to the presence of allergens and metals. These granulomatous lesions are generally considered to be the result of chronic antigenic stimulation (4,5). The tuberculous granuloma in humans is a focal collection of mononuclear cells surrounded by a halo of additional monocytes, lymphocytes and connective

tissue, including fibroblasts, collagen fibers and newly formed vessels (5-9). Granuloma formation occurs when an infected macrophage becomes encircled by other macrophages and the immune system attempts to wall-off the microorganism to prevent the bacteria from spreading locally and throughout the body. The granuloma physically restricts the bacilli and provides an environment for immune cells to interact and develop an effective immune response directed against the bacilli. This local environment leads to the inhibition of growth or to the death of *M. tuberculosis* due to the production of cytokines, activation of macrophages and cytotoxic killing by $CD8^+$ T cells.

Granulomas are composed mostly of macrophages, $CD4^+$ and $CD8^+$ lymphocytes and B lymphocytes (10), but a novel morphological characteristic of the granuloma is the presence of epithelioid cells, which are large mononuclear cells with increased cytoplasm and dispersed chromatin resembling epithelial cells (5). These epithelioid cells are derived from macrophages and their function in the center of the granuloma is suggested to be for secretion of biologically active factors. In fact, epithelioid cells have been shown to control the rate of multiplication of *M. tuberculosis* in granulomas in the hamster model (11); Langhans multinucleated giant cells can also be found in human and macaque granulomas (5,12).

Granulomas can exist as a solid mass of cells or can develop necrosis in the central portion of the structure. In humans, this necrotic center can develop further into a caseous granuloma (13). Currently, a progression model of tuberculous granulomas has not been established. Although a caseous granuloma generally is a solid mass, a caseous granuloma can undergo liquefaction if the infection is not controlled, and this liquefied milieu supports extracellular replication of *M. tuberculosis*. Some caseous granulomas evolve and develop cavities within the lung and have been associated with high bacterial burden (14). As the

granuloma controls infection, fibrosis of the lesion occurs and fibrosis is associated with a reduction in the inflammatory process. Characteristics of human granulomas have been observed in non-human primate models of tuberculosis (12).

Immune response to *Mycobacterium tuberculosis*

Mycobacterium tuberculosis infection induces a proinflammatory immune response, characterized by the expression of IFN-γ, TNF-α and IL-12 (3,9,15-21). Although information has been obtained from bronchoalveolar lavages (BAL) and lung biopsies during advanced disease in humans, only a small number of studies have examined the local cytokine expression patterns associated specifically within granulomas. Examination of BAL cells has indicated that *M. tuberculosis* induces a type 1 polarized cytokine response characterized by IFN-γ expression (22-25). Barry *et al.*, described strong IFN-γ and TNF-α responses in $CD4^+$ T cells isolated from BAL and activated with purified protein derivative (PPD) among patients with TB, while PPD-activated IFN-γ and TNF-α-producing $CD4^+$ T cells were low among control subjects (22). Another study revealed that the peripheral blood and BAL samples from patients with primary tuberculosis were characterized by high levels of IL-6 and IFN-γ (23). Robinson *et al.*, determined that the increased number of IFN-γ-producing cells in the BAL of tuberculosis patients were predominantly T lymphocytes (80% of IFN-γ mRNA-positive BAL cells) rather than alveolar macrophages (14.3%). This study also showed that there was not a significant difference in the proportion of cells expressing IL-2, IL-4, or IL-5 mRNA, which further demonstrated the importance of IFN-γ in the immune response against *M. tuberculosis* infection. Robinson *et al.*, concluded that the activation of Th1-like bronchoalveolar T-lymphocytes, in addition to the production of IFN-γ by alveolar macrophages, may contribute to the local cellular

immune response in pulmonary tuberculosis (26). Interestingly, expression patterns of IFN-γ relative to IL-4 in pulmonary granulomas from individuals with active tuberculosis were highly associated with the type of granuloma formed (27). Granulomas with no caseation expressed either IFN-γ mRNA or IFN-γ plus IL-4 mRNA, whereas caseous granulomas expressed little IFN-γ or IL-4 mRNA (27). These findings suggest that these cytokines play a role in determining granuloma architecture.

α/β and γ/δ TCR^+ lymphocytes

The central components of a protective immune response against *M. tuberculosis* involve the interaction of T cells and infected macrophages. $CD4^+$ T lymphocytes have an essential role in the immune response, and are supported by other T cell subtypes, such as $CD8^+$, γδ TCR^+ T cells and CD1-restricted T cell. Although these cells may have antibacterial mechanisms, such as perforin or granulysin, these T cell subsets also secrete type 1 cytokines, most notably IFN-γ (28-30). The level of involvement that each T cell subtype plays in an individual's immune response may vary, and the ability to study this in an animal model allows us to define further the potential of these other T cell subtypes to complement $CD4^+$ T cell function. This complementarity of $CD4^+$ T cells is illustrated in MHC Class II and CD4 knock-out mice, which produce large amounts of IFN-γ; however, the increased IFN-γ levels alone were still not sufficient to control infection (30). Macrophage activation is triggered by IFN-γ, which is augmented by TNF-α, and macrophage activation can lead to production of reactive oxygen intermediates (ROI) and reactive nitrogen intermediates (RNI), acidification of phagosomes, fusion of phagosomes and lysosomes, and iron restriction to restrict mycobacterial growth (28).

$CD4^+$ and $CD8^+$ T cells recognize antigen in the context of MHC II or I, respectively. This recognition is facilitated through the TCR, which is a heterodimeric transmembrane protein composed of two chains. The four different TCR polypeptide chains described are T-cell receptor α, β, γ and δ chains. Two chains bind together to form a heterodimer through disulfide bonds and resemble the immunoglobulin molecule. The predominant T-cell receptor is the α:β heterodimer and the αβ TCR is recognized by all functional classes of T cells. The other TCR complex that is important in the immune response is the γ:δ heterodimer and γδ TCR^+ T cells appear to play an important role in the immune response to *M. tuberculosis* by their ability to recognize nontraditional phosphoantigens (28). Ladel *et al.*, found that $TCR\beta^{-/-}$ mice succumbed to a low dose inoculum of *M. tuberculosis,* whereas $TCR\delta^{-/-}$ mice developed transient disease exacerbation (31). The development of granulomas and bacterial containment within these granulomas were impaired in $TCR\beta^{-/-}$ mice, and the $TCR\delta^{-/-}$ mice were less severely affected (31). Ladel *et al.*, further validated the function of αβ TCR^+ T cells in protection against tuberculosis infection and established a novel protective role of TCRγδ T cells in early stage of tuberculosis (31).

Experimental animal models

Animal models have further defined the general mechanisms underlying natural resistance and the acquisition of a protective immune response against *M. tuberculosis*, in addition to increasing our understanding of the pathology of tuberculosis. The most commonly used animal models for tuberculosis are the guinea pig, rabbit, mouse and non-human primate. The genetic manipulation and availability of immunologic reagents in mice has allowed researchers to study the role of distinct cells and surface molecules in an in vivo system. Many

initial observations in mice have been confirmed in humans, including the importance of IFN-γ, TNF-α and $CD4^+$ T cells in the control of *M. tuberculosis* [reviewed in (28)]. Unfortunately, the mouse model does not include the development of caseous granulomas consistent with pathology observed in humans, and cell types have slightly different specificities, e.g., γδ T cells (32). The most notable animal model for tuberculosis is the non-human primate. This model develops a slowly progressing disease with a lower percentage of animals developing primary disease and likely controlling the infection prior to a reactivation state The stages of disease closely resemble the course of infection in humans and histologically the granulomas appear strikingly similar (12). The negative aspect of this model is the cost of primates and necessity for more sophisticated containment precautions.

Another model of tuberculosis that demonstrated the full spectrum of disease seen in immunocompetent humans is the rabbit model. Rabbits also have a natural resistance to infection, and manifest pulmonary cavitary lesions during the course of progressive disease (14). Finally, guinea pigs have also been used as a model of tuberculosis due to the development of granulomatous lesions very similar to those observed in human tuberculosis patients. The use of guinea pigs is especially important when examining CD1-restricted lymphocytes, cells that recognize mycobacterial glycolipids, since these cells are found in humans and guinea pigs, but not in mice (33). In conclusion, there are several model systems in addition to the cell culture systems that have advanced the understanding of the immune response and pathogenesis of tuberculosis.

Recruitment of immune cells by chemokines

Granuloma formation likely requires the recruitment of cells to the site of inflammation

via the expression of chemotactic molecules, and prior to our publication of data from this dissertation only one study had examined chemokine expression directly in granulomatous tissue sections (34). Chemokines are approximately 8 to 10 kDa secreted proteins with chemotactic activity and play a major role in the recruitment of receptor-bearing cells to sites of inflammation (35,36). Chemokines are a family of small cytokines with four conserved cysteine residues linked by disulfide bonds (35). These chemokines are categorized into four families based on number of amino acids separating the cysteine residues in the amino acid sequence. The functions of chemokines include chemotaxis, integrin activation and degranulation of distinct leukocyte subsets expressing specific chemokine receptors (37). The expression of chemokines is controlled by local environmental signals, such as TNF-α or IFN-γ (35,38). Whereas the CC chemokines recruit lymphocytes, monocytes, basophils and eosinophils, suggesting a less selective recruiting process, the ELR^+ (Glutamic acid-Leucine-Arginine) CXC chemokines are potent recruiters of neutrophils and ELR^- CXC chemokines selectively recruit lymphocytes (35).

Granulomas induced experimentally in mice with mycobacterial antigen-coated beads lead to the development of type 1 cytokine and chemokine expression profiles (15,16,19). IFN-γ induces macrophages and DC to produce IFN-γ-inducible, CXCR3 ligands, CXCL9/monokine induced by γ-interferon (Mig), CXCL10/γ-interferon-inducible protein (IP-10), and CXCL11/IFN-inducible T-cell α-chemoattractant (I-TAC), which recruit $CXCR3^+$ cells (39). CXCR3 is a G-protein-coupled receptor that is expressed on memory and activated CD4 and CD8 lymphocytes, B cells and NK cells (40). Interestingly, $CXCR3^+$ cells characteristically express type 1 cytokines (41), and therefore, can potentially induce further upregulation of CXCR3 ligands, leading to chronic type 1 polarized inflammation.

Table 1. Chemokines examined in these studies

Family	Systemic Name	SCY Name	Human Ligand	Receptor
CXC	CXCL9	SCYB9	Mig	CXCR3
	CXCL10	SCYB10	IP-10	CXCR3
	CXCL11	SCYB11	I-TAC	CXCR3
CC	CCL2	SCYA2	MCP-1	CCR2
	CCL3	SCYA3	MIP-1α	CCR1, CCR5
	CCL4	SCYA4	MIP-1β	CCR5
	CCL5	SCYA5	RANTES	CCR1, CCR3, CCR5

Murine gene disruption and in vivo neutralization studies have shown the importance of recruitment of infiltrating CXCR3-bearing cells via CXCR3 receptor:ligand interactions. In vivo neutralization of CXCL9/Mig and CXCL11/IP-10 in mice reduced recruitment of the $CXCR3^+$ cells, but the disruption of the CXCR3 gene drastically disrupted this recruitment mechanism via its ligands and thus reduced the severity of idiopathic pneumonia syndrome (42) or prolonged functional graft survival (43). Recruitment of $CXCR3^+$ T cells by CXCL10/IP-10 have been implicated in allograft rejection (44). Interestingly, $CXCR3^{-/-}$ mice have been used to examine the role CXCR3 in fibroproliferation. Jiang *et al*., showed that CXCR3-deficient mice had increased fibrosis without increased recruitment, reduced early burst of IFN-γ and decreased expression of CXCL10/IP-10 (45). In the context of tuberculosis $CXCR3^{-/-}$ mice and anti-CXCL9/Mig-treated mice developed pulmonary granulomas, but the relative size of the granulomas were reduced 4.5- and 2-fold, respectively. Interestingly this same study showed that there was no difference in the survival or the mycobacterial load when comparing $CXCR3^{-/-}$ and anti-CXCL9/Mig-treated mice to wild-type controls (46).

Upregulated chemokines are likely produced by multiple cell types at the site of inflammation, especially by antigen presenting cells (APC). Macrophages have been shown to produce CXCR3 ligands in response to IFN-γ and *M. tuberculosis* infection alone (47), and DC also have been shown to produce IFN-γ-inducible chemokines during *M. tuberculosis* infection (48). DC are crucial to the induction of an adaptive immune response in *M. tuberculosis* infection and DC, in addition to macrophages, may potentially be responsible for the production of CXCR3 ligands at the site of the granuloma due to IFN-γ and or *M. tuberculosis* infection alone. The APC in the lung are typically submucosal and interstitial DC, and alveolar macrophages (49,50). Macrophages and DC perform surveillance functions within the pulmonary cavity, and DC, not macrophages, migrate to the regional lymph node based on a chemotactic gradient and adhesion molecules, leading to the priming of naïve T-lymphocytes (51,52). In addition, DC play a role in bridging the gap between the innate and adaptive immune response by recognizing pathogens and inducing a protective immune response. DC have been shown to bind *M. tuberculosis* via the DC-SIGN (dendritic cell-specific intercellular adhesion molecule 3-grabbing nonintegrin) molecule (53), thus, DC are also a target for *M. tuberculosis* infection and potentially aid in dissemination of the mycobacteria during migration.

Recent studies have shown the presence of DC in the granulomatous lesion of an experimental or spontaneous infection using immunohistochemical staining of DC-associated markers (54-56). In human tuberculosis patients, the numbers of peripheral blood $CD11c^+$ DC were lower than in control patients and $CD11c^+$ DC infiltrated the lymphocyte areas of the granulomatous lesion (56), suggesting the migration of DC from the peripheral blood to the inflammatory site. Other studies have utilized rodent animal models to assess the DC role in the immune response to mycobacterial infection. Tsuchiya *et al.*, demonstrated in a rat model with

bacillus Calmette-Guerin (BCG)-elicited pulmonary granulomas that DC were present at the site of the granulomatous lesion and these isolated DC had an effective ability to stimulate allogeneic T-lymphocytes (55). Thus, the DC likely may participate in the formation of granulomas based on their potent antigen presentation abilities.

In addition, DC were shown to play a key role in initiating granulomatous cell-meditated immunity in mice infected with purified protein derivative (PPD)-coated beads (54). The $CD11c^+$ DC in all granulomas were in contact with the beads and DC expressed IL-12p40 mRNA as determined by ISH. In addition, when isolated on day 1 these DC stimulated PPD-specific T-lymphocyte proliferation (54). The migration of these DC to regional lymph nodes is a dynamic process that involves the maturation of the DC from an immature to a mature DC, which includes the upregulation of costimulatory molecules and chemokine receptors, specifically CCR7 (57). The migration to the regional lymph node is facilitated by the expression of CCR7 chemokines, CCL19/MIP3-β and CCL21/6Ckine. Interestingly, in the granulomatous lesions of giant cell arteritis, mature DC expressing CCR7 are maintained within the granuloma likely due to the overexpression of CCL19/MIP3-β and CCL21/6Ckine (58). It is not clear whether the DC present in the tuberculous granulomas are maintained at the site by the CCR7 chemokines or are continuously recruited by other potential mechanisms.

In summary, the local chemokine expression patterns in granulomatous tissues have not been fully examined in tissue sections directly and the DC populations present at the site of the granuloma are not well characterized. Experimental *M. tuberculosis* infection in a macaque model induces granuloma formation remarkably similar to that seen in humans infected with this pathogen (12,59). Here, I have established that the chemokine and cytokine mRNA expression patterns in lung tissues from *M. tuberculosis*-infected cynomolgus macaques (*Macaca*

fascicularis) were abundant as determined by *in situ* hybridization (ISH). In addition, I have determined that these IFN-γ-inducible chemokine mRNAs were predominantly expressed by macrophages by simultaneous ISH and IHC; DC also expressed some of these chemokines. Additionally, I characterized the DC populations within granulomatous lesions to find a large number of DC-associated genes expressed in the granulomatous lesion. Finally, I examined the mycobacterial burden within the granulomatous tissues to potentially clarify whether the abundant expression of IFN-γ-inducible chemokines is likely a function of immune dysregulation or of continuous antigenic stimulation. Altogether, these data reveal the presence of DC and an abundant expression of several recruitment molecules and proinflammatory molecules known to drive immune responses. These findings are important, because previous studies have shown the upregulation of certain cytokines, but have not shown that the source of IFN-γ-inducible chemokines is within the granulomatous structure itself. These findings altogether have further defined the granuloma microenvironment in an attempt to understand how a granuloma is maintained, whereas further studies must be performed to explain the formation of tuberculous granulomas.

II.

SPECIFIC AIMS

Tuberculosis is a global epidemic, which is exacerbated by the breakdown of health services, the emergence of multi-drug resistant TB, and the global spread of HIV/AIDS. *Mycobacterium tuberculosis* infects humans through the inhalation of aerosolized microorganisms and primarily targets the pulmonary compartment. In an immunocompetent individual, the host's immune system controls the infection by surrounding the mycobacteria in a structure called a granuloma, a histological hallmark of tuberculosis. The factors initiating the formation of these granulomas are not well understood. However, granulomas characteristically are composed primarily of macrophages and lymphocytes, which are potentially recruited to the site of inflammation to prevent the dissemination of the microorganism. Chemokines and cytokines play important roles in the recruitment of immune cells, and **our hypothesis is that DC (in conjunction with macrophages) recruit immune cells to the granulomatous site by the expression of proinflammatory cytokines and the IFN-γ-inducible chemokines, which are expressed due to their exposure to mycobacterial antigens.** Since tuberculosis is a disease characterized by a type 1 polarized immune response, specifically IFN-γ and TNF-α, we examined the expression levels and patterns of the IFN-γ-inducible chemokines and proinflammatory cytokines and characterized the DC populations within the granulomatous lesions. These studies were performed using a nonhuman primate model infected with a low dose of *M. tuberculosis* and performing single-cell based and in vitro assays on cynomolgus macaque

tissues and peripheral blood cells. These studies have provided novel information on the local chemokine expression patterns and the expression patterns of DC-associated genes.

The overall aim of this project was to understand further the development/maintenance of granulomatous structures in cynomolgus macaques infected with *M. tuberculosis*. My specific aims to achieve this goal are listed below.

Specific Aim 1. Determine the local expression of IFN-γ-inducible chemokine and proinflammatory cytokine mRNAs in pulmonary granulomatous tissue sections of cynomolgus macaques (*Macaca fascicularis*) experimentally infected with a low dose of *Mycobacterium tuberculosis* Erdman strain. Since tuberculosis is characterized by a polarized IFN-γ and TNF-α expression profile, I examined the expression levels of recruitment molecules directly induced by IFN-γ, the IFN-γ-inducible chemokines. To achieve this, I studied cynomolgus macaques that were infected with a low dose of *M. tuberculosis* Erdman strain via bronchoscope and sacrificed at various states of disease. These resources were available through a collaborative study with Dr. JoAnne L. Flynn. I used *in situ* hybridization (ISH) to examine paraformaldehyde-fixed, cryopreserved lung tissues for chemokine and cytokine mRNA expression patterns, which were quantified by quantitative image analysis (QIA). In addition, I determined which cells are expressing the chemokine/cytokine mRNAs by performing simultaneous *in situ* hybridization and immunohistochemistry.

Specific Aim 2. Characterize the dendritic cell population in the pulmonary granulomatous tissue sections of cynomolgus macaques experimentally infected with *Mycobacterium*

***tuberculosis*.** DC serve a major function in the development of an appropriate adaptive immune response and DC have been described in granulomatous lesions, through the application of a small number of antigenic markers. Therefore, I sought to further characterize the DC populations in granulomatous lesions. Using paraformaldehyde-fixed, cryopreserved lung tissues harvested at necropsy, we characterized the DC populations in the granulomatous lesions using ISH with eight DC-associated riboprobes. The specific genes selected to characterize the type of DC are CD11c, CD123, DC-SIGN, DC-LAMP, B7-DC, DC-STAMP, CCR6 and CCR7.

Specific Aim 3. Determine whether mycobacterial antigen can stimulate the expression of inflammatory chemokines in dendritic cells. Tuberculosis is characterized by an abundant type 1 immune response, which is stimulated by the mycobacterial antigens, and we sought to examine the direct association between mycobacterial antigen and the IFN-γ-inducible chemokines in situ and in vitro. Using paraformaldehyde-fixed, cryopreserved lung tissues harvested at necropsy, we examined the lung tissues for mycobacterial 16S rRNA associated with granulomatous lesions by ISH. The intensity and distribution of ISH signal were examined and correlated with the chemokine and cytokine expression patterns. In addition, monocyte-derived DC were infected with *M. tuberculosis* in the presence and absence of IFN-γ and the IFN-γ-inducible chemokine mRNA expression levels were analyzed by real-time RT-PCR.

Collectively, these studies executed under these aims provided further insight into the maintenance of the granulomatous lesion and provide further insight into how DC might affect the granuloma by their presence. Whereas the field is aware of the macrophage's role in the immune response and ability to control the mycobacteria, the role of the DC within the

granuloma is not fully understood. We sought to further define the DC populations in the granulomatous lesion by using these DC-associated markers. We have shown in these studies that the expression of IFN-γ-inducible chemokines is abundant at the site of the granuloma and that these chemokines are expressed predominantly by macrophage and not by DC. We also have shown a potential marker for IL-4 expression, DC-STAMP. The development of the granuloma is still not well understood, but these studies show a consistent pattern of chemokine expression illustrating a potential coordination of the maintenance of a granuloma structure.

III.

IN SITU STUDY OF ABUNDANT EXPRESSION OF PROINFLAMMATORY CHEMOKINES AND CYTOKINES IN PULMONARY GRANULOMAS THAT DEVELOP IN CYNOMOLGUS MACAQUES EXPERIMENTALLY INFECTED WITH MYCOBACTERIUM TUBERCULOSIS

(Published 2003 Infection and Immunity Volume 71:7023-7034 (60))

This chapter includes a manuscript published in Infection and Immunity in its entirety with permission from American Society for Microbiology. Additional studies were performed to address questions not included in the final manuscript. These sections are presented at the end of the Results section under the following sections:

Expression of IFN-γ in the lymphocyte population

Characterization of the expression and distribution of T Cell receptor chains in granulomas from cynomolgus macaques

ISH analyses in hilar lymph node 5 weeks post-infection

Expression of CCR5 ligands in granulomas from cynomolgus macaques

All of the tissue-based studies were performed by Craig Fuller, while all of the animal care needs and medical services were performed by the staff in Dr. JoAnne Flynn's laboratory and by the Division of Laboratory Animal Resources (DLAR).

A. PREFACE

In this section I have described published data related to IFN-γ-inducible chemokines and proinflammatory cytokines observed in pulmonary granulomas in cynomolgus macaques infected with *M. tuberculosis*. This chapter contains data from ISHs for IFN-γ-inducible chemokine and proinflammatory mRNAs, which was abundant in both solid and caseous granulomas. I revealed in these studies that CXCL9/Mig mRNA was the most abundant by quantitative image analysis and the CXCR3 ligand mRNA expression correlated with an increased observation of $CXCR3^+$ cells within the granuloma, as compared to normal lung tissues. I also observed an increased expression of IFN-γ and TNF-α mRNAs associated with granulomatous tissues, compared to uninfected lung tissues. In addition, I developed an ISH assay for mycobacterial 16S rRNA to overcome limitations observed in formalin-fixed tissues. Using this ISH assay, I observed mycobacterial 16S rRNA within the acellular portions of caseous granulomas. Altogether, these studies provided further information on the expression of IFN-γ-inducible chemokine, IFN-γ and TNF-α mRNAs and cell populations directly within the granulomatous structure. These studies suggest that CXCR3 ligands likely play a role in the recruitment of CXCR3-bearing cells to the site of the granuloma.

Abundant expression of pro-inflammatory chemokines and cytokines in pulmonary granulomas developing in cynomolgus macaques experimentally infected with *Mycobacterium tuberculosis*: An *in situ* study

Craig L. Fuller[1], JoAnne L. Flynn[2], and Todd A. Reinhart[1‡]

Running title: *In situ* chemokine/cytokine expression in granulomas

[1]Department of Infectious Diseases and Microbiology, Graduate School of Public Health, University of Pittsburgh, Pittsburgh, PA; [2]Department of Molecular Genetics and Biochemistry, School of Medicine, University of Pittsburgh, Pittsburgh, PA

[‡]Corresponding author and reprint requests: Mailing address: Department of Infectious Diseases and Microbiology, Graduate School of Public Health, University of Pittsburgh, 130 DeSoto St., Pittsburgh, PA 15261. Phone: (412) 648-2341. Fax: (412) 624-4873. (reinhar@pitt.edu).

B. ABSTRACT

Tuberculosis remains a major public health problem worldwide. Chemokines and cytokines organize and direct infiltrating cells to sites of infection, and these molecules likely play crucial roles in granuloma formation and maintenance. To address this issue, we used *in situ* hybridization (ISH) to measure chemokine and cytokine mRNA expression levels and patterns directly in lung tissues from cynomolgus macaques (*Macaca fascicularis*) experimentally infected with a low dose of virulent *M. tuberculosis*. We examined more than 300 granulomas and observed abundant expression of IFN-γ-inducible chemokine mRNAs (CXCL9/Mig, CXCL10/IP-10, and CXCL11/I-TAC) within solid and caseous granulomas, with only minimal expression in nongranulomatous regions of tissue. The mRNA expression patterns of IFN-γ and TNF-α were examined in parallel and revealed that cytokine $mRNA^+$ cells were abundant and generally localized to the granulomas. Mycobacterial 16S rRNA expression was also measured by ISH and revealed localization predominantly to the granulomas with the highest signal intensity in caseous granulomas. We observed several granulomatous lesions with exceptionally high levels of RNA for mycobacterial 16S rRNA, IFN-γ, and IFN-γ-inducible chemokines suggesting that the local presence of mycobacteria is partly responsible for the upregulation of IFN-γ-inducible chemokines and recruitment of $CXCR3^+$ cells, which were also abundant in granulomatous lesions. These studies suggest that expression of CXCR3 ligands and the subsequent recruitment of $CXCR3^+$ cells are involved in granuloma formation and maintenance.

C. INTRODUCTION

Tuberculosis (TB) is a global public health epidemic in which 2 billion people are currently infected with *Mycobacterium tuberculosis* and 2.2 million deaths occur annually (1). Infection by *M. tuberculosis* typically occurs by inhalation of aerosolized microorganisms into the lungs, which serve as the primary site of infection. A granulomatous lesion develops to contain the bacteria, which is effective given that 90% of all *M. tuberculosis* infections do not result in active disease (2,3). *M. tuberculosis* preferentially infects macrophages and appears to be capable of residing in macrophages in a state that is resistant to immune responses. Infected macrophages release cytokines, which increase local inflammation and result in the development of the granulomatous lesion (2).

Granulomas are hallmarks of chronic infectious diseases, such as tuberculosis, brucellosis, and schistosomiasis, and also develop due to the presence of allergens and metals. These granulomatous lesions are generally considered to be the result of chronic antigenic stimulation (4,5). The tuberculous granuloma is a focal collection of mononuclear cells surrounded by a halo of lymphocytes and additional monocytes (5-9). This reaction occurs when an infected macrophage becomes encircled by other macrophages and the immune system attempts to wall-off the microorganism to prevent the bacteria from spreading locally and throughout the body. This complex cellular structure can be surrounded by connective tissue, including fibroblasts, collagen fibers and newly formed vessels (5). A novel morphological characteristic of the granuloma is the presence of epithelioid cells, which occupy the center of the lesion. These epithelioid cells are activated macrophages, which have increased cytoplasm

and disperse chromatin resembling epithelial cells (5). Langhans multinucleated giant cells are also be found in granulomas.

M. tuberculosis induces a proinflammatory immune response, characterized by the expression of IFN-γ, TNF-α and IL-12 (3,9,15-18,21,61,62). Although information has been obtained from bronchoalveolar lavages (BAL) and lung biopsies during advanced disease in humans, only a small number of studies have examined the local cytokine expression patterns associated specifically with granulomas. Examination of BAL cells has indicated that *M. tuberculosis* induces a type 1 polarized cytokine response characterized by IFN-γ expression (22-24,63). However, when Fenhalls *et al.* studied pulmonary granulomas from individuals with active tuberculosis, they found that the expression patterns of IFN-γ relative to IL-4 were highly associated with the type of granuloma formed (64). Granulomas with no evidence of caseation expressed either IFN-γ mRNA or IFN-γ plus IL-4 mRNA, whereas caseous granulomas expressed little IFN-γ or IL-4 mRNA (65). These findings suggest that these cytokines play a role in determining granuloma architecture.

The development of a granuloma likely depends on the movement of cells toward the site of inflammation due to expression of chemotactic molecules, although only one study to date has examined local chemokine expression directly in granulomatous tissue sections (34). Proinflammatory chemokines are chemotactic cytokines, which play a major role in the recruitment of receptor-bearing cells to sites of inflammation (35,36). The functions of chemokines include chemotaxis, integrin activation and degranulation of distinct leukocyte subsets expressing specific chemokine receptors (66). The expression of proinflammatory chemokines is induced by local environmental signals, such as TNF-α or IFN-γ (35,38). Granulomas induced experimentally with mycobacterial agents lead to the development of type 1

cytokine and chemokine expression profiles (15,16,67). IFN-γ induces macrophages and dendritic cells (DC) to produce IFN-γ-inducible, CXCR3 ligands, CXCL9/monokine induced by γ-interferon (Mig), CXCL10/γ-interferon-inducible protein (IP-10), and CXCL11/IFN-inducible T-cell α-chemoattractant (I-TAC), which recruit $CXCR3^+$ cells (39). $CXCR3^+$ cells typically express type 1 cytokines (41), and therefore, can potentially induce further upregulation of CXCR3 ligands, leading to chronic type 1 polarized inflammation, as we have proposed occurs during simian immunodeficiency virus (SIV) infection of rhesus macaques (*Macaca mulatta*) (68).

The local chemokine expression patterns in granulomatous tissues have not been fully examined directly in tissue sections thus far. Experimental *M. tuberculosis* infection in a macaque model induces granuloma formation remarkably similar to that seen in humans infected with this pathogen (59,69,70). In this report, we have examined the chemokine and cytokine mRNA expression patterns in lung tissues from *M. tuberculosis*-infected cynomolgus macaques (*Macaca fascicularis*) by *in situ* hybridization (ISH). These studies provide direct evidence that IFN-γ mRNA is present and abundant in the granulomas of infected cynomolgus macaques, and that IFN-γ-inducible chemokine mRNAs are upregulated and potentially responsible for the recruitment of $CXCR3^+$ cells that could further skew the immune environment through ongoing IFN-γ production. The abundant expression of IFN-γ-inducible, CXCR3 ligands and inflammatory cytokines IFN-γ and TNF-α directly within solid and caseous granulomas suggests that continual cell recruitment and a state of chronic inflammation likely contribute to the formation and maintenance of tuberculous granulomas.

D. MATERIALS AND METHODS

Animals and tissue processing

All animal studies were performed under the guidance and approval of the University of Pittsburgh Institutional Animal Care and Use Committee. Nine adult cynomolgus macaques were inoculated with a low dose (approximately 25 colony forming units) of virulent *M. tuberculosis* (Erdman strain) via bronchoscope into the lower right lobe, as described elsewhere (70). Infection was allowed to proceed until macaques reached disease states that spanned a spectrum from no apparent disease to advanced disease. At necropsy, tissues were collected and fixed in 4% paraformaldehyde/1X phosphate buffered saline (PF/PBS) for 5 hr at 40^{o}C, as previously described (71). After fixation, the tissues were cryoprotected and snap frozen in isopentane cooled on dry ice to -65^{o}C.

Immunohistochemistry

Immunohistochemical staining of 14μm tissue sections was performed using cell-type specific antibodies: anti-CD3 (clone CD3-12, NovoCastra), anti-CD68 (clone KP1, Dako), anti-CD20 (clone L26, Dako) and anti-CXCR3 (clone 1C6, Pharmingen). Tissue sections were pretreated in 0.01M sodium citrate (pH 6.0) by microwaving followed by application of the primary antibody (diluted in 1X PBS) to the tissues for 1 hr in a humid chamber at room temperature. Primary antibodies were detected with the PicTure^{TM}-Plus detection system (Zymed Laboratories), using 3,3'-diaminobenzidine as the final substrate.

In situ *hybridization (ISH)*

Riboprobe syntheses and ISHs were performed on 14μm tissue sections as previously described (68,71,72). Cytokine and chemokine mRNAs were detected by ISH using gene-specific riboprobes. Plasmids containing macaque IFN-γ and TNF-α cDNAs were kindly provided by Francois Villinger (Emory University). Plasmids encoding CXCL9/Mig, CXCL10/IP-10 and CXCL11/I-TAC genes were previously described (68,73). Autoradiographic exposure times were 7, 10 and 11 days for chemokine and cytokine mRNA and *M. tuberculosis* 16S rRNA ISHs, respectively.

Quantitative image capture and analysis

Each granuloma present in lung tissue sections was categorized as a solid or caseous granuloma. ISH signal intensities were measured by quantitative image analysis. Using a RT Slider Spot camera (Diagnostic Instruments, Inc.), we captured images of all granulomas using a 4X objective lens. The MetaView software package (Universal Imaging Corp.) was used to measure the surface area covered by autoradiographic silver grains, as well as the total surface area of the granuloma. After color separation, the green channel was converted to pseudocolor and the image was thresholded to measure the surface area covered by silver grains.

M. tuberculosis 16S rRNA subcloning, sequencing

The 16S rDNA from *M. tuberculosis* strain H37Rv was amplified by PCR using sequence specific forward (5'-GGCGTGCTTAACACATGCAA-3') and reverse (5'-CGCTCACAGTTAAGCCGT-3') primers, as previously described (74). The amplified product

(550 bp) was subcloned into pGEMT and DNA sequenced, which revealed 100% homology to 16S rRNA genes of both H37Rv and CDC1551 strains of *M. tuberculosis* (data not shown).

E. RESULTS

Classic granulomatous lesions arise in macaque pulmonary tissues

To address key issues regarding granuloma formation and maintenance in a nonhuman primate model, cynomolgus macaques were inoculated intrabronchially with a low dose of virulent *M. tuberculosis* (Erdman strain). All nine animals examined in this study were successfully infected as demonstrated by tuberculin skin test, PBMC lymphoproliferative response to mycobacterial antigens, positive bacterial cultures from BAL and by radiographic observations. Detailed clinicopathological and bacteriological findings are being presented separately (70). These animals varied in their rates and extents of disease progression, but all had macroscopic (gross) lesions within lung tissues at necropsy. They were classified as exhibiting minimal/moderate disease or advanced disease based upon their clinical condition, and gross and microscopic pathological findings. The pulmonary granulomas detected in these tissue sections varied in size and structure (Table 2). We examined more than 300 granulomas in 7 of the 9 animals, with 93% of the granulomas observed in animals with advanced disease (Table 2). The surface areas of the granulomas in 14μm tissue sections ranged from 1.5×10^4 to 5.5×10^6 μm^2, and approximately two-thirds of the granulomas were caseous. If macaque M15300, which harbored the majority of the granulomas examined, was removed from the summary, the mean surface areas for solid and caseous granulomas were 1.4×10^5 and 7.1×10^5 μm^2, respectively, and 37% of the granulomas were caseous. Caseous granulomas were present in all animals with granulomas, but the majority was observed in the macaques with advanced disease. Solid granulomas were present more frequently than caseous granulomas in animals with minimal/moderate disease. However,

Table 2. Animals and clinicopathological findings.

Animal	Duration of Infection (wpi)	Radiographic Readings[a]	Disease Course	Granulomas			
				Total[e]	Solid	Necrotic	Size[f]
M7100	9[b]	+	moderate disease	2	0	2	424,136 – 1,820,000
M15300	10[c]	+++	advanced disease	233	56	177	16,836 – 5,486,090
M15000	16[b]	++	moderate disease	13	12	1	20,185 – 996,507
M14600	17[b]	-	no disease[d]	0			
M15100	17[b]	+	moderate disease	7	6	1	33,606 – 1,020,000
M11301	32[c]	+++	advanced disease	15	9	6	40,992 – 1,250,000
M11201	37[c]	+++	advanced disease	24	12	12	28,620 – 2,327,970
M7200	41[c]	+++	advanced disease	7	4	3	14,882 – 2,060,000
M15200	64[b]	-	minimal disease	0			

[a]Radiographic readings at necropsy. M14600 is the only macaque to not have a positive radiographic reading. However, viable *M. tuberculosis* bacilli could be cultured from lung homogenates at necropsy

[b]Sacrificed at a scheduled timepoint.

[c]Sacrificed due to extreme clinical symptoms.

[d]Only a few macroscopic granulomas were observed at necropsy.

[e]Number of granulomas examined in tissues.

[f]Surface area in 14μm tissue sections (μm^2)

animals with advanced disease harbored more granulomas, and therefore, the majority of the solid granulomas were observed in these macaques.

The cellular compositions of these granulomatous structures were examined by immunohistochemical staining (IHC) of formalin-fixed, cryopreserved tissue sections. Both solid and caseous granulomas were predominantly comprised of macrophages ($CD68^+$) and lymphocytes (Fig. 1). Lymphocytes were mainly T-lymphocytes ($CD3^+$), but B-lymphocytes ($CD20^+$) were also detected in the granulomatous lesions as a mixed population of diffusely and intensely staining cells (Fig. 1G,H). Regardless of disease state, the compositions of the numerous granulomas were similar in all macaques. $CD68^+$ cells (Fig. 1C-D) were more abundant than the other cell types examined and the staining pattern was distributed throughout the cellular portions of the lesions. The T-lymphocytes ($CD3^+$, Fig. 1E-F) were dispersed throughout the cellular portions of the granulomatous lesions, whereas the rare B-lymphocytes ($CD20^+$, Fig. 1G,H) were not within a particular location, but were localized in peripheral focal collections in caseous granulomas. The $CD4^+$:$CD8^+$ ratio of T-lymphocytes for a small number of disaggregated granulomas from five animals ranged from 0.37 to 1.11 with a mean of 0.68. Taken together, these data indicate that cynomolgus macaques inoculated intratracheally with a low dose of virulent *M. tuberculosis* develop classic granulomas.

Abundant expression of IFN-γ-inducible CXCR3 ligands in granulomatous lesions

Chemokines likely play multiple roles in *M. tuberculosis*-associated granuloma formation and maintenance, including the shaping of the local immune environment. Given that IFN-γ is a cytokine critical to host resistance to *M. tuberculosis* disease progression in mice and humans (75-78), we determined the patterns and levels of expression of mRNAs encoding the

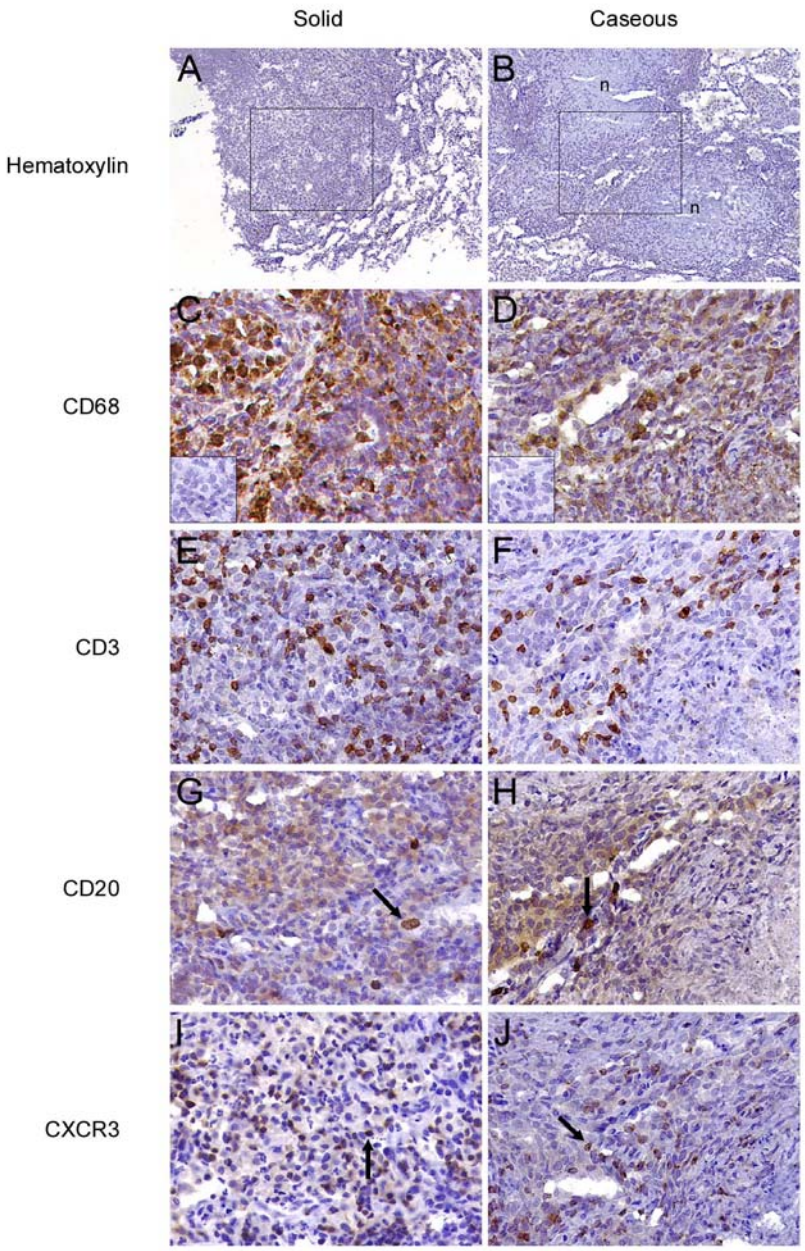

Figure 1. Structures and cellular compositions of lung granulomas of cynomolgus macaques experimentally infected with *M. tuberculosis*. Each granuloma in lung tissue sections was categorized as solid (e.g., M11201, A,C,E,G,I) or caseous (e.g., M11301, B,D,F,H,J). The open box in (A,B) identifies the region of the granuloma on subjacent sections, which are presented in (C-J), and the necrotic portions of the granulomas are also noted (n). Specific cell types were identified by IHC using antibodies directed against CD68 (C,D), CD3 (E,F), CD20 (arrow, G,H) and CXCR3 (arrow, I,J). $CXCR3^+$ cells were also detected as an indirect measure of the recruitment of $CXCR3^+$ cells to the granuloma (I,J). The necrotic portions of the granulomas are in the top left and bottom right corners of the micrographs (D,F,H,J). Parallel analysis with isotype control antibodies yielded no IHC signal (inset, C,D). Original magnification, 100X (A-B), 200X (C-J).

IFN-γ-inducible chemokines, CXCL9/Mig, CXCL10/IP-10 and CXCL11/I-TAC, directly in lung tissues from experimentally infected macaques. This approach can reveal changes in mRNA expression levels that might not be as evident using RNAs from homogenized tissues in population analyses. ISH for these CXCR3 ligand mRNAs revealed extremely abundant expression within the granulomatous lesions, with the highest signal observed for CXCL9/Mig and the lowest for CXCL11/I-TAC in both solid and caseous granulomas (Fig. 2). In contrast, nongranulomatous regions of lung tissue and lung tissue from *M. tuberculosis*-naïve control macaques rarely exhibited appreciable expression of any CXCR3 ligand mRNA (Fig. 2, data not shown). Solid granulomas had intense ISH signal concentrated only over the central portion of the granuloma, whereas caseous granulomas had intense ISH signal concentrated over the cellular portions of the granulomas surrounding the acellular centers (Fig. 2).

To provide a measure of mRNA expression, we performed quantitiative image analysis of the tissue sections using the MetaView software package. We measured the total surface area of each granuloma, as well as the proportion of the cellular surface area covered by autoradiographic silver grains. Acellular, necrotic regions were excluded from these calculations. As expected, the amount of thresholded surface area attributed to silver grains increased as the total surface area of the granuloma increased in both solid and caseous granulomas (data not shown). We then determined the percentage of cellular surface area covered by ISH signal (Fig. 3). The percent thresholded surface area measured over cellular portions of granulomas for CXCL9/Mig ISH signal was the highest of the three CXCR3 ligand mRNAs with mean percentages of thresholded area of 48% and 51% for solid and caseous granulomas, respectively (Table 3). The mean percentages of thresholded surface area for CXCL9/Mig, CXCL10/IP-10

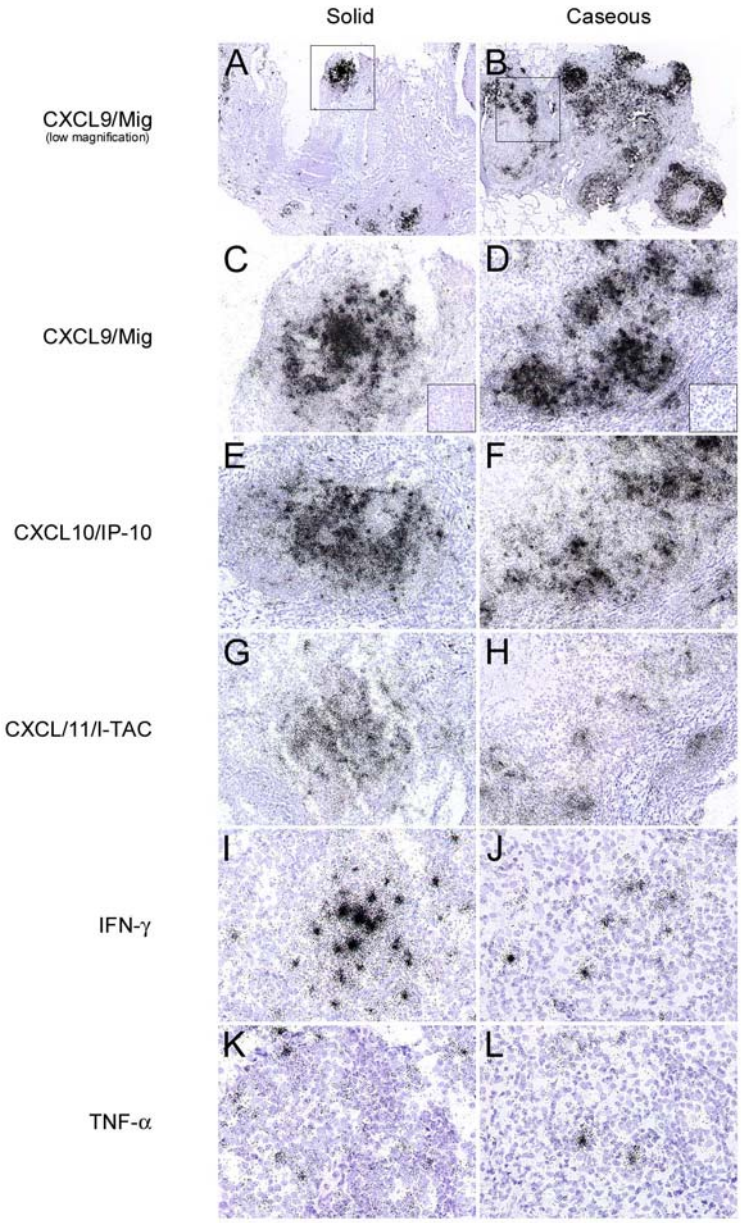

Figure 2. *In situ* hybridization detection of IFN-γ-inducible chemokine and cytokine mRNAs in granulomatous lung tissues from *M. tuberculosis*-infected cynomolgus macaques. ISH was performed on lung tissue sections with IFN-γ-inducible chemokine- and cytokine-specific riboprobes and representative fields from subjacent sections are presented. A low magnification micrograph of the ISH for CXCL9/Mig is shown to highlight the granulomatous tissue (A,B) and the open box demarcates the granulomatous region further presented in the remaining micrographs (C-L). ISH was performed for CXCL9/Mig (C,D), CXCL10/IP-10 (E,F) and CXCL11/I-TAC (G,H) mRNAs in solid (C,E,G) and caseous (D,F,H) granulomas. IFN-γ (I,J) and TNF-α (K,L) mRNAs were detected by ISH in solid (I,K) and caseous (J,L) granulomatous lesions. The necrotic portion of the granuloma is in the top left corner of the micrographs (D,F,H,J,L). Parallel hybridizations with control sense riboprobes provided no autoradiographic signal (inset, C,D). Original magnifications, 20X (A,B), 100X (C-H), 200X (I-L).

and CXCL11/I-TAC in the granulomas from animals with advanced disease were approximately two-fold higher than the animals with minimal/moderate disease (Fig. 3, Table 3). In summary, IFN-γ-inducible chemokines were dramatically upregulated in macaque pulmonary granulomatous lesions relative to nongranulomatous tissue and naïve controls.

The high levels of expression of CXCR3 ligands would be expected to lead to recruitment of $CXCR3^+$ cells into the local environment. To identify $CXCR3^+$ cells, we performed IHC using an anti-CXCR3 monoclonal antibody (Fig. 1I,J). $CXCR3^+$ cells were more abundant in granulomatous regions compared to nongranulomatous regions of macaque lung tissues. The distribution of $CXCR3^+$ cells was not concentrated uniquely in specific areas of the granulomatous lesions, but was generally well localized with the expression of the CXCR3 ligand mRNAs. The increased abundance of these receptor-bearing cells in the granulomatous lesions was concordant with increases in CXCR3 expression in BAL cells examined from these same macaques (data not shown).

Expression of IFN-γ and TNF-α mRNAs is elevated in granulomatous lesions.

Previous studies have shown that IFN-γ plays a protective role in the host response to *M. tuberculosis*, that TNF-α is important in granuloma formation and maintenance (38,79-81), and that both cytokines can induce the expression of subsets of chemokines (35,38). Therefore, we examined the patterns and levels of expression of these cytokine mRNAs in *M. tuberculosis*-induced granulomatous lesions in cynomolgus macaques. TNF-α and IFN-γ $mRNA^+$ cells were abundant in the granulomatous lesions of these macaques (Fig. 2I-L), but were extremely rare in nongranulomatous regions of lung tissue sections. These TNF-α and IFN-γ $mRNA^+$ cells were

Table 3. Quantitation of chemokine, cytokine, and mycobacterial RNA expression in granulomatous lesions of cynomolgus macaques experimentally infected with *M. tuberculosis*.

Animal[a]		Granuloma size[b] (μm^2)	Mycobacterial rRNA[c]	IFN-γ mRNA$^+$ cells[d]	TNF-α mRNA$^+$ cells[d]	CXCL9/Mig ISH signal[e]	CXCL10/IP-10 ISH signal[e]	CXCL11/I-TAC ISH signal[e]
Solid								
Minimal/Moderate disease								
M15000	(12)	184,882	0.9	38.2	31.2	23.54	35.89	8.47
M15100	(6)	157,386	0.0	6.5	2.5	9.54	6.83	1.56
Avg	(18)	175,717	0.8	27.0	21.1	18.29	17.58	6.17
Advanced disease								
M7200	(4)	189,597	2.0	46.0	N/A[f]	26.96	19.37	31.07
M11201	(12)	135,894	N/A	2.8	3.1	55.68	43.10	6.82
M11301	(9)	131,056	1.4	39.4	11.2	49.53	42.59	27.11
M15300	(56)	337,018	3.9	20.6	14.1	57.15	28.37	15.87
Avg	(81)	277,057	3.5	23.1	11.6	55.02	32.08	17.15
Avg	(99)	258,631	2.8	24.1	14.0	48.03	29.15	14.48
(range)				(0 - 156)	(0 - 130)	(1.33 - 84.22)	(0.16 - 90.53)	(0.08 - 75.44)
Caseous								
MinimalModerate disease								
M7100	(2)	1,122,068	N/A	114.0	42.0	40.23	23.48	10.01
M15000	(1)	996,507	0.0	47.0	N/A	30.60	22.60	0.26
M15100	(1)	1,020,000	N/A	20.0	10.0	16.86	8.17	1.99
Avg	(4)	1,065,161	0.0	60.3	26.0	29.23	18.09	5.57
Advanced disease								
M7200	(3)	875,262	4.3	92.3	N/A	32.61	27.14	22.95
M11201	(12)	591,442	N/A	39.6	13.0	60.11	41.27	12.88
M11301	(6)	634,611	246.0	112.8	28.8	51.93	44.15	22.16
M15300	(177)	678,735	4.1	49.1	28.0	51.32	32.75	11.52
Avg	(198)	675,010	45.17	51.8	26.9	51.58	33.53	12.00
Avg	(202)	682,892	45.0	51.9	26.9	51.19	33.25	11.83
(range)				(1 - 238)	(2 - 135)	(14.14 - 99.38)	(0.35 - 74.44)	(0.26 - 40.16)

[a]Number of granulomas examined in parentheses.

[b]Average surface area of granulomas per 14μm section.

[c]Average number of mycobacterial 16S rRNA focal collections per 14μm section of granuloma.

[d]Average number of mRNA$^+$ cells per 14μm section of granuloma.

[e]Average percentage of cellular surface area comprised of autoradiographic silver grains.

[f]N/A, not available.

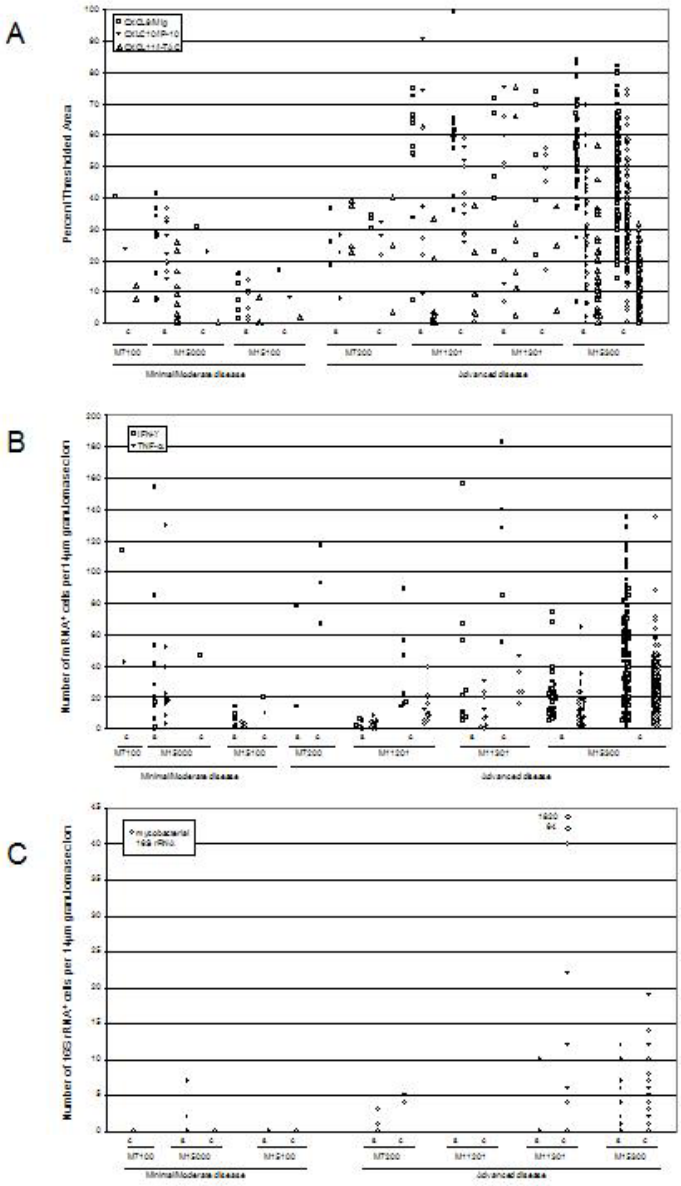

Figure 3. Quantitative image analysis of ISH signals for IFN-γ-inducible chemokine and cytokine mRNA and mycobacterial 16S rRNA in granulomatous lesions. Chemokine-, cytokine- and mycobacterial-specific ISHs were performed on granulomatous lung tissues from experimentally infected macaques. For quantitation of chemokine mRNA ISH signal, a digital image of each granuloma was captured. The proportion of cellular surface area covered by silver grains was determined using the threshold and measure tools of the MetaView software package (A). The numbers of IFN-γ and TNF-α mRNA$^+$ cells per 14μm section of granuloma were determined for each solid and caseous granuloma (B). To measure local mycobacterial load, ISHs for mycobacterial 16S rRNA were performed and the numbers of mycobacterial 16S rRNA$^+$ cells and focal collections were enumerated in 14μm sections of each solid and caseous granuloma (C). Each data point represents the value obtained for an individual granuloma. c, caseous; s, solid.

found in the cellular regions of granulomas, and co-localized with the IFN-γ-inducible chemokine ISH signal (Fig. 2C-H). In contrast, no IL-4 mRNA$^+$ cells were observed in any of these same tissue sections (data not shown). As a measure of local cytokine mRNA expression, we manually counted the cytokine mRNA$^+$ cells in each granuloma. ISH signal for IFN-γ mRNA was present as a dense focal collection of silver grains (Fig. 2I,J), whereas ISH signal for TNF-α mRNA was present as networks of more diffuse signal (Fig. 2K,L). The numbers of IFN-γ mRNA$^+$ cells per 14μm granuloma section were more abundant than TNF-α mRNA$^+$ cells in both groups of animals (Fig. 3B, Table 3), with caseous granulomas harboring higher numbers of IFN-γ mRNA$^+$ cells per granuloma than solid granulomas (Fig. 3B, Table 3). The average number of IFN-γ mRNA$^+$ cells was 24 and 52 mRNA$^+$ cells per 14μm section of granuloma for solid and caseous granulomas, respectively (Table 3), whereas the average number of TNF-α mRNA$^+$ cells of was 14 and 27 mRNA$^+$ cells per section of granuloma for solid and caseous granulomas, respectively. However, the mean values in Table 2 indicate that the number of IFN-γ mRNA$^+$ cells present in the cellular regions of granulomas were roughly proportional to granuloma size.

Detection and quantitation of M. tuberculosis 16S rRNA in pulmonary granulomatous lesions

The high levels of chemokine and cytokine mRNA expression we observed in granulomatous lesions might be associated with high numbers of local mycobacteria or mycobacterial products. To address this issue, we performed ISH using a riboprobe specific for mycobacterial 16S rRNA. ISH with this riboprobe readily allowed detection of the mycobacterial 16S rRNA in lung tissue sections of cynomolgus macaques (Fig. 4). No specific ISH signal was detected in the corresponding sense control probe experiments (Fig. 4E, inset). The ISH signal

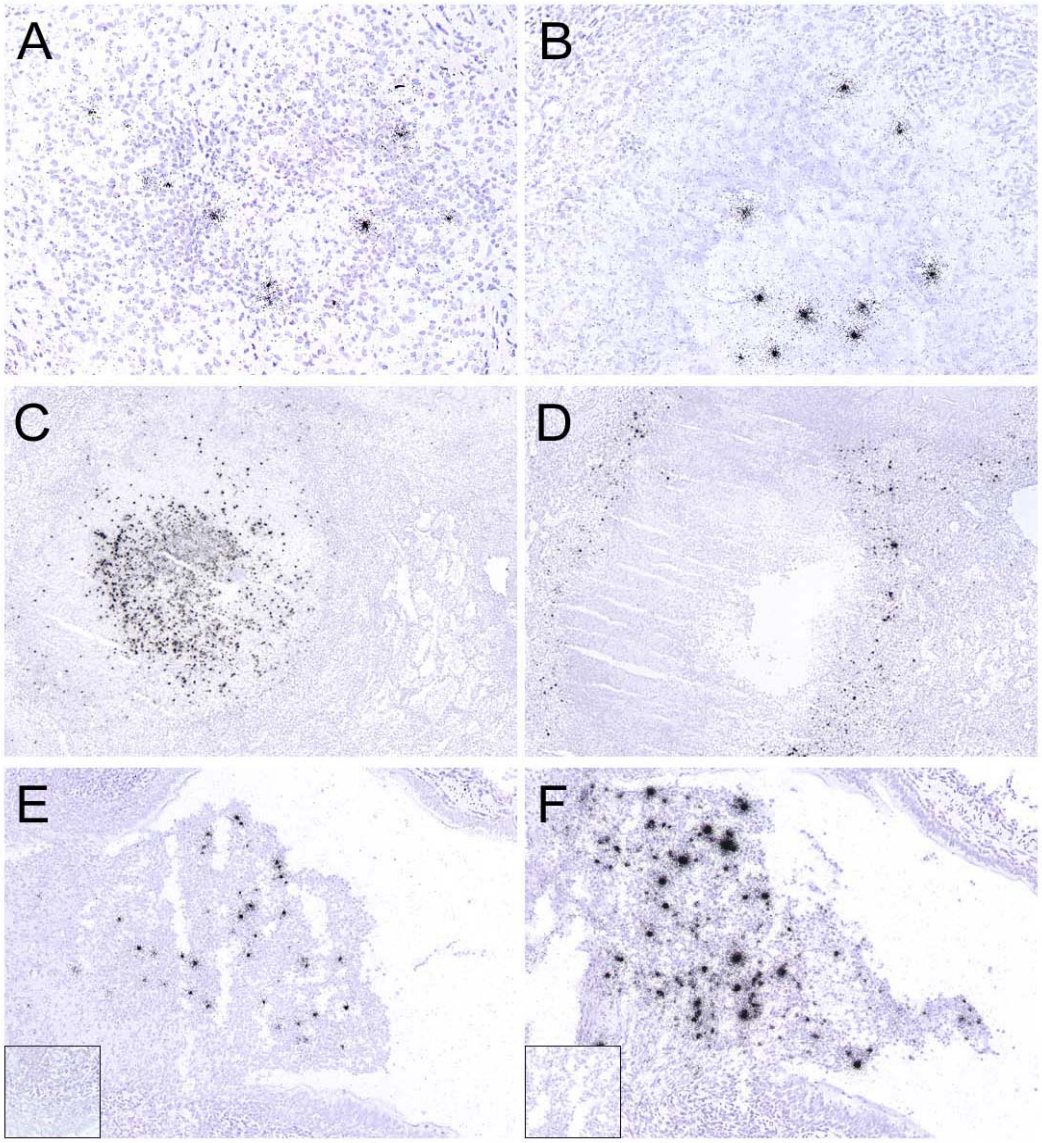

Figure 4. *In situ* hybridization detection of mycobacterial 16S rRNA and IFN-γ mRNA in granulomatous experimentally infected cynomolgus macaques. ISH was performed on lung tissues with riboprobes specific for the mycobacterial 16S rRNA and IFN-γ RNAs and representative fields are presented. Mycobacterial 16S rRNA was detected in tissues with solid (e.g., M15000, A) and caseous (e.g., M15300, B) granulomas in animals with moderate (A) and advanced disease (B). A necrotic granuloma with abundant mycobacterial 16S rRNA (M11301, C) and IFN-γ mRNA (M11301, D) ISH signals is shown. A cavitating lesion with abundant 16S rRNA (M15300,E) and IFN-γ mRNA (M15300,F) ISH signals is shown. Parallel hybridizations with control sense riboprobes provided no autoradiographic signal (inset, E, F). Original magnifications, 20X (E,F), 100X (A, C, D), 200X (B).

observed was typically a compact collection of silver grains or more rarely, a more diffuse collection of silver grains over an entire lung cell. We based our enumeration of the mycobacterial 16S $rRNA^+$ focal collections on the assumption that a focus identified either a single bacterium or a collection of bacteria that cannot be individually distinguished. Although mycobacterial 16S $rRNA^+$ foci were detected in both solid (Fig. 4A) and caseous (Fig. 4B) granulomas, they were more abundant in the caseous granulomas and in the macaques with advanced disease compared to the macaques with minimal/moderate disease. The mycobacterial 16S $rRNA^+$ focal collections were observed both in the cellular regions and the central caseating portions of granulomas. Frequently, 16S $rRNA^+$ focal collections were in close proximity to each other in cellular regions of granulomas, but the greatest ISH signals were observed in the acellular centers of caseous granulomas. In animal M11301 with advanced disease, 1,820 16S $rRNA^+$ foci were detected in a single 14μm section of an exceptional granuloma (Fig. 4C). If we assume a spherical shape for this entire granuloma and the tissue section represents the largest diameter of the granuloma, the entire granuloma (2.5×10^{10} μm^3) is estimated to harbor a minimum of 303,394 mycobacteria. The IFN-γ mRNA ISH signal obtained in a subjacent section of this same granuloma was extremely abundant (Fig. 4D), as were the intense ISH signals for TNF-α and CXCR3 ligand mRNAs (data not shown).

In another animal with advanced disease (M15300), we observed a cavitating lesion (Fig. 4E-F). This lesion, which protruded into an airway, had high numbers of mycobacterial 16S $rRNA^+$ focal collections in the protruding region (Fig. 4E). The local expression of IFN-γ mRNA was also exceptionally abundant (Fig. 4F), with the ISH signal co-localized with the 16S $rRNA^+$ foci. CXCR3 ligand mRNA expression was similarly abundant in this cavitating lesion (data not shown).

Expression of IFN-γ in the lymphocyte population

Interferon-γ is secreted by activated natural killer (NK) cells, cytotoxic T cells, Th1 cells and Th0 cells. The majority of the IFN-γ expression is attributed to the Th1 cells and we sought to identify which cells were expressing IFN-γ in these granulomatous tissues. We performed simultaneous ISH for IFN-γ mRNA and IHC for CD3, CD20 and CXCR3 protein. In these studies, $CD3^+$/IFN-γ $mRNA^+$ cells were 74% of the total IFN-γ $mRNA^+$ cells (Fig. 5A) and IFN-γ mRNA was rarely expressed by $CD20^+$ B-lymphocytes (Fig. 5B). In addition, we revealed that a large proportion of the IFN-γ $mRNA^+$ cells were also $CXCR3^+$. These findings further validate our model that the recruitment of $CXCR3^+$ cells into the site of the granuloma will upregulate the local IFN-γ production; thus, an amplification loop of IFN-γ-induced processes continue at the site of inflammation. We were unable to account for all of the IFN-γ $mRNA^+$ cells. This was partially due to difficulty in identifying subtypes of the $CD3^+$ lymphocytes as well as immunohistochemically staining NK cells and NKT cells.

Characterization of the expression and distribution of T cell receptor chains in granulomas from cynomolgus macaques

Lymphocytes expressing αβTCR are necessary in the formation of granulomas and control of infection, whereas the γδ TCR^+ T cells have a protective role in the early stage of infection (14,31). To determine the expression of TCR receptor chain mRNAs in the granulomatous tissues of these cynomolgus macaques, we used ISH to specifically detect the presence of TCRβ and TCRγ/δ mRNA within these tissues. These studies clearly illustrated the presence of TCRβ and TCRγδ mRNA present in the examined granulomatous structures (Fig.

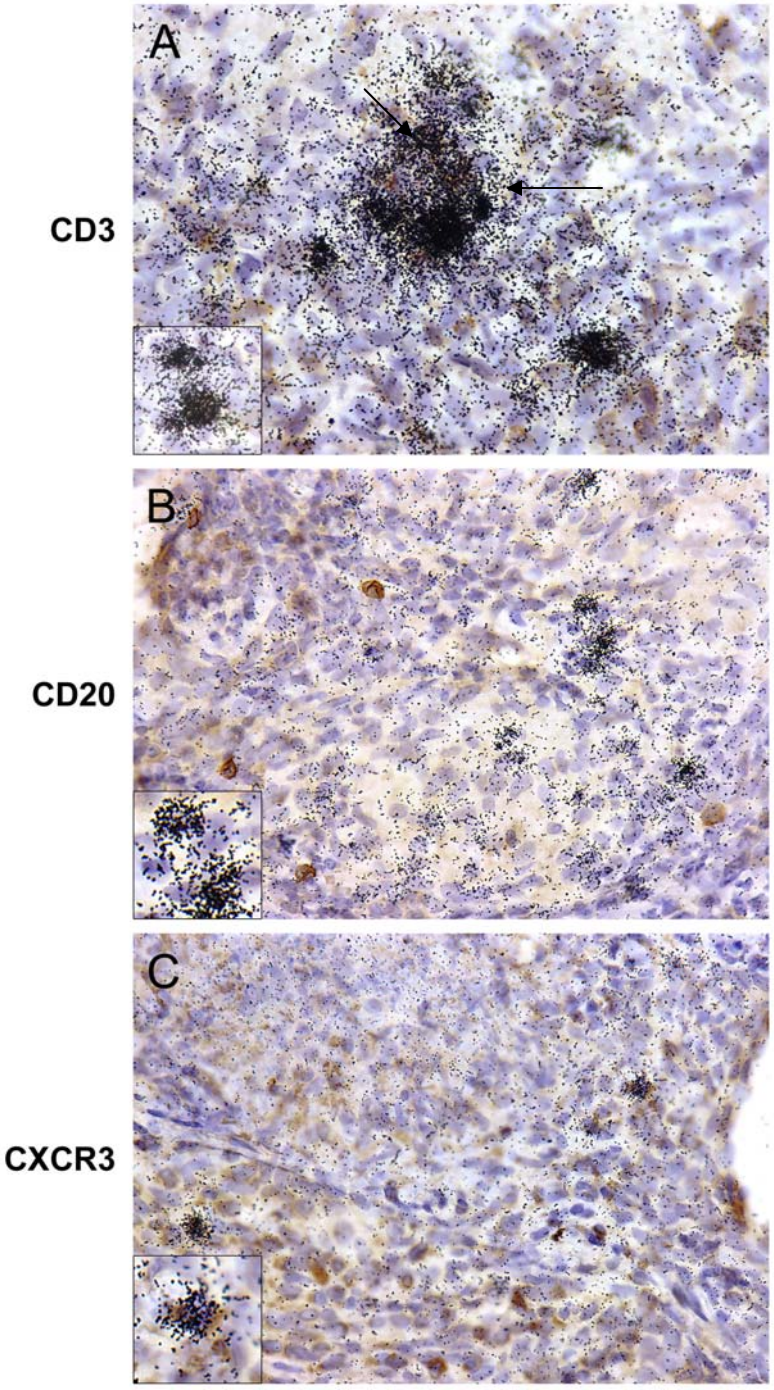

Figure 5. Simultaneous ISH for IFN-γ and IHC for CD3, CD20 and CXCR3 in granulomas from cynomolgus macaques infected with *M. tuberculosis*. The majority of the IFN-γ mRNA$^+$ cells were immunohistochemically stained as CD3$^+$ lymphocytes (A), while none of the IFN-γ mRNA$^+$ cells stained CD20$^+$ (B lymphocytes, B). Additionally, the IFN-γ mRNA$^+$ cells frequently were stained as CXCR3$^+$ cells (C). Original magnifications, x400.

6). We consistently found the TCRβ mRNA was dispersed and widespread throughout the granuloma (Fig. 6A-B), and the TCRγδ mRNA was in punctate accumulations of silver grains (Fig. 6C-D). The abundant expression of TCRβ mRNA compared with the expression of TCRγδ mRNA correlates with the current understanding that $\alpha\beta TCR^+$ T cells are the predominant cells and also that $\gamma\delta TCR^+$ T cells are likely complementing the type I immune response within these granulomas. Although our data are slightly skewed due to the fact that we only used TCRβ riboprobes, without inclusion of TCRα riboprobes, we are still able to see the general pattern of expression and distribution of the $\alpha\beta TCR^+$ and $\gamma\delta TCR^+$ T cells by this method.

ISH analyses in hilar lymph node 5 weeks post-infection

Dendritic cells are present in the bronchoalveolar space, airway epithelium and lung parenchyma, and immature DC function as sentinels for inhaled pathogens (82,83). DC likely play a key role in the initial immune response to *M. tuberculosis* infection, by ingesting the pathogen at the site of infection and migrating to the regional lymph node. *Mycobacterium*-infected DC have an upregulated expression of MHC and costimulatory molecules, which help DC acquire the ability to efficiently prime naïve T lymphocytes (84-86). To analyze the IFN-γ-inducible molecules in the development of an immune response in the regional lymph node, we examined the hilar lymph nodes of cynomolgus macaques that were infected intrabronchially with *M. tuberculosis* Erdman strain and sacrificed at 3, 4, 5 or 6 weeks post-infection (p.i.).

Our studies revealed that very few granulomas were present in the lymph nodes of these early time-point macaques tested. We also examined lung tissues from these macaques and were only able to find one caseous granuloma in a 5wk p.i. macaque and no apparent signs of

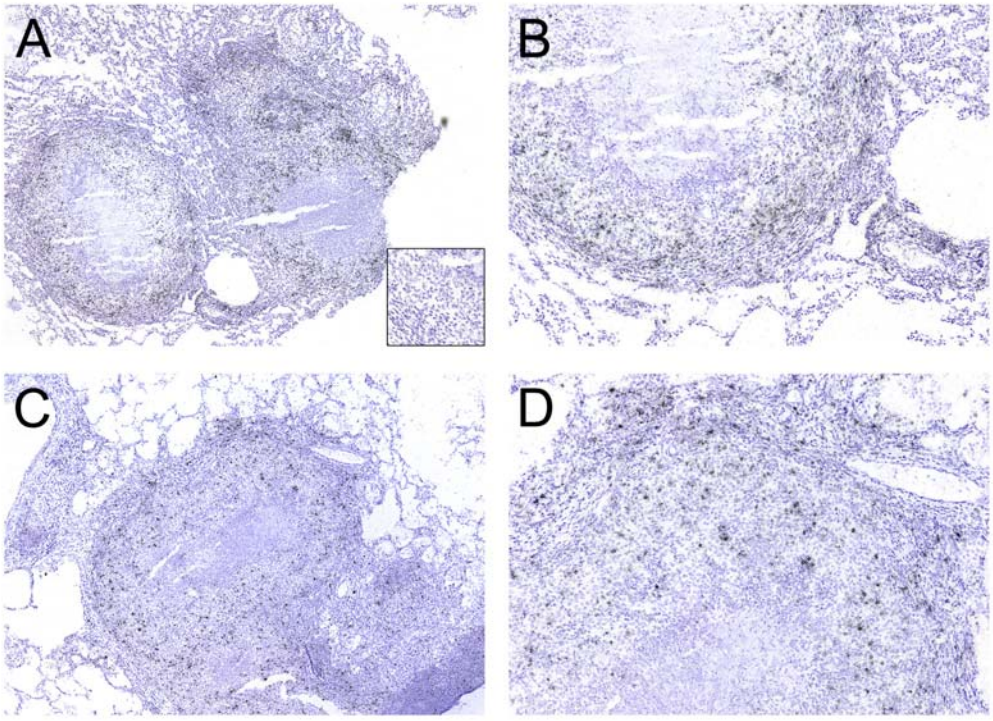

Figure 6. ISH for TCR chains (β,γ, and δ) in granulomas from cynomolgus macaques infected with *M. tuberculosis*. The expression of TCR β chain (A, B) was abundantly expressed in a dense manner throughout the cellular region of the granuloma. The simultaneous expression of TCR γ and δ chains (C, D) was also abundant and the ISH signal was more punctate throughout the granuloma. Parallel ISH using sense riboprobes were performed (inset, A). Original magnifications, x40 (A, C), x100 (B, D).

---

pregranulomatous lesions were observed in the tissues examined. Upon analysis of the ISH studies in the hilar lymph nodes (Fig. 7), we discovered an abundance of the IFN-γ-inducible chemokines as early as 3wk p.i. and the signal intensity increased with duration of infection (Table 4). In addition, IFN-γ and TNF-α mRNA$^+$ cells were observed in the hilar lymph nodes as early as 3wk p.i., whereas IL-12p40 mRNA$^+$ cells were not detected in these tissues (data not shown). We also detected low numbers of mycobacterial 16S rRNA focal collections in hilar lymph nodes, with the exception of M24102 (5 wk p.i.), which had a caseous

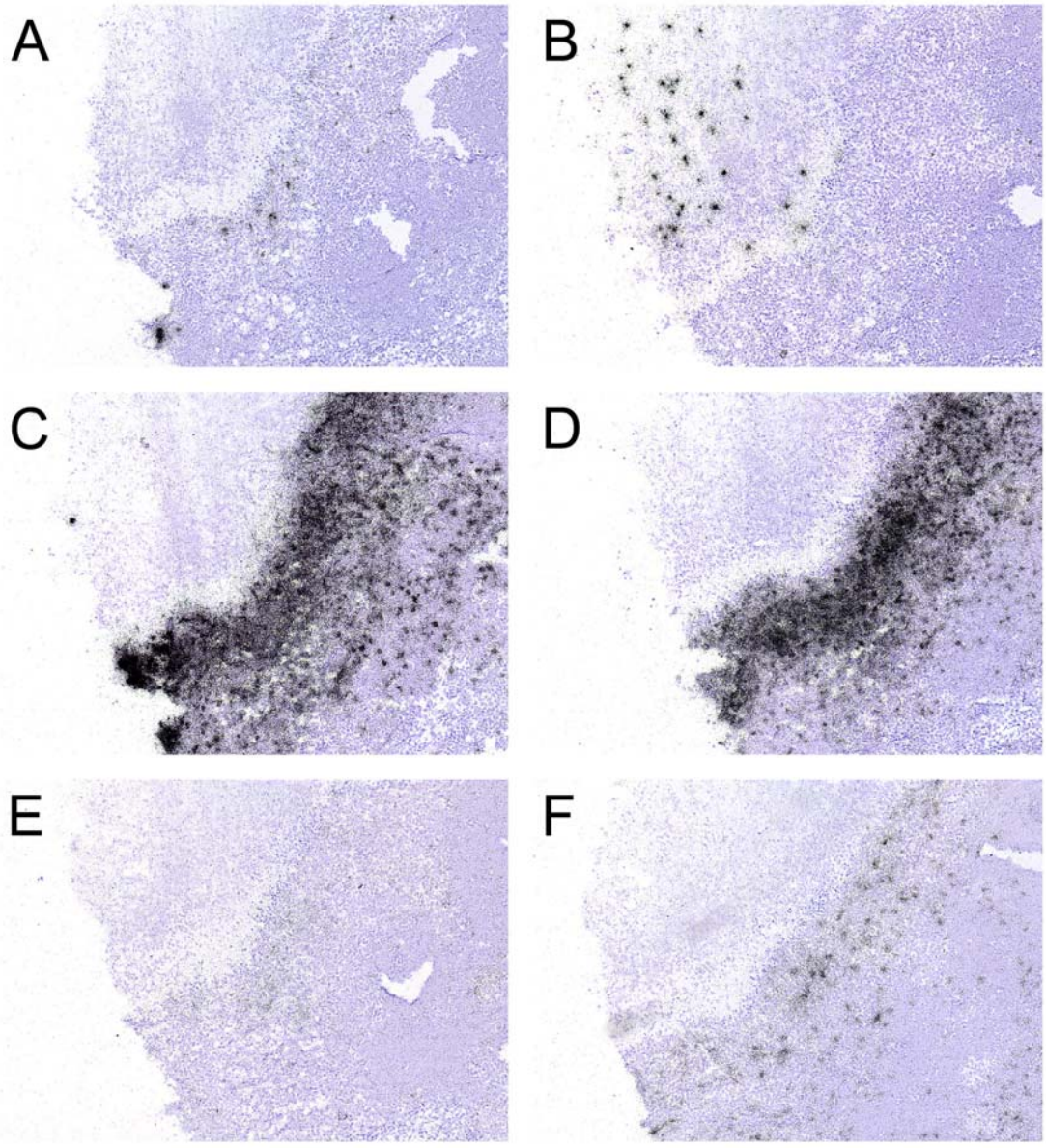

Figure 7. ISH analysis of a granuloma obtained from the left hilar lymph node of M24102 (5 wk pi). RNAs encoding for IFN-γ (A), mycobacterial 16S rRNA (B), CXCL9/Mig (C), CXCL10/IP-10 (D) CCL5/RANTES (E), and CCL2/MCP-1 (F) were detected within this granuloma. Original magnifications, x100.

Table 4. ISH for chemokine and cytokine mRNA$^+$ cells in hilar lymph node tissue sections from early timepoint infections.

					Number of mRNA$^+$ cells per 14μm section			
Animal	CXCL9 Mig[b]	CXCL10 IP-10	CCL5 RANTES	CCL2 MCP-1	IFN-γ	TNF-α	IL-12p40	Myco. rRNA[a]
3wk pi.								
M12202	NT[c]	NT	NT	NT	1	0	0	NT
M24002	+/++	+	-	-	13	3	0	0
4wk pi.								
M12302	++	++	+	++	51	23	0	0
M24702	NT	NT	NT	NT	0	NT	NT	0
5wk pi.								
M21902	+++	+++	-	++	1	0	0	3
M24102	+++	+++	±	++	64	1	0	132[d]
6wk pi.								
M24302	++	+	±	±	2	2	0	0
M22102	+	++	-	++	0	0	0	0

[a]Mycobacterial 16S rRNA.
[b]Chemokine ISH signal intensity was evaluated as follows: -, absence of ISH signal; +, 0-4 mRNA$^+$ cells per field (20x); ++, 5-20 mRNA$^+$ cells per field (20x); +++, >20 mRNA$^+$ cells per field (20x)
[c]NT, tissue repeatedly came off slide during processing.
[d]Mycobacterial 16S rRNA was only observed in the acellular region of the caseous granuloma.

granuloma with 132 mycobacterial 16S rRNA focal collections within the central portion of the caseous granuloma found in a 14μm section. The caseous granuloma in M24102 had abundant expression of CXCL9/Mig, CXCL10/IP-10, and IFN-γ mRNA, revealing that regardless of disease state the IFN-γ and IFN-γ-inducible chemokine expression patterns are the same in caseous granulomas. Interestingly, we also observed CCL5/RANTES mRNA in the cellular portion of the caseous granuloma, as well as CCL2/MCP-1 mRNA.

Expression of CCR5 ligands in granulomas from cynomolgus macaques

CCR5 chemokine ligands recruit T lymphocytes and macrophages, and previous studies have observed elevated expression levels of these chemokines in active pulmonary tuberculosis in humans (87-89) and in experimental infections with mice (87,90). In vitro studies have also shown that *M. tuberculosis* infection of THP-1 cells, a human macrophage cell line, induces a large number of genes that encode proteins involved in cell migration and homing, including the CCR5 ligands: CCL3/macrophage inflammatory protein (MIP)-1α, and CCL4/MIP-1β and CCL5/regulated on activation, normal, T-cell expressed and secreted (RANTES) (91). CCL3/MIP-1α, CCL4/MIP-1β and CCL5/RANTES are expressed to high levels in response to *M. tuberculosis* infection and MIP-1β and RANTES have also been shown to suppress intracellular mycobacterial growth, suggesting an innate immune function (92). In addition, CXCR3 and CCR5 are preferentially expressed on Th1 lymphocytes (93). Immature DC also have been shown to migrate toward the CCR5 ligands prior to activation/maturation (94). Since the expression of these CCR5 ligands may be involved in the migration of multiple relevant cell types and may be associated with the ability to control infection, we examined the granulomatous tissues in these cynomolgus macaques for CCL3/MIP-1α, CCL4/MIP-1β and CCL5/RANTES mRNAs by ISH. The CCR5 ligand mRNA ISH signal intensity was abundant within the granuloma (Fig. 8), although not as abundant as the CXCR3 ligands (Fig. 2). Even though the general expression patterns were very similar in distribution, CCL4/MIP-1β mRNA expression was the most abundant CCR5 ligand in these granulomas and CCL5/RANTES the least abundant. The expression of the CCR5 ligands could contribute to further skewing of the immune response to a type 1 immune response. The recruitment of activated Th1 cells induces a

microenvironment of high IFN-γ expression, thus facilitating a further skewed microenvironment comprised of greater numbers of $CXCR3^{+}/CCR5^{+}$ cells at the inflammatory site.

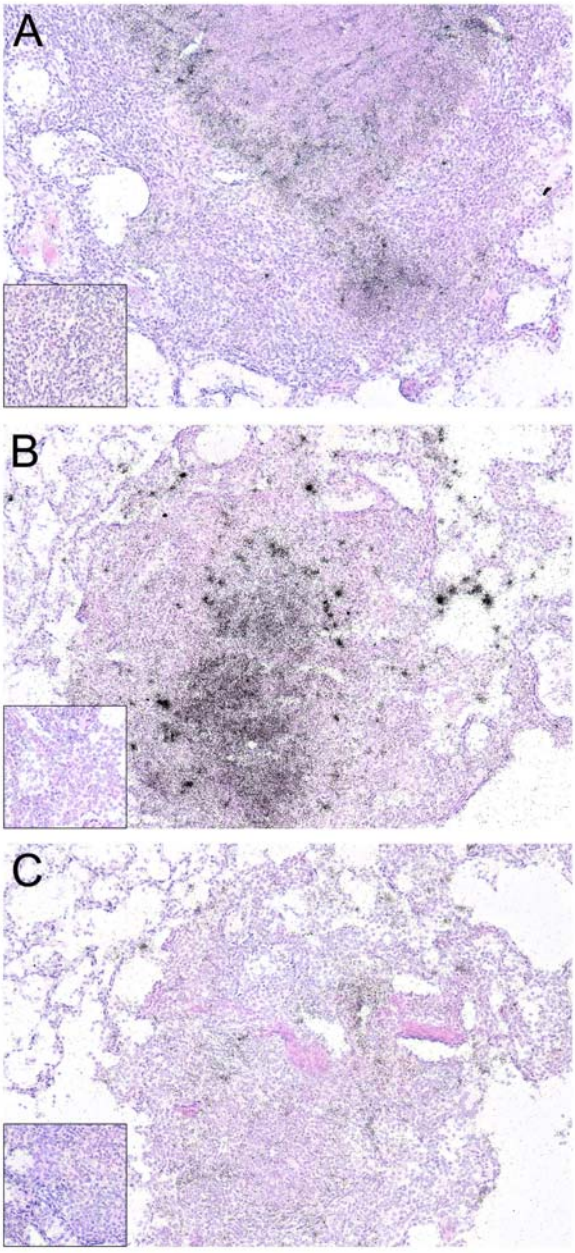

Figure 8. ISH analysis of the CCR5 ligands in granulomatous tissues from cynomolgus macaques infected with *M. tuberculosis*. Expression patterns of the CCR5 ligands, CCL3/MIP-1α (A), CCL4/MIP-1β (B), and CCL5/RANTES (C), were examined by ISH. Parallel ISH using sense riboprobes were performed (inset; A, B and C). Original magnifications, x100.

F. DISCUSSION

In this study we have examined local chemokine and cytokine mRNA expression, and local mycobacterial burden in pulmonary granulomatous lesions resulting from intrabronchial infection of cynomolgus macaques with a low dose of virulent *M. tuberculosis*. This is one of the first studies of chemokine expression directly in granulomatous tissue sections. We found abundant expression of mRNAs encoding the proinflammatory cytokines, IFN-γ and TNF-α, as well as IFN-γ-inducible, CXCR3 ligands within all granulomas regardless of size or structure. The general absence of cells expressing these mRNAs in nongranulomatous regions of lung tissues suggests they play a local role in granuloma formation and maintenance. Based on these findings we propose here a model for *M. tuberculosis*-initiated, IFN-γ-driven chronic inflammation in pulmonary granulomas that is similar to our model for the events occurring in lymphoid tissues of SIV infected rhesus macaques (68).

Cynomolgus macaques are susceptible to *M. tuberculosis*, and develop disease that is clinically, immunologically, and pathologically similar to humans (59,69,70). Interestingly, approximately 40% of cynomolgus macaques infected with a low dose of *M. tuberculosis* were able to contain the infection in a subclinical state during the period of study. This clinical state resembles clinical latency in humans (59,70) and indicates that cynomolgus macaques are an appropriate animal model for latency (59,70) and reactivation (70) during *M. tuberculosis* infection. Although the proportion developing active disease in cynomolgus macaques is higher, it is similar to the outcome of infection in humans in which only 10% of individuals infected with *M. tuberculosis* develop overt disease. At the tissue level, *M. tuberculosis* induced

granulomas in cynomolgus macaques are structurally similar to granulomas that develop in humans.

We have demonstrated here by direct analysis in tissue sections using ISH that there is a high level expression of IFN-γ-inducible chemokine mRNAs and increased numbers of IFN-γ and TNF-α mRNA$^+$ cells in pulmonary granulomas. CXCR3$^+$ cells, which are predominantly activated T- and B-lymphocytes and NK cells (39,95-97), are likely recruited into the local environment. Our detection of abundant CXCR3$^+$ cells in pulmonary granulomas provides evidence for this recruitment. Although not examined here, local proliferation and apoptosis are also likely contributing to accumulation and loss of cells, respectively, and affect overall granuloma size and structure.

Previous studies of chemokine expression during *M. tuberculosis* infection include *in vivo* murine studies and *ex vivo* and limited tissue-based human studies. Mice infected by the aerosol route have increases in CCL3/MIP-1α, CXCL2/MIP-2, CXCL10/IP-10 and CCL2/MCP-1 expression in lungs (98). In addition, granulomas elicited in mice by PPD-coated beads have a polarized type 1 immune response with increased expression levels of CXCL2/MIP-2, CXCL5/LIX, CXCL10/IP-10 and CXCL9/Mig (16,99). In these studies, neutralization of IFN-γ with antibodies greatly reduced the expression of CXCL9/Mig and CXCL10/IP-10. Human studies of patient-derived BAL or alveolar and peripheral macrophages revealed increased expression of CXCL8/IL-8, CCL5/RANTES, CCL3/MIP-1α, CCL2/MCP-1 and CXCL10/IP-10 (9,34). The one other ISH and IHC report of chemokine expression in human tuberculous granulomas demonstrated localized expression of CXCL10/IP-10, CXCL8/IL-8, and CCL2/MCP-1 within granulomas (34).

The strategy we have used for the detection of cells producing proinflammatory chemokines and cytokines is targeted toward mRNA expressed by the producing cell. This approach reveals the locations and numbers of cells that produce these immunomodulatory proteins, but does not indicate the locations or amounts of actual protein. Although this is a limitation of our study, the detection of chemokine and cytokine protein is complicated by the diffusion of protein that will occur after release into the extracellular milieu. The detection of different proteins through IHC is also complicated by the unique physiochemical properties of each antigen/antibody pair, in comparison to RNA/RNA hybrids, which will generally have the same physiochemical properties. Our ISH strategy has the additional advantage that it can reveal focal changes in mRNA expression that might not be detected using population analyses of extracted tissue RNAs due to dilution.

Previous *in situ* studies of human tuberculous granulomas identified local production of TNF-α and IFN-γ mRNA in all granulomatous lesions, but only a fraction of these lesions expressed IL-4 mRNA (100). Our data are consistent with these findings, in that IFN-γ mRNA was much more abundant than IL-4 mRNA, but they differ in that we did not detect any IL-4 mRNA with our ISH assay, as was also observed by others in human granulomas (101). Limited expression of both IFN-γ and IL-4 mRNA has been suggested to be associated with progression of granulomas to a necrotic state (102). However, we observed an association between the numbers of local IFN-γ and TNF-α $mRNA^+$ cells and the size (and necrotic state) of pulmonary granulomas. The reasons for the differences between our findings and those of others (103) are not clear but could include differences with respect to: (1) the host species of study; (2) the disease and treatment status of the study subjects; (3) the tissue processing protocols; and/or (4) the ISH probe and detection strategies.

Based on our findings of abundant expression of CXCR3 ligands, IFN-γ and TNF-α in pulmonary granulomatous lesions, we propose a model of their contributions to the chronic inflammation that results in granuloma formation and maintenance, which is similar to a model we previously proposed for chronic inflammation in SIV infected lymphoid tissues (68). First, infection of alveolar macrophages or DC leads to the induction of proinflammatory cytokines and chemokines, for example, by interaction of mycobacterial antigen with toll-like receptors (TLRs). Additional cells are therefore recruited into the local environment. Immune responses specific to *M. tuberculosis* develop following the trafficking of pulmonary DC to draining lymph nodes, which results in the trafficking of type 1 $CD4^+$ and $CD8^+$ T-lymphocytes to the site of *M. tuberculosis* infection, and these cells produce IFN-γ. IFN-γ function is enhanced in the presence of TNF-α, which is well-documented as an important cytokine in the immune response to *M. tuberculosis* and in granuloma formation (38,79-81). Local production of IFN-γ and TLR stimulation will both induce the expression of CXCR3 ligands, and thus recruit $CXCR3^+$ T-lymphocytes and NK cells to the site of *M. tuberculosis* infection. CXCR3 ligands contribute to further polarization of the local environment because they augment the ability of IFN-γ to induce additional CXCR3 ligand production and lead to a type 1 outcome following stimulation of T-lymphocytes with polyclonal activators or specific antigens (104). In this model, the collective outcome will be the establishment and maintenance of a positive feedback loop in which local IFN-γ production leads to the ongoing recruitment of additional IFN-γ producing cells. Also, this suggests a role for IFN-γ in granuloma formation and maintenance beyond the induction of an antimicrobial state in infected cells. Thus, there are common themes in *M. tuberculosis* and SIV infection of macaques that if recapitulated in humans infected with both organisms, might

contribute to significantly poorer prognosis relative to individuals infected with either pathogen alone.

In addition to effects of antigen-specific type 1 immune responses, *M. tuberculosis* bacilli or mycobacterial components will also have direct effects on local cytokine and chemokine expression profiles in and near pulmonary granulomas. *In vitro* analyses have demonstrated that mycobacterial cell wall components induce the expression of proinflammatory cytokines via TLR-2 and TLR-4 (105,106). Although alveolar macrophages are initially involved in the uptake of *M. tuberculosis*, DC and monocyte-derived interstitial macrophages also phagocytose and process *M. tuberculosis* (107). Interestingly, Lande *et al.* recently demonstrated that *M. tuberculosis* infection of DC leads to induction of CXCL9/Mig and CXCL10/IP-10, the latter in an IFN-αβ-dependent fashion (48).

In this model we have not included other complex factors, such as complex multi-chemokine gradients that lead to simultaneous synergistic or antagonistic signals on cells (108). In addition, there are likely to be negative regulatory activities occurring at the same time. A candidate for such regulation is the lymphocyte cell surface protein CD26 (also known as dipeptidylpeptidase IV), which catalyzes the removal of N-terminal dipeptides from suitable substrates containing a penultimate proline or alanine (109). Cleavage by CD26 differentially affects the activity of specific chemokines, rendering some chemokines inactive and others more potent (109). CD26 proteolytically processes all three CXCR3 ligands, and converts them to antagonists of CXCR3-mediated chemotaxis (110). Determination of the roles played by such complex factors in granuloma formation and maintenance will require further analysis.

To determine whether the immunologic events occurring in granulomatous lesions are due to the abundance of local *M. tuberculosis* bacilli or products, we developed an ISH strategy for the

detection of mycobacterial 16S rRNA directly in tissue sections. Among the strategies previously used for *in situ* detection of *M. tuberculosis*, acid-fast staining is frequently used. However, the sensitivity of this procedure is reduced by the common treatment of tissues with formalin and xylene (111). Overall, we found a relatively low number of foci hybridizing to the mycobacterial 16S rRNA probe in most animals, although two animals with advanced disease had much higher levels of signal. Most of the mycobacterial 16S rRNA ISH signal was localized to the necrotic portion of the granulomas, although some signal was localized to the cellular regions of caseous and solid granulomas. Our probe for detection of *M. tuberculosis* will not discriminate between viable and nonviable organisms, or metabolically active and inactive states of the bacillus, but detects an RNA target that is stable and abundant (112-114). This might explain the different localization of *M. tuberculosis* ISH signal in our study compared to those by Fenhalls *et al.* (115,116), in which ISH signal was localized to cells in the cellular and surrounding regions of the granulomas. Once reaching a certain size or fluidic composition, the necrotic centers of caseous granulomas might provide a hospitable environment for the organism. Further studies with additional probes and tuberculosis cases and stages are required to fully understand the importance of the numbers and states of mycobacterial organisms for granuloma formation and maintenance.

In summary, through the examination of over 300 *M. tuberculosis* induced pulmonary granulomas in experimentally infected cynomolgus macaques, we have demonstrated abundant IFN-γ-inducible chemokine and IFN-γ and TNF-α cytokine mRNA expression within the granulomas. Abundant staining of $CXCR3^+$ cells in the same microenvironments is consistent with recruitment of these cells to the granulomas. These findings, as well as our findings of colocalized *M. tuberculosis* 16S rRNA in the pulmonary granulomas, suggest that the nature of

the type 1 immune response and the direct action of mycobacterial components together lead to the establishment of chronic inflammation. There must be a complex balance between these inflammatory responses, antigen-specific responses, and negative regulatory mechanisms, that determines the extent to which a granuloma contains the bacillus or develops into a structure that allows the organism to multiply and spread within and among hosts. Additional definition of the contributions of IFN-γ-inducible and other chemokines to these processes will elucidate mechanisms by which granulomas successfully limit or eliminate *M. tuberculosis* bacilli. These data will be important for developing additional strategies to combat *M. tuberculosis* morbidity and mortality.

Acknowledgements

We thank Beth A. Fallert and Kelly Whelton for expert technical assistance, Dr. Denise Croix and Dr. Saverio Capuano III for their assistance and care of the animals, Dr. Santosh Pawar for flow cytometric information on granuloma T-lymphocyte populations, and Dr. Francois Villinger for plasmids containing macaque cytokine cDNAs. These studies were supported by NIH grant AI-47485 (JLF).

IV.

INTERACTION BETWEEN DENDRITIC CELLS AND *MYCOBACTERIUM TUBERCULOSIS* IN VIVO AND IN VITRO

The majority of this work was performed by Craig Fuller. The initial in situ hybridizations performed for DC-LAMP, DC-SIGN, DC-STAMP and B7-DC mRNAs on a subset of pulmonary tissues were performed by Kelly Whelton.

A. PREFACE

In this section I have described experiments and data related to DC associated with pulmonary granulomas in cynomolgus macaques infected with *M. tuberculosis*. I have performed ISH and IHC to reveal the DC populations present in the granulomatous lesions. We also performed in vitro studies to determine whether DC were capable of producing the IFN-γ-inducible chemokines in the presence of *M. tuberculosis*. The results indicated that multiple DC-associated mRNAs and antigens are present in the granulomatous lesion and DC are capable of producing IFN-γ-inducible chemokines upon exposure to *M. tuberculosis* and IFN-γ but not after a short exposure (4 hr) to *M. tuberculosis* alone. I also determined that the abundant expression of IFN-γ-inducible chemokines is predominantly by macrophages and not DC. Therefore, I have determined that DC are present within the granulomatous structure, but are not responsible for the ample expression of IFN-γ-inducible chemokines. Interestingly, I did discover the expression of an IL-4-inducible molecule (DC-STAMP/FIND) at the interface between the cellular and acellular region of the granuloma. The function of this molecule is currently unknown. Altogether, these studies reveal that DC are present in granulomas observed in non-human primates and are not responsible for the production of chemokines examined in this study, but may function in the immune response in another manner, such as IL-12 secretion and T cell priming, most likely in draining lymph nodes.

Expression of dendritic cell-associated markers in pulmonary granulomas arising in cynomolgus macaques infected with *Mycobacterium tuberculosis*

Craig L. Fuller[1], Kelly Whelton[1], JoAnne L. Flynn[2] and Todd A. Reinhart[1‡]

Running Title: Dendritic cell-associated markers in pulmonary granulomas

[1] Department of Infectious Diseases and Microbiology, Graduate School of Public Health, University of Pittsburgh, Pittsburgh, PA; [2]Department of Molecular Genetics and Biochemistry, School of Medicine, University of Pittsburgh, Pittsburgh, PA

[‡]Corresponding author and reprint requests: Mailing address: Department of Infectious Diseases and Microbiology, Graduate School of Public Health, University of Pittsburgh, Pittsburgh, PA 15261. Phone (412) 648-2341. Fax: (412) 624-4873. (reinhar@pitt.edu)

B. ABSTRACT

Dendritic cells (DC) are professional antigen presenting cells that bridge innate and adaptive immune responses. DC are responsible for surveillance of mucosal surfaces and the presentation of foreign antigen by DC is a critical step in the immune response. DC have previously been observed in granulomas, including tuberculous granulomas. These cells were identified as $CD11c^+$, $fascin^+$ and $HLA\text{-}DR^+$, but have not been well characterized based on other DC-associated markers. In this study, we characterized a repertoire of DC-associated markers by in situ hybridization (ISH) to understand the composition of DC populations within granulomas. We have found abundant local expression of several DC-associated genes, including a potential surrogate marker for IL-4 production, DC-STAMP. To define the role of DC in local chemokine production, we performed simultaneous ISH/immunohistochemistry (IHC) to determine the cell types producing IFN-γ-inducible chemokines and performed in vitro infections of monocyte-derived DC with *M. tuberculosis* in the presence of IFN-γ or *M. tuberculosis* infection alone. I observed that the majority of the IFN-γ-inducible chemokines were expressed by $CD68^+$ macrophages and not by $fascin^+$ DC, although DC were capable of producing IFN-γ-inducible chemokines upon IFN-γ stimulation, but not after a short *M. tuberculosis* infection alone. These findings further illustrate the presence of DC within the granulomatous structure, but provide evidence that the DC are not responsible for the abundant expression of IFN-γ-inducible chemokines.

C. **INTRODUCTION**

Tuberculosis has been classified as a global health emergency since 1993 by the World Health Organization (WHO) and remains a major public health problem today, causing approximately 2 million deaths each year. Although tuberculosis is a preventable disease and curable in many cases, multiple demographic and socioeconomic factors render prevention and treatment difficult. One-third of the world's population is infected, with 10% of the infected individuals developing active disease, usually within the first two years (117). The remaining 90% of the infected population contain the infection and this clinical latency may persist throughout the life of the individual. Acquired immunity to *M. tuberculosis* involves multiple T lymphocyte subsets, including $CD4^+$ and $CD8^+$ T lymphocytes directed against mycobacterial antigens (29,118).

Dendritic cells (DC) are a heterogeneous population of antigen presenting cells (APC) that are central to the integration of innate and adaptive immunity. DC are present in multiple anatomic sites, including lymphoid organs, afferent lymph, blood and nonlymphoid sites. The nonlymphoid sites include skin, heart, kidney, liver, kidney, gut and lung (51,119), and DC play a major role in the surveillance in these nonlymphoid mucosal sites, which is a large interface between the host and the environment. DC surveillance in these mucosal sites enhances the opportunity for DC to encounter microbial organisms and allows the DC play to initiate and modulate the host's adaptive immune response.

Immature DC, which survey the environment, have high phagocytic activity, but are inefficient at stimulating T lymphocytes (120). DC express many of the germ-line encoded pattern recognition receptors (PRRs) (49) that recognize pathogen-associated patterns. DC maturation occurs in response to pathogen-associated molecular patterns (PAMPs) signaling

through the Toll-like receptors (TLRs) or in response to pro-inflammatory stimuli secreted by cells induced through PAMPs (121,122). Mature DC have increased expression of MHC and costimulatory molecules and migrate from peripheral tissues to the regional lymph nodes, where mature DC efficiently present the captured antigen to naïve T cells and B cells. In addition to presentation of antigen, DC also secrete cytokines and chemokines, while also expressing cell surface costimulatory molecules to coordinate the immune response by serving as a second signal (e.g., B7/CD28 interaction). This efficient cell-cell process may be limited in vivo due to the small percentage of DC in tissues and blood (51). FLT3 ligand (Flt3L)-treatment in mice can preferentially increase the number of functionally active DC in the lung (123), although the Flt3L-treated mice were more susceptible to *Listeria*, an intracellular pathogen (124). These findings support the notion that DC must be properly controlled within the physiological condition to optimize the host defense to an intracellular bacterial pathogen.

Previously, DC have been characterized by surface phenotyping or by immunohistochemical staining for DC-associated antigens and these data revealed that multiple types of DC subtypes existed. The origin of a DC can be categorized as either lymphoid or myeloid. Plasmacytoid DC are believed to be lymphoid-derived and express high levels of CD123 (125). CD123 is the IL-3 receptor α chain, which forms a heterodimer with a β chain to form the IL-3 receptor (IL-3R). IL-3/CD123 interactions promote proliferation and differentiation of multipotential stem cells and of neutrophils, basophils, eosinophils, and monocyte bone marrow precursors (126) and CD123 is constitutively expressed on a variety of hematopoietic cells (126). In contrast, myeloid DC are characterized by the abundant surface expression of the adhesion molecule, CD11c. Although myeloid DC are not the only cell expressing CD11c, the surface expression of CD11c aids in distinguishing DC subtypes.

The maturation of DC involves the increased or altered surface expression of chemokine receptors, MHC molecules, costimulatory and adhesion molecules, as well as reduced phagocytic capacity, and increased morphological changes, cytoskeleton reorganization, secretion of cytokines, chemokines and proteases (51). Immature DC express multiple chemokine receptors including CCR1, CCR2, CCR5, CCR6 and CXCR1 (57). These DC are chemotactically recruited primarily through CCR6 by CCL20/macrophage inflammatory protein (MIP)-3α, but also respond to CCL5/RANTES and CCL3/MIP-1α (57). Upon maturation of DC, CCR6 expression is downregulated and the increased expression of CCR7 on mature DC allows these cells to migrate toward the regional lymph nodes via CCL21/6-Ckine and CCL19/MIP-3β (94).

The surface marker DC-SIGN (DC-specific ICAM-3 grabbing nonintegrin) has been used to classify DC as immature, and functions as an adhesion molecule. DC-SIGN has recently been shown to bind multiple pathogens, including *M. tuberculosis* (53,127-129), thereby serving as a broad-spectrum pathogen recognition receptor (PRR), as well as a potential receptor for pathogen infection of the DC. The binding of *M. tuberculosis* to DC-SIGN may enhance the dissemination of the bacilli to the regional lymph nodes by binding the bacillus and carrying the organism to the lymph node without degrading the pathogen, thus providing access to a compartment outside of the pulmonary cavity.

Another characteristic of DC maturation state is the expression of DC-LAMP/CD208, a lysosome-associated membrane glycoprotein homologous to CD68 (130). DC-LAMP was previously reported to be induced during maturation and was exclusively found in DC and interdigitating DC within the lymphoid organs (130). DC-LAMP was determined to be associated with the MHC class II compartment prior to the translocation of MHC class II molecule to the cell surface and then concentrated in the perinuclear lysosomes, possibly

changing the lysosome function after the transfer of the peptide-MHC class II molecule exits (130).

Another group of surface markers associated with DC maturation/activation is the B7 family. The B7 family members are costimulatory molecules, which deliver critical signals in the T-cell-dependent immune responses initiated by DC. There are five members in the B7 family: B7.1, B7.2, B7-H1, B7h and B7-DC. Two members of the B7 family, B7.1 (CD80) and B7.2(CD86), provide positive costimulatory signals by binding to CD28 or counterregulatory signals by binding CTL-associated antigen (CTLA)-4 on T cells. In contrast, B7-H1, B7h and B7-DC bind PD-1, which is upregulated upon T cell activation (131,132). B7-DC was shown to strongly costimulate IFN-γ production, while not stimulating IL-4 and IL-10 production, suggesting that B7-DC may be an important mediator of Th1 responses (132). The expression of B7-DC was restricted to DC, while the other B7 family members are broadly distributed on multiple hematopoietic and nonhematopoietic tissues (132).

Interestingly, $CD11c^+$ DC have been observed within the granulomatous structures in patients with tuberculosis with a simultaneous reduction in $CD11c^+$ DC in the blood (56). Uehira *et al*., demonstrated that the DC population infiltrating the lymphocyte area of the tuberculous granuloma was $fascin^+$, $CD11c^+$ and $HLA\text{-}DR^+$. In another study, DC pretreated with bacillus Calmette-Guerin (BCG) augmented the polarization of Th1 cells (133), suggesting that trafficking of DC to the site of the granuloma further skewed the immune response toward type 1.

In the studies described in this section, I sought to characterize further the DC population within the granulomatous lesion using DC-associated markers not previously examined in tissues and not applied to an experimental nonhuman primate model of tuberculosis. I also sought to

determine whether DC express CXCR3 ligands upon infection with *M. tuberculosis*, treatment with IFN-γ, or treatment with a proinflammatory inhibitor to IFN-γ responsiveness, IL6. Lastly, I sought to determine whether DC in situ were responsible for the abundant expression of CXCR3 ligands observed in the granulomatous lesions (Fig. 2). These studies have revealed an abundance of DC-associated molecules at the site of the granulomatous lesion, including fascin (p55) mRNA and protein, and CD11c mRNA. I determined that DC were capable of producing CXCR3 ligands upon IFN-γ treatment by 4 hr, but not due to *M. tuberculosis* infection after 4 hr. However, after an 8 hr infection, monocyte-derived DC did produce CXCR3 ligands from *M. tuberculosis* infection alone. Finally, we also revealed that IFN-γ-inducible chemokine mRNAs were predominantly expressed by $CD68^+$ macrophages rather than $fascin^+$ DC within the granulomatous lesion. Although DC may perform an important immune function at the site of the granuloma, macrophages were responsible for the abundant expression of IFN-γ-inducible chemokines associated with granulomatous lesions.

D. MATERIALS AND METHODS

Animals and tissue processing

All animal studies were performed under the guidance and approval of the University of Pittsburgh Institutional Animal Care and Use Committee. Adult cynomolgus macaques were inoculated with a low dose (approximately 25 colony forming units) of virulent *M. tuberculosis* (Erdman strain) via bronchoscope into the lower right lobe, as described elsewhere (70). Infection was allowed to proceed until macaques reached disease states that spanned a spectrum from no apparent disease to advanced disease. At necropsy, tissues were collected and fixed in 4% paraformaldehyde/1X phosphate buffered saline (PF/PBS) for 5 hr at 40^{o}C, as previously described (71). After fixation, the tissues were cryoprotected and snap frozen in isopentane cooled on dry ice to -65^{o}C.

Immunohistochemistry

Immunohistochemical staining of 14μm tissue sections was performed using cell-type specific antibodies for fascin (clone 55K-2, Dako, Carpinteria, CA) and CD68 (clone KP1, Dako). Tissue sections were pretreated in 0.01M sodium citrate (pH 6.0) by microwaving followed by application of the primary antibody (diluted in 1X PBS) to the tissues for 1 hr in a humid chamber at room temperature. Primary antibodies were detected with the PicTure^{TM}-Plus detection system (Zymed Laboratories), using 3,3'-diaminobenzidine (DAB) as the final substrate.

In situ *hybridization (ISH)*

Riboprobe syntheses and ISHs were performed on 14μm tissue sections as described (68,71,72). Cytokine and chemokine mRNAs were detected by ISH using gene-specific riboprobes of DC-associated genes. Plasmids (pGEM-T, Promega, Madison, WI) containing macaque DC-LAMP, DC-SIGN, B7-DC, DC-STAMP, CCR6, CCR7, CD123 and CD11c were generated and sequenced in our laboratory (134). Autoradiographic exposure times were 8 days for DC-LAMP, DC-SIGN, B7-DC, DC-STAMP ISHs and 21 days for CCR6, CCR7, CD123 and CD11c ISHs.

In situ hybridization and immunohistochemistry

In situ hybridizations (ISHs) and simultaneous ISH and immunohistochemistry (IHC) were performed as described (68,71).

Isolation of monocyte-derived DC

Peripheral blood mononuclear cells were isolated from human buffy coats (Central Blood Bank) by Ficoll density gradient centrifugation (Histopaque, Sigma-Aldrich, ST. Louis, MO) or from cynomolgus macaque peripheral blood by Percoll gradient (Amersham Biosciences). $CD14^+$ monocytes were isolated by positive selection using anti-CD14 microbeads, per the manufacturer's recommendations (Miltenyi Biotech, Auburn, CA). The purity of CD14+ cells after enrichment was >93% as determined by flow cytometry. $CD14^+$ cells were cultured in RPMI 1640 media supplemented with L-glutamine, nonessential amino acids, 1M HEPES, 10% heat-inactivated fetal calf serum and penicillin/streptomycin for 5 days; the medium was changed on days 2 and 4.

DC infection with M. tuberculosis

Immature human DC (day 5 culture of monocyte-derived DC) were harvested using 20mM EDTA to remove adherent cells and centrifuged at 1200 rpm for 10 min. The DC were counted and resuspended to a concentration of 1 x 10^6 cells/ml in DC media without antibiotics. The cells were infected with *M. tuberculosis* Erdman strain at an MOI of 4 with or without 100 ng/ml of IFN-γ and 100ng/ml of IL-6. The cultures were incubated in 5% CO_2 at 37^{o}C for 4 or 8 hours. The infected cultures were then centrifuged at 1200 rpm for 7 min at room temperature and the supernatant was removed. The cells were resuspended in 1ml Trizol (Invitrogen Corporation, Carlsbad, CA) and total RNA was isolated by Trizol and chloroform extraction.

Real-time RT-PCR of CXCL9/Mig and CXCL11/IP-10

For each specimen, 400ng of total RNA was reverse transcribed using random hexamers and Superscript II reverse transcriptase (Life Technologies, Carlsbad, CA) in a 100μl reaction. Reverse transcriptase (RT)-negative controls were also performed in parallel with 400ng of each RNA sample. For PCR amplification, 5μl of each cDNA and 50nM of forward and reverse primers for either CXCL9/Mig or CXCL10/IP-10 mRNA were used. β-glucouronidase (β-GUS) was used as the endogenous control to normalize for the input of RNA. The primers were designed using Primer Express software (PE Applied Biosystems) and contained the following sequences: SSRhMigF2 (5'-CAGATTCAGCAGATGTGAAGGAA-3'), SSRhMigR2 (5'-ACGTTGAGATTTTCTAACTTTCAGAACTT-3'), SSRhIP10F4 (5'-TTGCTGCCTTGTCTTTCTGACTCTAA-3'), SSRhIP10R4 (5'-AATTCTTGATGGCCTTCGATT-3'), SSbGUSF3 (5'-CTCATCTGGAATTTTGCCGATT-3') and SSbGUSR3 (5'-CCGAGTGAAGACCCCCTTTTTA-3'). The PCR reactions were cycled at

95°C for 12 min followed by 40 cycles of 95°C for 15 s and 60°C for 1 min on an ABI Prism 7000 Sequence Detection System (PE Applied Biosystems, Foster City, CA) using SYBR Green PCR master mix (PE Applied Biosystems, Foster City, CA). The relative expression levels of CXCL9/Mig and CXCL10/IP-10 mRNA were calculated using the comparative C_T method (135)(Anonymous, ABI Prism 7700 Sequence detection system: relative quantitation of gene expression ([user bulletin #2], 1-36.1997, Norwalk, CT, Perkin-Elmer Corp.), with mock infected DC cultures used as a calibrator.

DC-STAMP expression in cytokine-treated cells by real-time RT-PCR

Rhesus macaque monocyte-derived DC were differentiated in GM-CSF plus either IL-4 or IL-15 (cellular RNAs were provided by Dr. Russ Salter, University of Pittsburgh). Human $CD19^+$ B cells were treated with CD40L and IL-4 (cell cultures were provided by Dr. Charles Rinaldo, University of Pittsburgh). The total RNA was extracted from treated cells by Trizol extraction and SYBR Green real-time RT-PCR was performed as described above using DC-STAMP-specific primers - CLF.DC-STAMP.F2 (5'-TAGATTATCTGCTGTATCGGCTCATTT-3') and CLF.DC-STAMP.R5 (5'-AAGAATCATGGATAATATCTTGAGTTCCTT-3'). β-GUS was utilized as an endogenous control as described above.

E. RESULTS

To characterize the DC populations within the tuberculous granulomas, we examined pulmonary granulomas from cynomolgus macaques, which were inoculated intrabronchially with a low dose of virulent *M. tuberculosis* (Erdman strain). All animals examined in this study were successfully infected and detailed clinicopathological and bacteriological findings have been presented elsewhere (70). These animals varied in their rates and extents of disease progression, but all had macroscopic (gross) lesions within lung tissues at necropsy. The pulmonary granulomas had abundant expression of IFN-γ-inducible chemokines and proinflammatory cytokines (60) and in this study we sought to define the DC population(s) present in granulomas in a relevant nonhuman primate model of tuberculosis. The determination of the type and maturation of DC in these granulomas may further clarify the potential role of DC within the granulomatous structure.

Expression of DC-associated genes in granulomatous lesions

To define the DC populations present in the pulmonary granulomatous lesions, we performed immunohistochemistry and in situ hybridization for multiple DC targets. Given that there are two major types of DC, myeloid and plasmacytoid, we performed ISH for their respective CD11c and CD123 markers to determine whether the DC populations in the lungs were more generally of the myeloid or plasmacytoid lineage. Within granulomatous lesions, we found that CD11c mRNA (Fig. 9A-B) was abundant and was dispersed throughout the granuloma. Previous studies have used CD11c in combination with other markers to label DC; however, some populations of macrophages can also express CD11c. In addition, we examined the expression of CD123

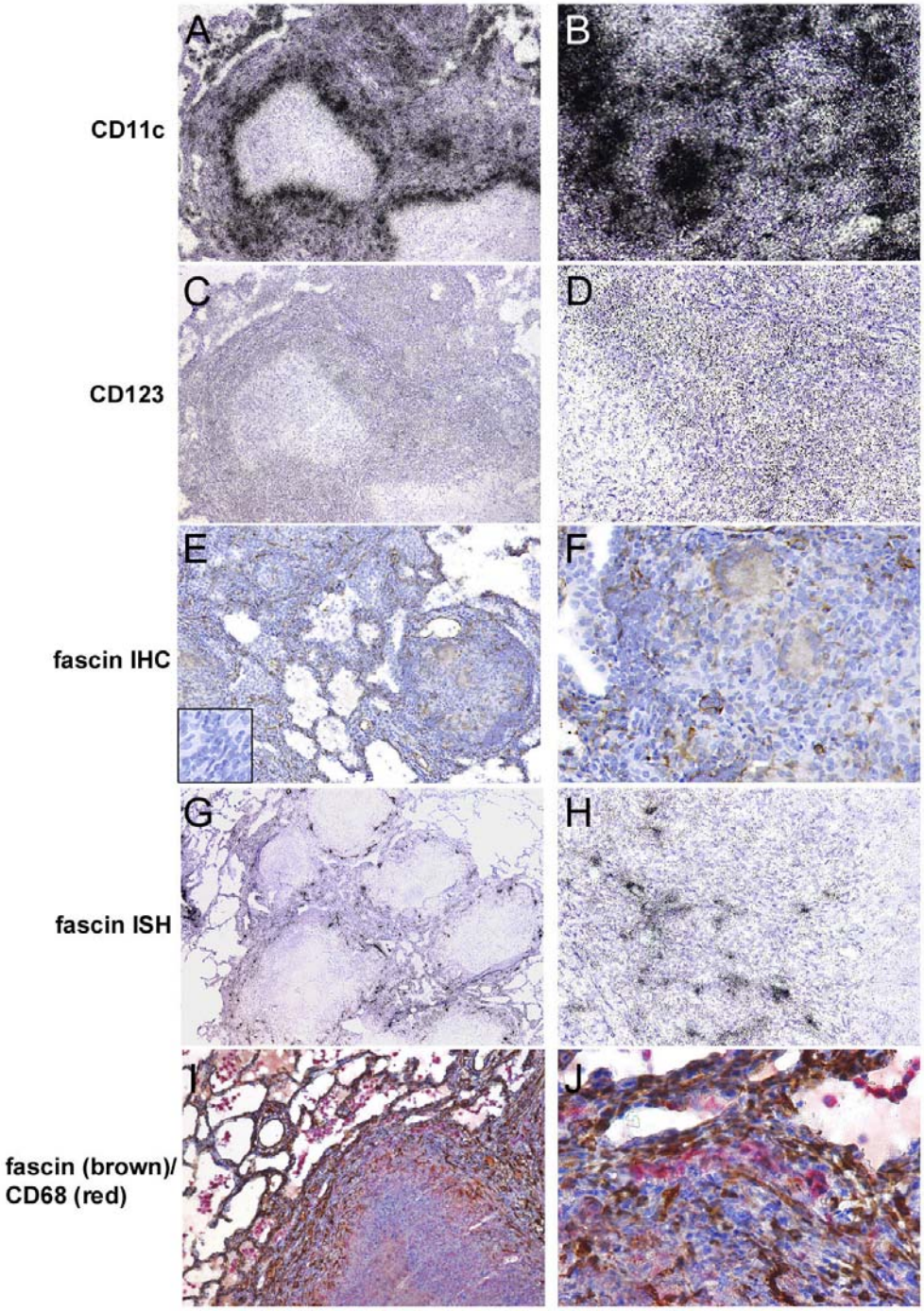

Figure 9. In situ hybridization for DC-associated mRNAs in pulmonary granulomatous tissues from cynomolgus macaques infected with virulent *M. tuberculosis*. The expression of CD11c (A, B) and CD123 (C, D) mRNAs were examined to determine the presence of myeloid and plasmacytoid DC. Fascin-positive cells were also identified in the granulomatous tissues by IHC (E, F) and ISH (G, H), with the isotype control shown (inset, E). The expression of fascin was restricted to DC as shown by double IHC (I, J), with fascin-positive cells (DC, brown) and CD68-positive cells (macrophages, red). Original magnifications, x40 (D, G), x100 (A, C, I), x400 (B, D, F, H), x600 (J).

mRNA (IL-3 receptor α chain), which is expressed abundantly by plasmacytoid DC. We found that CD123 mRNA (Fig 9C-D) was also expressed in the granulomatous lesion and that the expression was dispersed throughout the granuloma, but at a much lower intensity than CD11c (Fig. 9A-B).

Fascin (p55) is a 55kDa protein involved in the formation of microfilament bundles and is expressed by interdigitating and follicular DC within the lymph node (136), and by DC in thymus, spleen and peripheral blood (137,138). Fascin mRNA (Fig. 9G-H) and fascin protein (Fig. 9E-F) had relatively the same distribution patterns in these granulomatous lesions, with staining observed throughout the entire lung tissue. The fascin^{+} cells were distinct from pulmonary macrophages as shown by simultaneous immunohistochemical staining for fascin and CD68 (Fig. 9I-J). Taken together, the mRNA expression of fascin antigen and mRNA suggests that myeloid DC are present in the granulomatous lesions and that the abundant expression of CD11c mRNA is predominantly being expressed by macrophages.

To determine if the DC were the major producers of IFN-γ-inducible chemokine mRNA in the granuloma, I performed simultaneous ISH for chemokine mRNA and IHC for cell-type specific markers. These experiments revealed that CXCL9/Mig and CXCL10/IP-10 mRNAs within granulomas were expressed mainly by macrophages (Fig 10A-B), occasionally by DC (Fig. 10C-D) and not by B cells (Fig. 10E-F).

In addition to identifying DC expressing lineage-specific (CD11c, CD123) and pan-DC (fascin) markers, we sought to obtain data regarding the maturation/activation states of the dendritic cell populations. Previous studies have shown that DC-SIGN is abundantly expressed by immature DC and as the DC captures antigen, matures, and becomes activated, the expression of DC-SIGN decreases (51). DC-LAMP is a lysosomal marker homologous to CD68 in

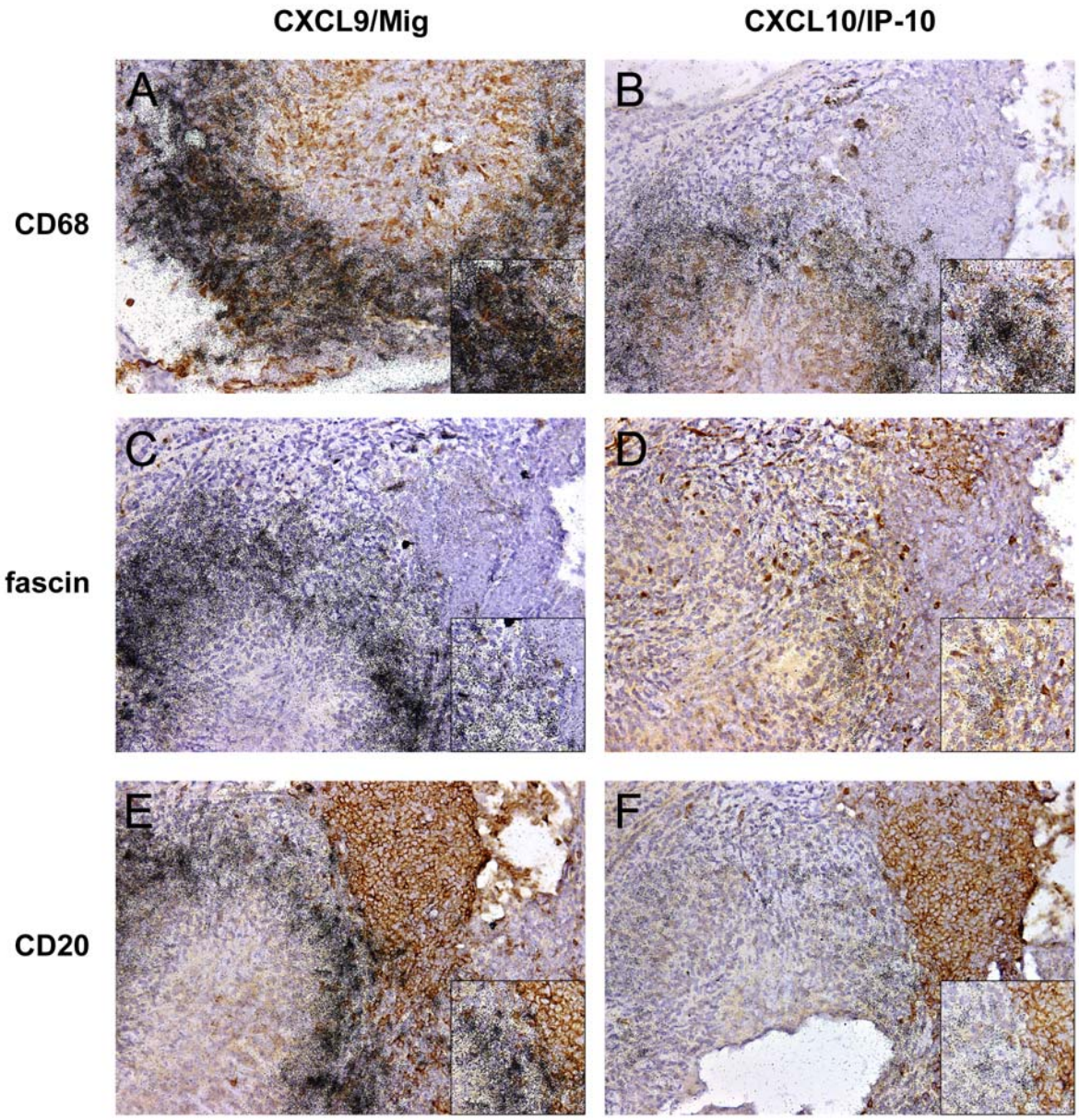

Figure 10. Simultaneous in situ hybridization for CXCL9/Mig or CXCL10/IP-10 mRNAs combined with immunohistochemical staining for macrophages (CD68), DC (fascin) or B (CD20) cells. CXCL9/Mig (A, C and E) and CXCL10 (B, D, F) mRNA was expressed by $CD68^{+}$ macrophages (A, B), less frequently by $fascin^{+}$ DC (C,D) and rarely by $CD20^{+}$ B cells (E, F). Original magnifications, x100 (A-F), x400 (inset) .

macrophages and DC-LAMP expression in DC is increased during maturation and activation (130). We also sought to examine the distribution of mRNA for the costimulatory molecule B7-DC, which is highly restricted to DC and a potential mediator of Th1 response (132).

We performed ISH for DC-SIGN, DC-LAMP and B7-DC mRNAs on these granulomatous tissues. Although previous studies in rodents have shown that pulmonary DC populations have functional characteristics of an immature DC (120), we did not detect any DC-SIGN mRNA within these granulomatous tissues utilizing ISH. However, we were able to detect DC-SIGN mRNA in submucosal areas of the lung tissues (Fig. 11A) and in hilar LN and spleen tissues of these macaques (Fig. 11B). In situ hybridizations for mRNA encoding the lysosomal marker DC-LAMP revealed that (1) DC-LAMP$^+$ cells encircled the granulomas (Fig. 11C) and (2) the ISH signal patterns in the normal lung architecture were consistent with our previous findings in rhesus macaques (139). All granulomas had this characteristic distribution of DC-LAMP mRNA$^+$ cells. The cells expressing DC-LAMP mRNA were abundant on the outside surfaces of the granulomas with a small number of DC-LAMP mRNA$^+$ cells also observed within the cellular portion of the granuloma. These findings suggested that DC were present in and around the granulomatous structure.

However, two recent reports have shown that DC-LAMP protein co-localizes with markers for human type II pneumocytes (140,141). Thus, we examined whether the DC-LAMP ISH signal within the lung was consistent with these previous reports by performing ISH for surfactant B mRNA, which is expressed by type II pneumocytes (142). ISH on subjacent sections for DC-LAMP (Fig. 11D, left) and surfactant B (Fig. 11D, right) mRNAs exhibited the same distribution patterns. These data indicate that the DC-LAMP mRNA expression observed in these tissues is predominantly contributed by type II pneumocytes lining the alveolar spaces or

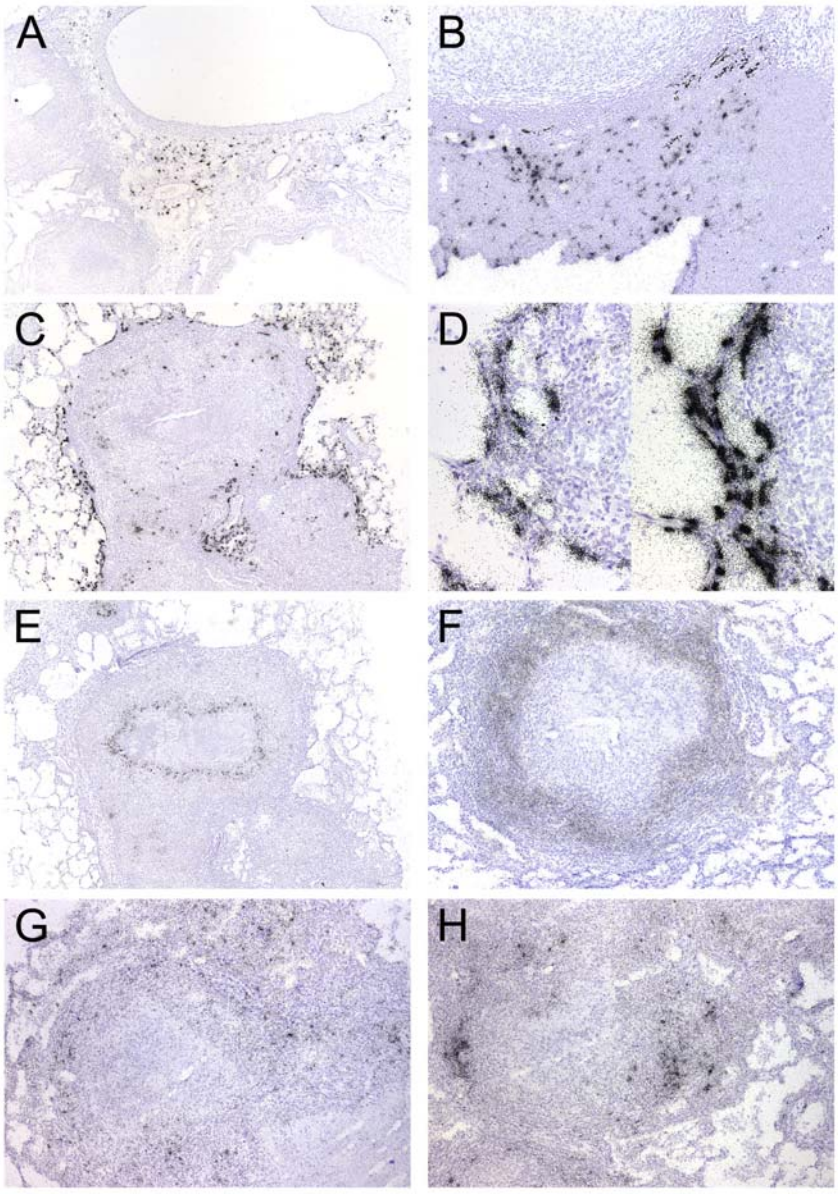

Figure 11. In situ hybridization for additional DC-associated mRNAs in pulmonary granulomatous tissues from cynomolgus macaques infected with virulent *M. tuberculosis*. The expression of DC-SIGN was rare in lung tissues (A) and was more abundant in the medullary sinuses of hilar lymph nodes (B). DC-LAMP $mRNA^+$ cells were abundant surrounding the granuloma and dispersed within the cellular region of the granuloma (C). Further characterization of these cells showed that the DC-LAMP $mRNA^+$ cells (D, left) were colocalized with type II pneumocytes expressing surfactant B mRNA (D, right). DC-STAMP mRNA expression (E) was confined to the interface between the caseation and cellular region of the granuloma, whereas B7-DC mRNA (F) was dispersed throughout the entire granuloma structure, but with increased intensity near the same interface. Focal collections of CCR6 mRNA (G) were spread out over the granuloma, whereas CCR7 mRNA (H) was more focalized to distinct regions of the granuloma. Original magnifications x40 (A, C, E-H), x100 (B), x400 (D).

trapped within the granulomatous structure forming around them, and suggest that there are only few mature DC in the pulmonary granulomas.

Another marker that is expressed by activated DC is the B7 family costimulatory molecule, B7-DC, which is considered to be DC-restricted. Unlike DC-LAMP, B7-DC ISH signal (Fig. 11F) is highly dispersed throughout and did not label distinctive cells, consistent with the cells potentially having numerous intertwining DC processes.

Surveillance of the pulmonary mucosal interface with the external environment is performed by DC characterized by a rapid turnover (143). One of the mechanisms influencing the movement of DC is the interaction between chemokine and chemokine receptors. Immature DC express abundant CCR6, which is signaled by CCL20/MIP-3α, whereas mature DC express CCR7, which is signaled by CCL19/MIP-3β and CCL21/6-Ckine (144,145). Therefore, we sought to determine the mRNA expression patterns of these two chemokine receptors within pulmonary granulomatous tissues using ISH. We detected CCR6 mRNA expression in the lung tissues examined. The expression pattern was dispersed diffusely around the granuloma (Fig. 11G). In contrast, CCR7 mRNA was abundant in the lung tissues, specifically in the granulomatous lesions (Fig. 11H). In addition, CCR6 and CCR7 mRNAs were abundantly expressed in the hilar lymph nodes and the expression was mutually exclusive.

Expression of CCR6 and CCR7 ligands in granulomas from cynomolgus macaques

Maturation and migration of DC from the mucosal surfaces to the regional lymph nodes is associated with their activation (51) and responsiveness to expressed chemokines (146). Immature DC are dispersed throughout peripheral tissues to function as sentinels surveying the sites for foreign antigens. In a study using intranasal delivery of BCG, DC were recruited to the

lungs quickly to induce a type 1 immune response (133). In addition, Legge *et al.*, have demonstrated that respiratory DC have an accelerated migration during the first 24 hr after pulmonary virus challenge, but after that time the DC are refractory to further migration (147). Thus, we sought to determine if chemokines, which specifically recruit immature or mature DC, were present in the granulomatous lesion. Immature DC are characterized as $CCR6^+$, which is the receptor for CCL/20MIP-3α, and the mature DC are characterized as $CCR7^+$, which is the receptor for CCL19/MIP-3β and CCL21/6Ckine. Thus, I performed ISH for CCL/20MIP-3α, CCL19/MIP-3β and CCL21/6Ckine mRNA in the granulomatous tissues of cynomolgus macaques infected with *M. tuberculosis*. Interestingly, we found very few MIP-$3\alpha^+$ cells expressed within the granuloma (Fig. 12A), whereas the CCR7 ligands (CCL19/MIP-3β and CCL21/6Ckine) were more abundant. CCL19/MIP-3β mRNA was expressed as a dispersed signal in the cellular portion of the granulomas and was concentrated just outside the acellular region of the caseation (Fig. 12B). In contrast, ISH signal for CCL21/6Ckine mRNA was intense in specific sites along the outer portion of the cellularity of the granuloma (Fig. 12C). Our laboratory is investigating this expression profile further as we think that CCL21/6Ckine is a suitable marker for lymphatic vessels. While we were unable to show large numbers of immature DC at the site of the granuloma, we also found very little CCL/20MIP-3α mRNA within the granuloma, suggesting that immature DC were not recruited to the existing granuloma structures. However, we found both CCR7 ligands within the granulomatous structure. The distribution of the silver grain patterns is consistent with CCR7 mRNA expression previously described (Fig. 11H), suggesting that mature DC may be present in the granuloma and possibly are expressing these CCR7 ligands themselves. Previously, Krupa *et al.*, found a similar phenomenon in giant cell arteritis, a granulomatous vasculitis, which contained mature DC expressing CCR7. These

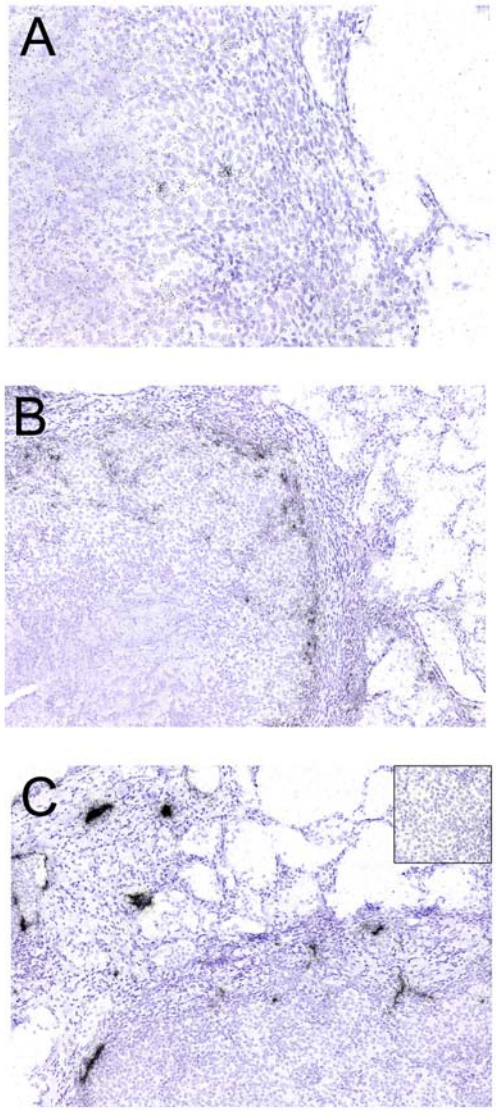

Figure 12. ISH analysis of CCL/20MIP-3α, CCL19/MIP-3β and CCL21/6-Ckine mRNA in the granulomatous tissues of cynomolgus macaques infected with *M. tuberculosis*. CCL/20MIP-3α (A) mRNA was relatively rare within the cellular region of the granuloma. CCL19/MIP-3β (B) mRNA was more abundant and expressed as a dispersed ring on the internal portion of the cellularity of the granuloma. CCL21/6Ckine (C) mRNA was detected as intense focal collections, presumed to identify lymphatic vessels. Original magnifications, x100.

granulomas also abundantly expressed CCL18/pulmonary and activation-regulated chemokine (PARC), CCL19/MIP-3β and CCL21/6Ckine (58). Altogether, their data suggested that DC in granulomas may be trapped and prevented from migrating to the region lymph nodes, thus, maintaining T cell activation and granuloma formation. This may also be occurring in these granulomas, where we detect fascin^{+} DC, CCR7^{+} cells and the CCR7 ligand-producing cells.

Abundant expression of Interleukin-6 within the granulomatous lesion

Interleukin (IL)-6 is a pleitropic cytokine that has roles in the immune response during inflammation, hematopoiesis and the differentiation of T cells. IL-6 has been shown to suppress T cell responses in mycobacterial infections, which may account for unresponsiveness apparent in both human and murine mycobacterial disease (148,149). IL-6 is potentially involved in the initial innate response to *M. tuberculosis* as observed by the increased early bacterial burden and low IFN-γ production following low dose aerosol infection in IL-6$^{-/-}$ mice (150). The development of acquired immunity correlated with mice survival and memory responses remained intact in the IL-6$^{-/-}$ mice (150). A key observation described in the previous studies with IL-6 and *M. tuberculosis* infection is the reduced production of IFN-γ and an increased production of IL-4 in IL-6$^{-/-}$ mice (148). Saunders *et al*., demonstrated that IL-6 is responsible for inducing the production of IFN-γ early in infection, but that IL-6 is not critical to the development of specific immunity to *M. tuberculosis* (150). Interestingly, another study examined the ability of IL-6 secreted by *M. tuberculosis*-infected macrophages to inhibit the responses of uninfected macrophages to IFN-γ, illustrating a bystander effect (151). Therefore, we sought to determine if IL-6 was expressed within the granulomatous lesions using ISH for IL-6 mRNA. We found that IL-6 mRNA expression was abundantly expressed within the cellular

regions of the granuloma (Fig. 13A) and in inflamed lung tissues (Fig. 13B), although IL-6 mRNA expression was virtually absent from the nongranulomatous tissues. These studies in conjunction with previous studies of IL-6 effect on the immune response suggests that IL-6 may be inhibiting the IFN-γ responses of newly recruited, uninfected macrophages, but none of the current studies have examined the potential inhibitory role of IL-6 on DC responsiveness to IFN-γ.

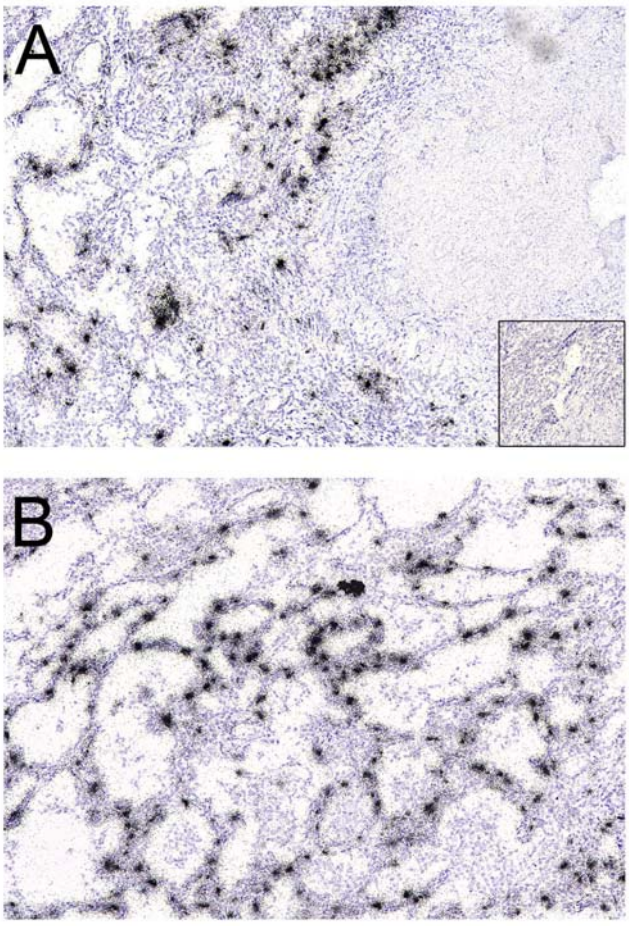

Figure 13. ISH for IL-6 mRNA in lung tissues of cynomolgus macaques infected with *M. tuberculosis.* IL-6 mRNA expression was observed as a focal collection of silver grains in outer portion of the cellular region of the caseous granuloma (A) and in the alveolar walls of the inflamed lung tissue (B) juxtaposed to the caseous granuloma. Original magnifications, x100.

Table 5. Summary of ISH studies performed on granulomas from cynomolgus macaques.

DC-associated marker	Region of the Granuloma[a]		
	External Surface[b]	Cellular[b]	Interface Cellular/Acellular[b]
CD11c	+	++	+++
CD123	+	+	+
DC-SIGN	-	-	-
DC-LAMP	++	+	-
B7-DC	-	+	±
DC-STAMP	-	-	++
CCR6	-	+	-
CCR7	-	+	-

[a]Over 250 granulomas were examined for all eight DC-associated markers in three different lobes from 9 cynomolgus macaques.

[b]ISH analysis was scored as follows: -, no ISH signal, +, rare focal collections or diffuse spray of silver grains observed; +, low intensity of silver grains covering cells; ++, mild intensity of silver grains covering cells; +++, high intensity of silver grains covering cells.

DC-STAMP/FIND is expressed in pulmonary granulomas and is induced upon IL-4 stimulation

DC-STAMP, DC-specific transmembrane protein, is a multi-membrane spanning molecule that was initially described as being expressed preferentially by DC (152). My analysis of related sequences in the GenBank database revealed that FIND was identical in nucleotide sequence. FIND (IL-Four INDuced) was initially described as a transmembrane molecule expressed by mononuclear phagocytes deactivated by IL-4 and not IL-10 treatment (153). Next, I examined the expression of DC-STAMP/FIND mRNA in granulomatous tissues and found that cells expressing this IL-4-inducible mRNA were exquisitely localized to the cellular and acellular interface of caseous granulomas (Fig. 11E), whereas DC-STAMP mRNA was not

observed in the solid granulomas or in normal lung tissue. Given that DC-STAMP and FIND are the same molecule, and that FIND was known to be induced by IL-4 (153), I reasoned that DC-STAMP could potentially serve as a locally expressed surrogate marker for local IL-4 production. In a previous study, IL-4 mRNA could be detected in certain human granulomas (27), but we were not able to detect IL-4 mRNA within these granulomas from cynomolgus macaques. To determine whether DC-STAMP/FIND could serve as a surrogate marker for IL-4 expression, I measured DC-STAMP/FIND mRNA expression in rhesus macaque monocyte-derived DC, which were differentiated in GM-CSF plus either IL-4 or IL-15. By real-time RT-PCR and gel electrophoresis, we detected DC-STAMP mRNA in the cell populations that were derived with IL-4, but not in the IL-15-derived DC (Fig. 14, Table 6). These data confirmed that human monocyte-derived DC using GM-CSF and IL-4 expressed DC-STAMP, as previously reported (152), but that monocytes differentiated without IL-4 did not express this IL-4-inducible molecule. To further examine the potential of IL-4 to induce the production of DC-associated genes in other cells, we examined the ability of freshly-isolated $CD19^+$ cells to express DC-STAMP/FIND mRNA by real-time RT-PCR. We determined that the freshly-isolated human $CD19^+$ B cells were unable to produce DC- STAMP/FIND, but that CD40L and IL-4 treated $CD19^+$ B cells were capable of expressing DC-STAMP/FIND (Table 6). While CD40L treatment has been previously shown to downregulate DC-STAMP in monocyte-derived DC (152), it is possible that IL-4 treatment has overcome the downregulating capacity of the CD40L and IL-4 has induced a mild upregulation of DC-STAMP in $CD19^+$ B cells.

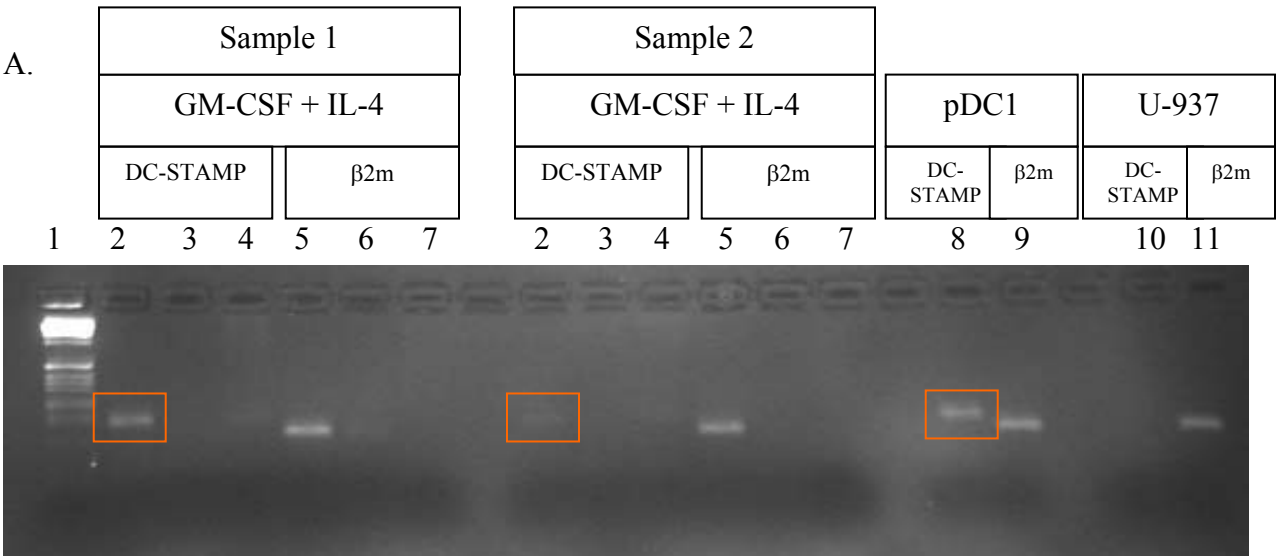

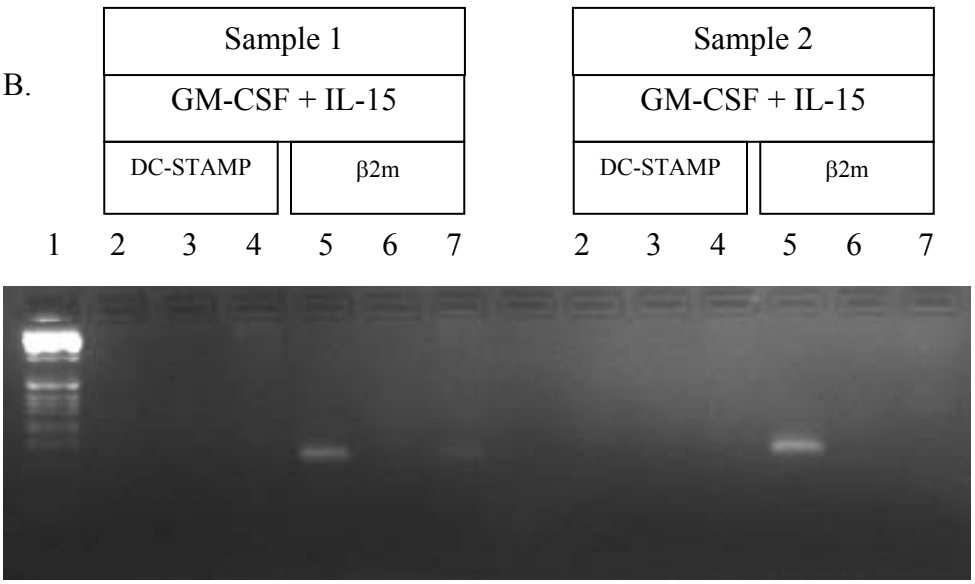

Figure 14. Electrophoretic gel of DC-STAMP/FIND amplification in dendritic cells derived from rhesus macaque monocytes with IL-4 or IL-15. The amplification of DC-STAMP/FIND is observed (red squares, lane 2 and 8, A) in IL-4 derived DC, while DC-STAMP/FIND was not amplified in DC cultures derived with IL-15 (lane 2, B). The 1 kb marker is in Lane 1, rhesus macaque monocyte derived DC derived with GM-CSF + IL-4 (A) in lanes 2-7 or IL-15 (B) in lanes 2-7, rhesus macaque precursor DC1 cells (pDC1)derived with GM-CSF + IL-4 in lanes 8 - 9, and human U937 monocyte cell line in lanes 10-11. Parallel amplification of b2m was performed and observed in lanes 5-7 (A and B), 9 and 11. No reverse transcriptase controls (NRT, lane 6, A and B) and NRT plus genomic DNA controls (lane 7, A and B) were also performed.

Table 6. Real-time RT-PCR analysis of DC-STAMP/FIND expression in rhesus macaque monocyte-derived dendritic cells and human $CD19^+$ B cells.

Sample	ΔC_T[a]	$2^{-\Delta\Delta C_T}$	Band (Electrophoresis)
Dendritic cells[b]			
GM-CSF + IL-4	15.7	1.32	+
GM-CSF + IL-4	16.6	0.71	+
GM-CSF + IL-15	ND[c]	ND	-
GM-CSF + IL-15	ND	ND	-
pDC1[d]	16.1	1.00	+
$CD19^+$ B cells[e,f]			
No treatment	ND	1.00	-
CD40L + IL-4	8.78	>1.12	+

[a] ΔC_T, change in C_T value was provided here if there was no mRNA detected. $\beta_2$microglobulin was used as the endogenous control.
[b] Rhesus macaque monocyte-derived DC were differentiated with GM-CSF plus either IL-4 or IL-15.
[c] ND, not detected after 40 cycles.
[d] pDC1 are precursor DC (lin^-CD11c^+) isolated from rhesus macaque peripheral blood and treated with GM-CSF and IL-4.
[e] βGUS was used as the endogenous control.
[f] To determine the fold change in the DC-STAMP expression for CD40L + IL-4 treatment, we used 40.0 as the C_T value for the freshly isolated human $CD19^+$ B cells, although it was below our level of detection.

Expression of CXCL9/Mig and CXCL10/IP-10 in human monocyte-derived dendritic cells

To determine whether DC could be induced to produce the CXCR3 ligands in response to *M. tuberculosis* infection and/or IFN-γ induction, we derived DC from $CD14^+$ monocytes isolated from human peripheral blood. Human peripheral blood was used instead of cynomolgus macaque peripheral blood, because the number of $CD14^+$ monocytes isolated from macaque peripheral blood was low and the volume of blood we were able to use was limited. The isolated

$CD14^+$ cells were incubated for 5 days in medium supplemented with GM-CSF and IL-4 to induce differentiation into immature DC. On day 5, the monocyte-derived DC were examined for surface phenotype to reveal >95% of the population expressed DC-SIGN, as determined by flow cytometry. The monocyte-derived DC were infected with *M. tuberculosis* (Erdman strain) at a multiplicity of infection (MOI) of 4 for 4h and then RNA was harvested from the infected cells. The expression of CXCL9/Mig and CXCL10/IP-10 mRNA was quantitated by SYBR Green real-time RT-PCR. CXCL9/Mig mRNA was not detectable in the mock and *M. tuberculosis*-infected cultures after 4 hr (Table 4.3), whereas CXCL10/IP-10 mRNA was only upregulated (>5-fold) in two samples of 4 (Table 4.3). Similar to previous studies showing that IFN-γ induces CXCR3 ligand expression (96,154,155), I observed an induction of the CXCR3 ligands (1,900- to 56,000-fold increase) by monocyte-derived DC upon IFN-γ treatment in a dose-dependent manner after a 4 hr *M. tuberculosis* infection. In a preliminary study, we observed appreciable expression of IL-6 mRNA in granulomatous tissues (Fig. 13) and the inhibitory effects of IL-6 on IFN-γ signaling in DC has not been well studied. Therefore, we also treated the monocyte-derived DC with IL-6 to determine if IL-6 treatment would reduce the DC responsiveness to IFN-γ. Interestingly, IL-6 had a mildly suppressive activity on CXCL9/Mig (1.5-fold) and CXCL10/IP-10 (1.2-fold) expression with IL-6 treatment. Taken altogether, these findings reveal that IFN-γ-induced expression of CXCL9/Mig and CXCL10/IP-10 does appear to be influenced by IL-6 treatment of the monocyte-derived DC.

Table 7. Real-time RT-PCR analysis of CXCL9/Mig and CXCL10/IP-10 expression in *M. tuberculosis*-infected dendritic cells.

		CXCL9/Mig				CXCL10/IP-10			
				Mtb-infected				Mtb-infected	
	IFN-γ (μg/ml)	mock	Mtb-infected	IFN-γ	IFN-γ+IL-6	mock	Mtb-infected	IFN-γ	IFN-γ+IL-6
Sample #									
human									
KS84044	10	ND[a,b,c] (1.0)	ND (> 4.5)	> 1,951 (> 5,113)	4,705 (> 3,956)	1.0 (1.0)	ND (> 47)	> 787 (> 4,040)	> 1,314 (> 826)
KJ67282	10	ND	ND	> 5,874	> 5,442	1.0	> 5	> 8,364	> 3,019
KM13687	100	1.0 (1.0)	ND (> 82)	> 56,267 (> 48,645)	32,768 (> 46,988)	1.0 (1.0)	> 5 (> 60)	> 37,381 (> 3,769)	> 28,133 (> 3,795)
KM84905	100	ND (ND)	ND (> 147)	> 11,268 (> 20,032)	8,481 (> 12,590)	ND (ND)	>1.0 (> 2,778)	>24,147 (> 6,165)	>20,757 (> 431)
macaque									
M23102[f]	100	ND	ND	> 4,040	NT[d]	ND	ND	292	NT
M23202[f]	100	1.0	2	NT	NT	ND	3	NT	NT

[a]Fold expression of CXCL9 and CXL10 in monocyte-derived DC after 4hour incubation (8 hr incubation in parentheses) in the presence or absence of *M. tuberculosis* Erdman strain and cytokines.

[b]In order to calculate fold expression changes, a default CT value of 40.0 was used if there was no mRNA detected. βGUS was used as the endogenous control.

[c]ND, not detected.

[d]NT, not tested due to low number of cells in culture.

[f]Only 10^6 cells from cynomolgus macaques were infected at MOI of 4 due to low cell yields.

F. DISCUSSION

In this study we have examined local DC-associated mRNA expression in pulmonary granulomatous lesions resulting from intrabronchial infection of cynomolgus macaques with a low dose of virulent *M. tuberculosis*. Previously, DC within the granulomatous lesion have only been characterized by protein expression of CD11c, fascin and HLA-DR (56). Thus, we have analyzed the mRNA expression profiles of several DC-associated genes by ISH. These studies are the initial analyses of the DC population within a granulomatous lesion using this extensive array of DC-associated markers. Whereas some of these markers may be expressed by cells other than DC, the results here clearly show a wealth of information to further tease out the cell populations present within the granuloma and helps further distinguish between the cells expressing immune molecules. The function of DC within a granulomatous lesion is still unclear, but the presence of IL-12-producing DC within the granuloma (54) and the reported presence of newly arriving DC to the site of the granuloma supports the premise that one role of the DC is to serve as a key initiator of a type 1 immune response (54).

The fascin$^+$ cells and the fascin mRNA$^+$ cells were abundant in the granulomatous lesion (Fig. 9F-H), which are most likely DC. Previous studies have shown that fascin is present in the cell body and dendritic portions of cultured Langerhans cells and the expression of fascin increased in concordance with the maturation of the DC (156,157). Fascin can also be expressed by fibroblasts (158) and neuronal cells (156). Although we cannot definitively state that these fascin$^+$ cells are DC, the morphological structure of these cells does correlate with DC and less so with the fibrin-like structure of fibroblasts encircling the granuloma.

Previously, we have shown that DC-LAMP mRNA expression is present in cells lining the alveolar walls, consisting of approximately 10-15% of the total cells (139). We have also shown previously that DC-LAMP mRNA was abundant in the lymphoid tissue, distributed distinctly from the DC-SIGN mRNA signal (72). Other groups have recently shown that type II pneumocytes also express DC-LAMP in association with the MHC class II molecule, suggesting a similar function in both cell types (140,141). In the macaque tissues examined here we found that DC-LAMP co-localizes with surfactant B, which is a type II pneumocyte marker in the lungs (Fig. 11D). This suggests that the DC-LAMP mRNA we observed in macaque lung tissues and surrounding the granulomatous lesions are likely type II pneumocytes and not DC. While the appearance of DC-LAMP $mRNA^{+}$ cells inside the granuloma is suggestive that mature DC are present within the granuloma, our data also suggest that these are actually type II pneumocytes that became trapped upon the influx of immune cells into the inflammatory site and eventually are completely encased in the growing granuloma.

IFN-γ can stimulate DC to recruit and further activate IFN-γ-producing T cell responses important for cell-meditated immunity (159), whereas the induction of the immune response by IL-4 supports humoral immunity. IL-4 is recognized as a major cytokine in the type 2 immune response, which also inhibits IFN-γ production of type 1 responses. Standard differentiation of DC ex vivo utilizes IL-4 in combination with GM-CSF. GM-CSF supports the survival and proliferation of the DC progenitor, whereas IL-4 contributes to myeloid cell maturation. Interestingly, treatment of maturing DC with IL-4 increases the production of DC-STAMP (152). I observed that DC-STAMP mRNA was localized to the cellular/acellular border of the caseous granuloma (Fig. 11E), but I was unable to detect IL-4 mRNA by ISH (60). Interestingly, monocytes (153) and B cells (Fig. 14) also express DC-STAMP/FIND upon IL-4 stimulation,

suggesting that DC-STAMP/FIND could be used as a surrogate marker for local IL-4 production. IL-4 treatment of monocytes has illustrated a potential mechanism for an amplification loop of polarized Th2 responses (160) and IL-4 treatment also mediates the induction of IL-12p70 in human Th2 cells (161), which could serve to balance type 2 and type 1 responses. By real-time RT-PCR we clearly showed that IL-4, not IL-15, induced DC-STAMP in monocyte-derived DC (Fig. 14) and IL-4 induced DC-STAMP expression in B cells (Table 6). Whether IL-4 is contributing to a deactivation of the type 1 immune response in these tissues is still unclear, but treatment of maturing DC with IL-4 has shown a reduced responsiveness to CD40 stimulation (162) and CD40L treatment revealed a 10-fold decrease in DC-STAMP expression (152). DC-STAMP/FIND is a protein with an N-terminal signal anchor of 52 amino acids, seven transmembrane regions, one intracellular loop and two extracellular loops, which have three putative N-glycosylation sites, and a cytoplasmic C-terminus (153). This putative protein also contains several potential myristoylation and phosphorylation sites, a phospholipase A2 site and a G-protein β WD-40 repeat, a 40-residue domain containing a characteristic Trp-Asp motif (genome.ucsc.edu). The G protein β subunits do not have a clearly defined function, but seem to be required for the replacement of GDP by GTP and in membrane anchoring and receptor recognition (163). All of these findings suggest that DC-STAMP/FIND may be enhanced due to a type 2 cytokine and potentially could function as a receptor subunit to downregulate the type 1 immune response locally.

Mathematic modeling of *M. tuberculosis* infection suggests that DC are necessary for the development of protective immunity against *M. tuberculosis* (164) and are likely involved in the control of the granuloma, possibly by aiding in granuloma formation. DC-recruiting chemokines have been observed in granulomas of giant cell arteritis and potentially are responsible for the

continual presence of DC at the site of inflammation (58), and we have observed that tuberculous granulomas also have cells expressing CCL19/MIP-3β and CCL21/6Ckine mRNA (Fig. 12) and numerous dendritic cell markers (Fig. 9 and 11). The most convincing data within these studies are the fascin^{+} cells by ISH and IHC illustrating the abundance and distribution of the DC within granulomatous structures. It is true that the DC play a major role in the establishment of the immune response and that a rapid DC turnover at the site of infection combined with a strong activation of DC will lead to a minimal antigen presentation and lead to the production of cytokines responsible for a protective response.

Acknowledgements

We thank Beth A. Fallert, Kelly Whelton and Adam Straub for expert technical assistance, Dr Holly Scott Algood and Amy Myers for their assistance and advice with infections, Drs. Philana Lin and Saverio Capuano III for their assistance and care of the animals. We would also like to thank Drs. Charles Rinaldo, Jr., Russell Salter and Angus Thomson for providing cellular RNAs. These studies were supported by NIH grant AI-47485 (JLF).

V.

FINAL DISCUSSION

Tuberculosis is a worldwide epidemic that is continually causing deaths and is a major AIDS-related complication. Although a large amount of research has attempted to elucidate ways to understand, control and prevent *M. tuberculosis* infection, the processes of disease are not well understood. Tuberculosis is characterized by a predominant type I immune response, which has high levels of IFN-γ and proinflammatory cytokines. The objective of this body of work was to define the potential roles of IFN-γ-inducible chemokines and proinflammatory cytokines in the granulomatous tissues of cynomolgus macaques infected with *M. tuberculosis*, while examining the putative roles of DC in these processes. We have utilized single-cell based techniques to analyze the expression of chemokine and proinflammatory cytokine mRNAs and to determine what cell types are expressing these mRNAs. In addition, we also have utilized these single-cell based assays to examine the expression of DC-associated transcripts in an attempt to define the DC populations present within the granulomatous structure. Since CXCR3 ligands can be induced by IFN-γ stimulation of DC, we also examined the ability of DC to express these CXCR3 ligands and whether DC are the major producer of the abundant CXCR3 ligand expression.

Abundant IFN-γ-inducible chemokine expression

In these studies, we determined that the granulomas are the site of an abundant expression of IFN-γ-inducible chemokines and proinflammatory cytokines. Other cytokines consistent with IFN-γ expression, or a type I immune response (such as CCR5 ligands), were also observed. Whereas macrophages and lymphocytes were the predominant cells within granulomatous tissues, we did observe a considerable number of B cells and DC within the granulomatous structure. We also observed a large number of DC-associated transcripts, which are associated with different maturation and activation states. Although DC were capable of producing CXCR3 ligands upon IFN-γ stimulation in vitro, the majority of CXCR3 ligand mRNAs associated with the granuloma were expressed by $CD68^+$ macrophages rather than by $fascin^+$ DC (Fig. 9).

The CXCR3 ligands are IFN-γ-inducible chemokines, which are observed in type I immune responses and CXCL10/IP-10 can be upregulated upon innate activation, such as through Toll-like receptors (TLRs). IFN-γ-inducible chemokines were abundant in granulomas and the expression level of CXCR3 ligand was proportional to the granuloma size, but the signal intensity of each chemokine was relatively similar when the signal intensity/cellular area of solid granulomas was compared to caseous granulomas. Although no direct association was shown between the number of IFN-γ $mRNA^+$ cells and/or TNF-α $mRNA^+$ cells with increasing amounts of CXCR3 ligand mRNA expression, this is likely due to the fact that the granuloma sections we observed were 14μm sections of a much larger three-dimensional histological structure in the lung. If we had observed mRNA expression profiles from a disaggregated granuloma, we likely would be able to measure a potential association more accurately. The number of IFN-γ $mRNA^+$ and TNF-α $mRNA^+$ cells were approximately three times more numerous in the caseous

granulomas than in the solid granulomas (Table 3), and the average size of the caseous granulomas were also approximately three times the size of the solid granulomas. This potentially explains the three-fold difference in the cytokine mRNA, which appears in a dispersed pattern, and the same thresholded values obtained via quantitative image analysis of chemokine mRNA, which are extremely abundant.

The IFN-γ-inducible chemokines have been shown to inhibit bone marrow colony formation (165), possess antitumor activity in vivo (166-168), promote T cell adhesion to endothelial cells (169,170), and inhibit angiogenesis (171,172). The increased expression of angiogenic molecules, such as vascular endothelial growth factor (VEGF) is significantly correlated with active pulmonary tuberculosis (84,173,174). Thus, the abundance of IFN-γ-inducible chemokines recruit immune cells to aid in the immune response, but also work to counterregulate inflammatory events, such as neovascularization. Interestingly, Cole *et al*., have shown that IFN-γ-inducible chemokines have defensin-like antimicrobial activity against *Escherichia coli* and *Listeria monocytogenes* (175). These studies also showed that the concentration of IFN-γ-stimulated chemokines produced by PBMC was sufficient for antimicrobial activity suggesting that the IFN-γ-inducible chemokines may inhibit certain microbes in addition to the recruitment of immune cells to the site of inflammation (175). To this end, IFN-γ-inducible chemokines could also be antimycobacterial.

Additionally, the CXCR3 ligands are antagonists for CCR3, which is characteristically expressed by Th2 lymphocytes, thereby inhibiting the migration of $CCR3^+$ cells toward ligands, such as CCL11/eotaxin-1, though without causing internalization of CCR3 (176). Therefore, chemokines that attract Th1 cells via CXCR3 can concomitantly block the migration of Th2 cells in response to CCR3 ligands, thus further enhancing the polarization of the local environment.

CXCL11/I-TAC also has an additional interesting characteristic potentially relevant to tuberculosis and granuloma formation. CXCL11/I-TAC also binds to CCR5 and blocks migration of $CCR5^+$ cells, as well as inhibits the release of intracellular calcium and actin polymerization by CCR5 ligands (177). Thus, CXCL11/I-TAC likely has a different set of overlapping functions relative to CXCL9/Mig and CXCL10/IP-10. Although CXCL11/I-TAC has a higher binding affinity for CXCR3 compared to CXCL9/Mig and CXCL10/IP-10 (178), competitive binding studies have revealed that these IFN-γ-inducible chemokines are allotropic, or noncompetitive, ligands for CXCR3 (179). In addition to these studies, CXCL11/I-TAC-induced internalization of surface CXCR3 was significantly increased compared to the other two CXCR3 ligands (97) and CXCL11/I-TAC used a distinct domain in the CXCR3 molecule compared to CXCL9/Mig and CXCL10/IP-10 (180). These findings suggest that the differential requirement of these domains contributes to the complexity of the chemokine system and further suggest that true chemokine redundancy may not be operative in vivo.

Type 1 amplification loop

The identification of abundant expression of the IFN-γ-inducible chemokines and the proinflammatory cytokines directly in the granulomatous lesion is a novel observation. In addition, we also sought to determine the cell types expressing these immune molecules. Simultaneous ISH and IHC revealed that the CXCR3 ligands were produced most predominantly by $CD68^+$ macrophages, to a lesser extent by $fascin^+$ DC, and not by $CD20^+$ B cells (Fig. 10). Although previous studies have shown that macrophages, DC and B cells are all capable of producing CXCR3 ligands upon IFN-γ stimulation (96,181), we determined that the major producers of the IFN-γ–inducible chemokines in the granulomatous lesions were macrophages.

This is not unexpected since the predominant cell types in the granuloma are macrophages and T lymphocytes (164). Induction by the large amount of IFN-γ in the granulomatous lesion and the fact that macrophages can produce CXCR3 ligands upon *M. tuberculosis* infection (34) likely explains the massive expression of CXCR3 ligands in the granuloma. In a type 1-mediated pulmonary disease, the local expression of IFN-γ-inducible chemokines likely induces the trafficking of effector T cells and monocytes to the inflammatory site within the lung tissues, which leads to a local chronic inflammation in the lungs. This influx of activated type 1 immune cells further enhances the IFN-γ production and further amplifies this process producing an IFN-γ-driven positive feedback mechanism (Fig. 15). This amplification loop of chemokine production/IFN-γ-producing cell recruitment has been previously discussed in the context of SIV (68) and may represent the same amplification processes seen in tuberculosis and possibly in other type 1 diseases. Whereas the increased recruitment of IFN-γ-producing cell recruitment is important in the immune response to tuberculosis, an uncontrolled amplification loop potentially can lead to more devastating outcomes, such as tissue destruction.

Potential chemokine-altering molecules

The CXCR3 ligands recruit $CXCR3^+$ cells, which are predominantly activated IFN-γ-producing T cells (93,96,175,182,183). This massive expression of type 1 recruiting molecules further amplifies the recruitment signal into the inflammatory site. Although we studied the expression levels at the mRNA level, it was not determined whether or not the respective proteins were expressed or were functional. Multiple attempts in our laboratory to stain for CXCL9/Mig protein in tissue sections has not yielded conclusive results. Molecules such as CD26 or matrix metalloproteinases (MMPs) have the ability to counterregulate chemokine

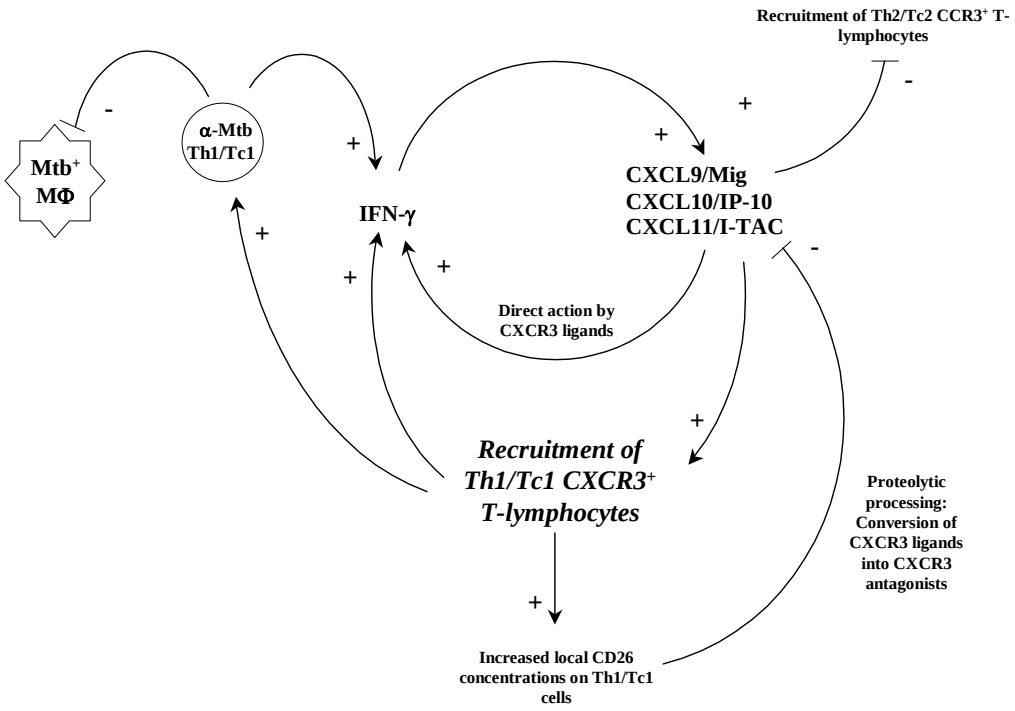

Figure 15. Proposed model for type 1 amplification loop in tuberculosis. Infected macrophages secrete chemokines, which attract IFN-γ-producing lymphocytes. The increased expression of IFN-γ leads to an increased production of CXCL9/Mig, CXCL10/IP-10 and CXCL11/I-TAC. The increased expression of the CXCR3 ligands recruits more IFN-γ-producing $CXCR3^+$ cells, which further upregulate the expression level of CXCR3 ligands. In addition, CXCR3 ligands also negatively impact the recruitment of $CCR3^+$ cells. The increased recruitment of CXCR3+ cells is associated with CD26 expression, which proteolytically cleaves CXCR3 ligands and converts them into CXCR3 antagonists.

---

function. CD26 is a dipeptidyl peptidase that cleaves behind the proline residue at the penultimate N-terminal amino acid position, altering the efficiency of chemotactic recruitment of a subset of chemokines (184). CD26 cleaves multiple chemokines, affecting their chemotactic potential differently, and has been shown to reduce the chemotactic potential of CXCL9/Mig, CXCL10/IP-10 and CXCL11/I-TAC (110). Preliminary studies performed in our laboratory have shown an abundant expression of CD26 mRNA associated with granulomatous tissues compared to normal lung tissues (data not shown). Interestingly, when the first two N-terminal amino

acids are truncated, CXCL11/I-TAC becomes a potent antagonist for CXCR3 (110). Therefore, N-terminal truncation is a potential feedback mechanism to help control the amplification loop that may develop in a recruitment schematic similar to this type I-dominated immune response.

Another chemokine-altering group of molecules is the family of MMPs, which are associated with extracellular matrix degradation and enzyme processing of bioactive molecules. Gelatinase A (MMP2) and B (MMP9) have been shown to cleave multiple CC- and CXC-chemokines with varying effects. Gelatinase B/MMP9 cleaves ELR^+ (Glutamic acid-Leucine-Arginine) CXC-chemokines in the amino terminus, but MMP9 has been shown to degrade CXCL10/IP-10 and cleave CXCL9/Mig at three locations in the carboxyterminus (185), neither of which are ELR^+ chemokines. Whereas basic residues at the carboxyterminal end of CXCL10/IP-10 are essential for the binding of CXCL10/IP-10 to CXCR3, these residues are less important for the binding to negatively charged polysaccharides (186). The carboxyterminal truncation of CXCL9/Mig greatly decreased its biological activity (181,187) and its ability to be immobilized through binding to extracellular matrix polysaccharides, which is a component of the chemotactic gradient (181). Thus, the MMPs, which are abundantly expressed in inflammatory tissues by the infiltrating cells, may be able to diminish or abolish the chemotactic potential of the CXCR3 ligands within these granulomatous lesions.

Expression of CCL5/RANTES, CCL3/MIP-1α, and CCL4/MIP-1β mRNAs in granulomas

Activated type 1 cells and macrophages are recruited to the site of inflammation through the receptor CCR5 (93). The CCR5 ligands, CCL5/RANTES, CCL3/MIP-1α, and CCL4/MIP-1β, were also expressed in the granulomatous tissues studied here, as determined by ISH (Fig. 8). The CCR5 ligands were concentrated within the granulomatous structures, although not to the

same levels as the CXCR3 ligands, whereas the CCR5 ligand mRNAs were virtually absent in the nongranulomatous regions of lung tissue. The increased expression of these chemokines, in addition to the abundant CXCR3 ligand expression, further suggests an overwhelming recruitment of immune cells capable of producing type 1 or pro-inflammatory cytokines, including activated Th1 cells, cytotoxic T cells, macrophages and DC. These findings further support the notion that the granulomatous environment contains numerous signals directing the recruitment of type 1 immune cells that are capable of producing IFN-γ, which can lead to further upregulation of CXCR3 ligands or to antimycobacterial actions by macrophages.

Potential inhibition of DC by Interleukin 6

Another important cytokine in the inflammatory process is IL-6. IL-6 has systemic and local properties that include activation of acute phase proteins, recruitment of neutrophils to inflammatory sites, activation of lymphocytes, and induction of fever. The differentiation of B cells into plasma cells and the differentiation of naïve T cells into Th2 cells are also activities attributed to IL-6 (188). We have observed IL-6 mRNA as abundantly expressed within pulmonary granulomas (Fig. 13) and previous studies have shown that IL-6 secreted from *M. tuberculosis*-infected macrophages has inhibited a subset of IFN-γ-responsive genes, including IFN-γ-inducible class II trans-activator (CIITA), CXCL9/Mig and IFN regulatory factor (IRF)-1 (151). Although previous studies have shown an increased expression of IL-6 upon *M. tuberculosis* or BCG infection of DC (85,86,189,190), no reports have shown the effects of IL-6 on DC responsiveness to IFN-γ. We examined monocyte-derived DC for their ability to produce IFN-γ-inducible chemokines upon *M. tuberculosis* infection and in the presence of IFN-γ or IFN-γ plus IL-6. We found that IL-6 during *M. tuberculosis* infection reduced CXCL9/Mig and

CXCL10/IP-10 expression (Table 7). Whereas this reduction of CXCL9/Mig (1.5 fold reduction) is similar to the studies in macrophages performed by Nagabhushanam *et al.*, DC may not be as responsive to IL-6 as macrophages. CXCL10/IP-10 was not significantly different in the previous study. The ability of IL-6 to inhibit IFN-γ-induced genes may also contribute to the host's inability to mount an appropriate cellular immune response sufficiently to eradicate infection. Reduction of other IFN-inducible genes may have a detrimental effect on the overall immune response. For example, the reduction of IRF-1 by IL-6 would lead to TNF-α-mediated activation of MMP-9 (191), which cleaves the carboxyterminus of CXCR3 ligands, as mentioned above, ultimately reducing the ability of CXCR3-ligands to bind to the extracellular matrix and form a chemotactic gradient.

Early granulomatous structures

Although many studies have attempted to elucidate the molecules responsible for the maintenance of a granuloma, we wanted to examine pulmonary tissues of *M. tuberculosis*-infected macaques for early stages of granuloma formation. Eight cynomolgus macaques were infected with *M. tuberculosis* Erdman strain and were sacrificed at weeks 3, 4, 5 or 6 p.i. The hilar lymph nodes and three lobes of the lung were analyzed for early granulomas (or pregranulomas) by hematoxylin/eosin (H/E) staining and ISH for mycobacterial 16S rRNA and CXCL10/IP-10 mRNA on 14μm sections every 280μm over a total of 2,800μm of lung tissue. We used these markers to examine the lung tissues for potential accumulations of either mycobacterial rRNA or chemokine mRNA, as an indicator of potential pregranulomatous structures. Unfortunately, we did not observe any pregranulomatous structures, but we did observe a caseous granuloma in the right lower lobe of M21902 and in the left hilar lymph node

of M24102 (both of which were sacrificed at 5wk post-infection). Whereas the ISH studies on these granulomas were concordant with our previous findings (Fig. 2, Table 3), there was an abundance of mycobacterial 16S rRNA within the granuloma from the lymph node compared to the pulmonary granuloma. In addition, the granuloma within the hilar lymph node had slightly higher CXCL10/IP-10 compared to CXCL9/Mig (Fig. 7). This was in contrast to our previous findings that CXCL9/Mig was the most abundant IFN-γ-inducible chemokine in more developed granulomas. This higher expression level of CXCL10/IP-10 was consistent with murine studies performed in which CXCL10/IP-10 was observed as early as 3 days p.i. and CXCL9/Mig was not observed until 6 days p.i. and only in a proportion of mice (87). In addition, Algood *et al*., also examined the effect of anti-TNF treatment on chemokine expression (87). The anti-TNF treatment caused a reduction in the expression of the two CXCR3 ligands further suggesting that TNF-α may have an inductive effect on local chemokine expression prior to granuloma formation.

Dendritic cell-associated studies

The studies described in Chapter IV have expanded the current knowledge of the populations of DC within the granuloma. Previous studies have suggested that DC in the lung tissues are immature in function, but we were not able to detect the immature DC marker, DC-SIGN. The expression level of DC-SIGN on immature DC in the lung may have been below the level of sensitivity of the assay, but this is unlikely since we were capable of detecting DC-SIGN in hilar lymph node and spleen of these macaques by ISH. Interestingly, DC-LAMP mRNA was abundantly expressed in and around the granulomatous structure, and we have previously shown that approximately 10% of the cells in rhesus macaque lung tissues express DC-LAMP mRNA

(139). This initially led us to believe that mature DC were extremely abundant and possibly forming a protective "surveillance" barrier around the granuloma. However, two recent studies (140,141) and our ISH studies for surfactant B mRNA (Fig. 11) have revealed that the DC-LAMP$^+$ cells in the lung tissues are actually type II pneumocytes. This contradicts our theory of DC forming a barrier around the granuloma, and brings into question why type II pneumocytes are so abundant around and within the cellular region of the granuloma. The most logical reason is that the granuloma forms and begins to expand into the lung alveoli and the type II pneumocytes become trapped on the inside and outside of the granulomatous structure.

Mature DC have been shown to preferentially express CCR7 (94) and we found the ISH signal for CCR7 mRNA concentrated within regions of the granuloma (Fig. 11), as was ISH signal for CCR7 ligands within the same regions (Fig. 12), suggesting that mature DC could be present within the cellular region. This is consistent with our fascin immunohistochemical staining and ISH findings (Fig. 9). Interestingly, B7-DC was abundantly expressed within the granuloma and this expression of B7-DC could play either a costimulatory or inhibitory role. Initial studies have not clarified whether B7-DC inhibits the stimulation of T cells by binding to the inhibitory receptor, programmed death (PD)-1 (192), or whether B7-DC costimulates T cell proliferation and cytokine production, such as IFN-γ (132). Previous studies have shown that cross-linking B7-DC with a naturally occurring antibody directly activated immune function in the DC (193), but recent studies have revealed that antibody binding of B7-DC augments T cell stimulation and results in the inhibition of a negative signal (194). PD-1 is a known inhibitory receptor of T cells (131) and B cells (195), and Chemnitz *et al.*, have shown that inhibition of T cell activation occurred with the apparent colocalization of PD-1 with CD3 and/or CD28 (196). Their data suggest that the T cell stimulation observed in the B7-DC studies was due to the

suboptimal levels of anti-CD3 used (132). This inhibitory action on T cell activation could be a further regulation of the immune response to prevent T cell anergy or T cell exhaustion.

Development of mycobacterial 16S rRNA ISH assay

Acid-fast staining is routinely used in laboratories to identify the presence of acid-fast bacilli (AFB) organisms in the sputum, BAL, and pleural effusions, but our initial efforts to stain for AFB in paraformaldehyde-fixed tissues had little success even though the lesions seemed histologically active. Previously, Fukunaga *et al.*, revealed that formalin and xylene greatly reduced the sensitivity of acid-fast staining and the numbers of bacilli estimated by real-time PCR were considerably higher than those counted manually with a microscope. These results suggest that the bacilli are frequently missed or underestimated with acid-fast microscopy on formalin-fixed, paraffin-embedded tissue (111). In an attempt to increase the sensitivity of *M. tuberculosis* detection in our paraformaldehyde-fixed tissue sections, I developed an ISH assay, which detected mycobacterial 16S rRNA, alpha-crystallin (*hspX*) and RNA polymerase beta subunit (*rpo*B). We did not detect *hspX* mRNA, which is a surrogate marker for latent infections (197), or *rpo*B mRNA, which is expressed during active replication (198), but we did detect mycobacterial 16S rRNA in granulomatous tissues. Although this 16S rRNA assay will also detect other mycobacterial 16S rRNA due to high levels of sequence similarity, lung tissue sections from uninfected controls and from nongranulomatous tissues had no detectable ISH signal for mycobacterial 16S rRNA. This is in contrast to the intense focal collections of silver grains observed in many granulomas observed in the lungs of cynomolgus macaques infected with *M. tuberculosis*. The main limitation of this assay is the possibility that this assay may also detect extracellular mycobacterial rRNA or dead mycobacteria, although it needs to be noted that

these nonviable mycobacterial components likely still have very potent biological activity. Even though this limitation exists, it is likely that the immune cells are recruited to the granulomatous lesion in an attempt to control the infection or remove the antigenic stimulation. Therefore, the assay described in this dissertation overcomes the limitations of certain fixation protocols and provides an increased level of specificity due to the RNA:RNA hybrids within the ISH assay.

Type 2 immune response in granulomatous lesions

In addition to examining type 1-associated chemokines, we also examined the expression of CCL2/monocyte chemotactic protein (MCP)-1, which is a chemokine regulated by Th2 cytokines, IL-4 and IL-13. Interestingly, CCL2/MCP-1 can stimulate IL-4 production and CCL2/MCP-1 overexpression is associated with defects in cell-mediated immunity (199-202). Although not strictly a "type 2 chemokine", these data are consistent with a potential role for CCL2/MCP-1 in type 2 processes. In the left hilar lymph node of a 5 wk post-infection cynomolgus macaque (M24102), a granuloma was observed in the hilar lymph node that expressed CCL2/MCP-1 mRNA, which had a higher signal intensity than CCL5/RANTES. The mRNA signal consistently was surrounding the perimeter of the caseous granuloma (Fig. 8). This particular granuloma also had high expression levels of CXCL9/Mig, CXCL10/IP-10, IFN-γ and TNF-α mRNAs in the cellular portion in addition to an abundant level of mycobacterial 16S rRNA within the central (acellular) portion of the granuloma (Fig. 7). Although it is unclear what role CCL2/MCP-1 may play during this early timepoint, it is interesting that we observed both type 1 cytokines and chemokines and a potentially type 2 chemokine present at such an early stage of the infection. This illustrates an early time in the immune response showing that IFN-γ and other type 1 molecules can be abundantly present early after infection, thereby contributing

to a predominant type 1 immune response. However, our study did not resolve whether IL-4 might have acted in a protective role in mycobacterial infection, as seen in conflicting reports in IL-4 knock-out mice (203,204), but does raise the question of the presence of these IL-4-inducible molecules and what potential function these molecules may have.

Putative model of DC-STAMP/FIND involvement in tuberculous granuloma

Interleukin-4-induced expression of DC-STAMP/FIND was initially described concurrently by two different groups studying DC and macrophages, respectively (152,153). In addition, my studies revealed that DC-STAMP/FIND expression was observed by real-time RT-PCR in DC and B cells derived or stimulated with IL-4 (Fig. 14) and DC-STAMP/FIND mRNA was exquisitely localized to the interface between the cellular and acellular portions of caseous granulomas (Figure 11E). It should be noted that thus far IL-4 is the only cytokine demonstrated to induce expression of DC-STAMP/FIND. IL-10 (153) and IL-15 (Table 6, Fig. 14) do not induce DC-STAMP/FIND expression. We did not detect IL-4 mRNA in any of the macaque tissues, but the level of IL-4 expression may have been below the level of detection in our assay. Frequently, IL-4 protein can not be detected by ELISA due to the very low concentrations and only the effects of IL-4-neutralizing antibodies are assessed (205). In addition, IL-4 has a low mRNA copy number and IL-4 mRNA has a short half-life (206,207), suggesting that detection of IL-4 mRNA would be extremely difficult without the immediate use of an mRNA stabilizing buffer. In fact, only one group has been able to detect IL-4 mRNA in granulomatous tissues (27,208,209) and conclusions from their findings suggest that IL-4 may be involved in reducing the amount of tissue damage by acting as an anti-inflammatory molecule at the local site.

Interestingly, CD1d-restricted T cells (NKT cells) are innate memory cells activated by glycolipid antigen and play important roles in the initiation and regulation of the immune response and secrete large quantities of cytokines, including IL-4 as well as IFN-γ (210). NKT cells can influence various immune responses, including tumor rejection, the maintenance of self-tolerance, autoimmunity and the response to infectious agents (210). Although pulmonary granulomatous lesions are not significantly different in NKT knock-out mice compared to wild-type (211) and Vα14 NKT cells contribute only minimally to the Th1 immune response in murine mycobacterial infections (212), NKT cells play a potential role in late-phase mycobacterial infections (211) and express granulysin in a CD1d-dependent manner, thereby restricting the intracellular growth of *M. tuberculosis* (213). Additionally, NKT cells express high levels of CXCR3 and CCR5 and have chemotaxis patterns similar to Th1 inflammatory homing cells, suggesting that the CD1d-restricted NKT cells perform their specialized function in peripheral tissue sites rather than in secondary lymphoid organs (214,215). The abundant expression of CXCR3 ligands, which I have demonstrated, could therefore recruit NKT cells to these inflammatory environments. If we extrapolate from the DC-STAMP ISH data that IL-4 is expressed in the internal portion of the granuloma, in concert or separately from IFN-γ production, potentially by NKT cells responding to *M. tuberculosis* in a CD1d-dependent manner, we can develop a preliminary model for the involvement of DC-STAMP/FIND and IL-4 in this type 1-biased chronic inflammatory environment (Fig. 16). This model was developed based on some of my preliminary data and previous studies showing an abundance of IFN-γ-inducible chemokine mRNAs, putative recruitment of IFN-γ-producing $CXCR3^+$ cells and expression of DC-STAMP/FIND mRNA. As cells are recruited to the granulomatous site by chemokines, $CXCR3^+$ cells are recruited, including Th1 cell, $CD8^+$ and TCRγδ T cells and NKT

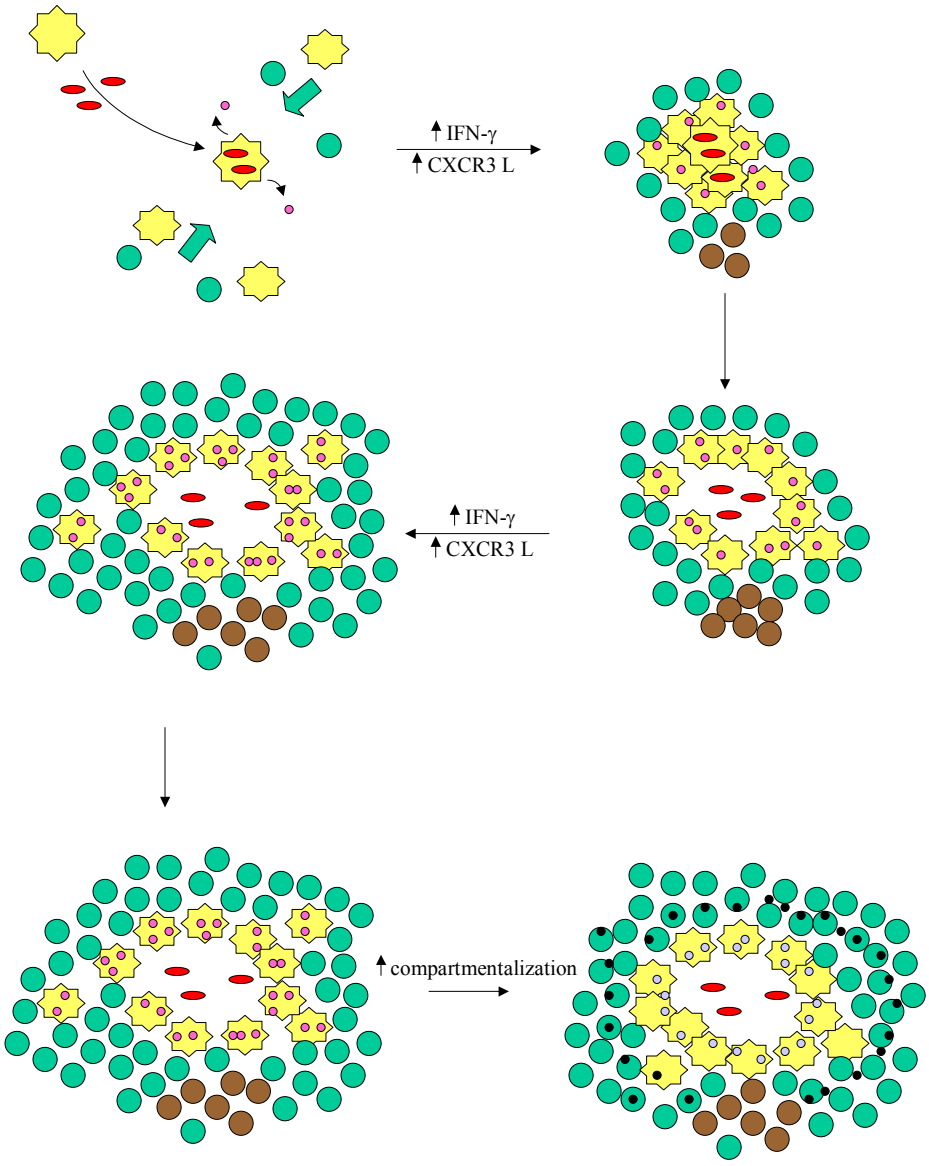

Figure 16. Schematic model of IFN-γ-inducible chemokines and DC-STAMP/FIND in the context of *M. tuberculosis* infection. An infected macrophage secretes chemokines that recruit many cell types including monocytes (yellow) and lymphocytes (T, green; B, brown). The increased presence of macrophages and lymphocytes produce IFN-γ in response to mycobacterial antigen. IFN-γ-induces macrophages to produce IFN-γ-inducible chemokines (pink circles), which in turn recruit more $CXCR3^+$ cells, including more lymphocytes and macrophages. As the granulomatous lesion grows, the central acellular region becomes less accessible to the external cellular components. This induces a reduced IFN-γ environment on the internal portion of the granuloma, causing a less controlled environment. Increased IL-4 centrally induces the increased expression of DC-STAMP/FIND (aqua) expressed along that acellular/cellular border.

cells. Although the main cytokine produced by these cells is IFN-γ, the possible expression of IL-4 by NKT cells could drive the expression of DC-STAMP/FIND. Additionally, previous studies in mice have shown an increased Th2 switch in tuberculosis. Whereas IL-4 was not detected in lymphocytes and macrophages treated with live mycobacteria, IL-4 was detected in lymphocytes treated with dead mycobacteria and hsp60 (216). This could be an indication of what we observed in the caseous granulomas. If the cellular debris within the caseous granulomas contains dead mycobacteria, then it is quite likely that the $CD4^+$ lymphocytes will produce IL-4, as previously reported (216). Since the function of DC-STAMP/FIND has not been elucidated, it is still unclear whether the expression of DC-STAMP/FIND will serve as a surrogate marker of IL-4 expression alone or will also negatively regulate the IFN-γ-dominated immune response and lead to disease progression or provide a function not currently understood.

The studies described in this dissertation provide additional information on the chemokine profile within the granulomatous lesions. The CXCR3 ligands are abundantly expressed, and likely in concert with CCR5 ligands, are providing a constant recruiting mechanism to continuously replenish the antigen-specific response directed against the microorganism present inside the granuloma. Although we did not directly show the recruitment of $CXCR3^+$ cells into the granuloma, we have shown that there is a definitive difference in the absence of $CXCR3^+$ cells in uninfected lungs correlating with the absence of CXCR3 recruiting molecules. Additionally, we have not directly shown that the CXCR3 ligands, instead of other factors, are actively recruiting these $CXCR3^+$ cells to the site of inflammation. We have definitely shown that the level of expression is massive and the growth of these granulomas potentially could be occurring due to uncontrolled mechanisms. These studies are relevant for therapeutic treatment studies, and complete blocking of CXCR3 might prevent further growth of

the granuloma, but this type of therapy would likely be devastating. The potential outcomes would be (1) the partial inhibition of the growth of the granuloma, if at all, or (2) destruction of the granuloma, similar to the anti-TNFα treatment studies (217,218), which would likely lead to the progression of disease.

In summary, these studies have shown that the IFN-γ-inducible chemokines, IFN-γ and TNF-α are abundantly expressed within the granulomatous lesions and are likely involved in the recruitment of the CXCR3-bearing cells to the inflammatory site. In addition, myeloid DC are present within the granulomatous structure. In vitro, myeloid DC are capable of producing high levels of IFN-γ-inducible chemokines, but macrophages are responsible for the abundant upregulation of the IFN-γ-inducible chemokines within these granulomatous tissues. In addition, this is the first report of the expression of an IL-4-inducible transmembrane molecule associated with a tuberculous granuloma. Even though the function of DC-STAMP/FIND is unknown, we believe that its expression can be used as a surrogate marker for IL-4 expression. All of these studies further expand the current knowledge about tuberculosis and the immune response induced during infection. In conclusion, tuberculosis is a chronic inflammatory disease that is characterized by a type 1 amplification process of chemokine/cytokine interactions and the host mechanisms, which counterregulate these processes do not appear to diminish the amplification processes observed in these studies.

VI.

FUTURE DIRECTIONS

While this dissertation has addressed a number of aspects pertaining to the potential roles of the IFN-γ-inducible chemokines in the maintenance of the pulmonary granuloma, many questions and alternative directions have arisen through the course of these studies. The following section discusses several questions that remain unresolved and if addressed, could offer valuable information regarding granuloma structure and/or DC biology.

Determine potential synergistic effects of CXCR3 and CCR5. I have exhaustively examined the expression of IFN-γ-inducible chemokines in the granulomatous structure, but only a preliminary examination of all three CCR5 ligand expression patterns was performed. Since activated Th1 lymphocytes commonly express both CXCR3 and CCR5 (93), examination of granulomatous lesions for the expression of CCR5 mRNAs could be done to determine if CCR5 is affected by *M. tuberculosis* infection. In addition, in vitro chemotaxis assays would clarify any potential synergistic effects of CXCR3 and CCR5 ligands and whether chemokines work in a coordinated manner to recruit type 1 lymphocytes capable of producing IFN-γ. Since CXCL11/I-TAC acts as an antagonist of monocyte recruitment through CCR5, we would investigate whether CXCL11/I-TAC acts in a similar manner on $CCR5^+$ lymphocyte population as well. Further investigation into the putative role of CXCL11/I-TAC will elicit information on the

increasing data that CXCR3 ligands are not merely redundant, but all serve a purported function. These additional studies could further define the interplay between CXCR3 and CCR5 ligands in the recruitment of immune cells to the site of granulomatous lesions within the pulmonary cavity during tuberculosis.

Establish an in vitro model system of granulomas. We have performed tissue-based and in vitro approaches in this dissertation, but these assays lack the ability to discern three-dimensional growth and maintenance of the granulomatous structure. Previously, many studies have used standard cell culture and chemotaxis assays to answer questions regarding the development of a chemotactic gradient and/or the migration of cells, but none of these assays have the potential to accurately mimic the formation of granuloma formation and maintenance that occurs in vivo. We have attempted to find pregranlomatous tissues in infected monkeys, but were unsuccessful. Thus, the establishment of a 3-dimensional cell culture model would potentially allow us to examine the formation of a granuloma, while preserving the cell-cell and cell-environment interactions observed in vivo. Three-dimensional cell cultures using varying forms of collagen-lattice networks have been used, including BD Matrigel matrix (Becton Dickinson), which has been used to study cell morphology, biochemical function, migration or invasion, and gene expression. This type of system consists of extracts from solublized basement membrane preparations extracted from an extracellular matrix (ECM) rich murine sarcoma, which resembles the mammalian cellular basement membrane. This system would enable us to examine, in vitro, the migration of immune cells to the site of infection and formation of granulomas in a three dimensional nature. Although the complexity of a tuberculous granuloma likely would never be replicated in vitro, this type of model system likely would provide us with

more information about the early events of granuloma formation, and possibly maintenance of granulomas also.

Further examination of DC-STAMP/FIND. I (Chapter IV) and others (152,153) have shown that DC-STAMP/FIND is an IL-4-inducible molecule expressed by macrophages, dendritic cells and B cells, but the function of DC-STAMP/FIND is still unknown and anti-DC-STAMP/FIND antibodies have not been successfully produced.

A. DC-STAMP/FIND mRNA expression. We have already observed DC-STAMP/FIND mRNA in dendritic cells, macrophages and B cells, but it is unclear whether DC-STAMP/FIND expression is a global marker for IL-4 stimulation. To address this issue, I would perform a comprehensive examination of multiple cell types treated with IL-4, in addition to an extensive array of other cytokines, to determine if DC-STAMP/FIND mRNA is detectable by RT-PCR. These studies will provide more information about the potential target population and possibly provide further information about a function of DC-STAMP/FIND.

B. Identify a protein-protein interaction. Previous studies have listed putative functional groups on the cytoplasmic domain of DC-STAMP/FIND (152,153), but no follow-up studies have been published about the function or potential binding partners. Since DC-STAMP/FIND has a small extracellular domain, multiple membrane spanning domains and a cytoplasmic tail, it is likely that the DC-STAMP/FIND protein may play a role in cell signaling. To determine if DC-STAMP/FIND has a binding partner I would utilize the yeast two hybrid system to screen a cDNA expression library of dendritic cells in pACT2. Our laboratory has

previously used this methodology to establish the association of simian immunodeficiency virus (SIV) with TCRζ chain (219) and we can use this technology to potentially identify a binding partner for DC-STAMP/FIND. Although the role of DC-STAMP/FIND is unknown, the detection of a binding partner or a protein clearly associated with DC-STAMP/FIND would elicit a greater understanding of the potential role of DC-STAMP/FIND.

As previously stated in this section, these are some of the interesting questions that have arisen throughout the course of this project. The completion of these experiments would further define the role of chemokines in the recruitment of immune cells to the site of granulomatous lesions during maintenance and also would provide a greater understanding of DC-STAMP/FIND expression and putative function.

APPENDIX

Table 8. Cynomolgus macaques included in these studies.

Animal	Duration of Infection (wpi)	Radiographic Readings[a]	Disease Course
M12202	3[b]	-	early infection necropsy
M24002	3[b]	-	early infection necropsy
M12302	4[b]	-	early infection necropsy
M24702	4[b]	-	early infection necropsy
M21902	5[b]	-	early infection necropsy
M24102	5[b]	-	early infection necropsy
M24302	6[b]	-	early infection necropsy
M22102	6[b]	-	early infection necropsy
M7100	9[b]	+	moderate disease
M15300	10[c]	+++	advanced disease
M15000	16[b]	++	moderate disease
M14600	17[b]	-	no disease[d]
M15100	17[b]	+	moderate disease
M12002	19	++	active/chronic disease
M11301	32[c]	+++	advanced disease
M11201	37[c]	+++	advanced disease
M11501	39	++	reactivated disease
M7200	41[c]	+++	advanced disease
M15200	64[b]	-	minimal disease

[a]Radiographic readings at necropsy (12). M14600 is the only macaque to not have a positive radiographic reading. However, viable *M. tuberculosis* bacilli could be cultured from lung homogenates at necropsy. Results are indicated as follows; -, negative film; ±, possibly small area of pneumonia, +, positive, ++ and +++, more extensive involvement.
[b]Sacrificed at a scheduled timepoint.
[c]Sacrificed due to extreme clinical symptoms.
[d]Only a few macroscopic granulomas were observed at necropsy.

BIBLIOGRAPHY

1. Dye, C., S. Scheele, P. Dolin, V. Pathania, and M. C. Raviglione. 1999. Consensus statement. Global burden of tuberculosis: estimated incidence, prevalence, and mortality by country. WHO Global Surveillance and Monitoring Project. *JAMA* 282:677-686.

2. Murray, P. J. 1999. Defining the requirements for immunological control of mycobacterial infections. *Trends Microbiol.* 7:366-372.

3. Kaufmann, S. H. 2001. How can immunology contribute to the control of tuberculosis? *Nat.Rev.Immunol.* 1:20-30.

4. Boros, D. L. 1978. Granulomatous inflammations. *Prog.Allergy* 24:183-267.

5. Mariano, M. 1995. The experimental granuloma. A hypothesis to explain the persistence of the lesion. *Rev.Inst.Med.Trop.Sao Paulo* 37:161-176.

6. Orme, I. M. 1998. The immunopathogenesis of tuberculosis: a new working hypothesis. *Trends Microbiol.* 6:94-97.

7. Orme, I. M. and A. M. Cooper. 1999. Cytokine/chemokine cascades in immunity to tuberculosis. *Immunol.Today* 20:307-312.

8. Roach, D. R., H. Briscoe, K. Baumgart, D. A. Rathjen, and W. J. Britton. 1999. Tumor necrosis factor (TNF) and a TNF-mimetic peptide modulate the granulomatous response to Mycobacterium bovis BCG infection in vivo. *Infect.Immun.* 67:5473-5476.

9. Saunders, B. M. and A. M. Cooper. 2000. Restraining mycobacteria: role of granulomas in mycobacterial infections. *Immunol.Cell Biol.* 78:334-341.

10. Gonzalez-Juarrero, M., O. C. Turner, J. Turner, P. Marietta, J. V. Brooks, and I. M. Orme. 2001. Temporal and spatial arrangement of lymphocytes within lung granulomas induced by aerosol infection with Mycobacterium tuberculosis. *Infect.Immun.* 69:1722-1728.

11. Sinhorini, I. L., J. L. Merusse, and M. Mariano. 1994. Role of lymphatic drainage on the development of Calmette-Guerin bacillus-induced granulomas in the hamster. *Int.Arch.Allergy Immunol.* 103:166-174.

12. Capuano, S. V., III, D. A. Croix, S. Pawar, A. Zinovik, A. Myers, P. L. Lin, S. Bissel, C. Fuhrman, E. Klein, and J. L. Flynn. 2003. Experimental Mycobacterium tuberculosis

infection of cynomolgus macaques closely resembles the various manifestations of human M. tuberculosis infection. *Infect.Immun.* 71:5831-5844.

13. Dannemberg, Jr. A. M., M. Ando, K. Shima, and T. Tsuda. 1975. Macrophage turnover and activation in tuberculous granulomas. In *Mononuclear phagocytes in immunity, infection and pathology*. R. V. Furth, ed. Oxford, Blackwell, pp. 959-967.

14. Yoder, M. A., G. Lamichhane, and W. R. Bishai. 2004. Cavitary pulmonary tuberculosis: The Holey Grail of disease transmission. *Current Science* 86:74-81.

15. Chensue, S. W., K. Warmington, J. Ruth, P. Lincoln, M. C. Kuo, and S. L. Kunkel. 1994. Cytokine responses during mycobacterial and schistosomal antigen-induced pulmonary granuloma formation. Production of Th1 and Th2 cytokines and relative contribution of tumor necrosis factor. *Am.J.Pathol.* 145:1105-1113.

16. Chiu, B. C., C. M. Freeman, V. R. Stolberg, E. Komuniecki, P. M. Lincoln, S. L. Kunkel, and S. W. Chensue. 2003. Cytokine-Chemokine Networks in Experimental Mycobacterial and Schistosomal Lung Granuloma Formation. *Am.J.Respir.Cell Mol.Biol.*

17. Kaufmann, S. H. 2002. Protection against tuberculosis: cytokines, T cells, and macrophages. *Ann.Rheum.Dis.* 61 Suppl 2:ii54-ii58.

18. Kawahara, M., T. Nakasone, and M. Honda. 2002. Dynamics of gamma interferon, interleukin-12 (IL-12), IL-10, and transforming growth factor beta mRNA expression in primary Mycobacterium bovis BCG infection in guinea pigs measured by a real-time fluorogenic reverse transcription-PCR assay. *Infect.Immun.* 70:6614-6620.

19. Qiu, B., K. A. Frait, F. Reich, E. Komuniecki, and S. W. Chensue. 2001. Chemokine expression dynamics in mycobacterial (type-1) and schistosomal (type-2) antigen-elicited pulmonary granuloma formation. *Am.J.Pathol.* 158:1503-1515.

20. Taha, R. A., T. C. Kotsimbos, Y. L. Song, D. Menzies, and Q. Hamid. 1997. IFN-gamma and IL-12 are increased in active compared with inactive tuberculosis. *Am.J.Respir.Crit Care Med.* 155:1135-1139.

21. Taha, R. A., E. M. Minshall, R. Olivenstein, D. Ihaku, B. Wallaert, A. Tsicopoulos, A. B. Tonnel, R. Damia, D. Menzies, and Q. A. Hamid. 1999. Increased expression of IL-12 receptor mRNA in active pulmonary tuberculosis and sarcoidosis. *Am.J.Respir.Crit Care Med.* 160:1119-1123.

22. Barry, S. M., M. C. Lipman, B. Bannister, M. A. Johnson, and G. Janossy. 2003. Purified protein derivative-activated type 1 cytokine-producing CD4+ T lymphocytes in the lung: a characteristic feature of active pulmonary and nonpulmonary tuberculosis. *J.Infect.Dis.* 187:243-250.

23. Belli, F., A. Capra, A. Moraiti, S. Rossi, and P. Rossi. 2000. Cytokines assay in peripheral blood and bronchoalveolar lavage in the diagnosis and staging of pulmonary granulomatous diseases. *Int.J.Immunopathol.Pharmacol.* 13:61-67.

24. Somoskovi, A., G. Zissel, P. F. Zipfel, M. W. Ziegenhagen, J. Klaucke, H. Haas, M. Schlaak, and J. Muller-Quernheim. 1999. Different cytokine patterns correlate with the extension of disease in pulmonary tuberculosis. *Eur.Cytokine Netw.* 10:135-142.

25. Robinson, D. S., S. Ying, I. K. Taylor, A. Wangoo, D. M. Mitchell, A. B. Kay, Q. Hamid, and R. J. Shaw. 1994. Evidence for a Th1-like bronchoalveolar T-cell subset and predominance of interferon-gamma gene activation in pulmonary tuberculosis. *Am.J.Respir.Crit Care Med.* 149:989-993.

26. Robinson, D. S., S. Ying, I. K. Taylor, A. Wangoo, D. M. Mitchell, A. B. Kay, Q. Hamid, and R. J. Shaw. 1994. Evidence for a Th1-like bronchoalveolar T-cell subset and predominance of interferon-gamma gene activation in pulmonary tuberculosis. *Am.J.Respir.Crit Care Med.* 149:989-993.

27. Fenhalls, G., A. Wong, J. Bezuidenhout, P. van Helden, P. Bardin, and P. T. Lukey. 2000. In situ production of gamma interferon, interleukin-4, and tumor necrosis factor alpha mRNA in human lung tuberculous granulomas. *Infect.Immun.* 68:2827-2836.

28. Kaufmann, S. H. 2003. Immune response to tuberculosis: experimental animal models. *Tuberculosis.(Edinb.)* 83:107-111.

29. Boom, W. H. 1996. The role of T-cell subsets in Mycobacterium tuberculosis infection. *Infect.Agents Dis.* 5:73-81.

30. Boom, W. H., D. H. Canaday, S. A. Fulton, A. J. Gehring, R. E. Rojas, and M. Torres. 2003. Human immunity to M. tuberculosis: T cell subsets and antigen processing. *Tuberculosis.(Edinb.)* 83:98-106.

31. Ladel, C. H., C. Blum, A. Dreher, K. Reifenberg, and S. H. Kaufmann. 1995. Protective role of gamma/delta T cells and alpha/beta T cells in tuberculosis. *Eur.J.Immunol.* 25:2877-2881.

32. Kaufmann, S. H. 1996. gamma/delta and other unconventional T lymphocytes: what do they see and what do they do? *Proc.Natl.Acad.Sci.U.S.A* 93:2272-2279.

33. Schaible, U. E. and S. H. Kaufmann. 2000. CD1 molecules and CD1-dependent T cells in bacterial infections: a link from innate to acquired immunity? *Semin.Immunol.* 12:527-535.

34. Ferrero, E., P. Biswas, K. Vettoretto, M. Ferrarini, M. Uguccioni, L. Piali, B. E. Leone, B. Moser, C. Rugarli, and R. Pardi. 2003. Macrophages exposed to Mycobacterium tuberculosis release chemokines able to recruit selected leucocyte subpopulations: focus on gammadelta cells. *Immunology* 108:365-374.

35. Baggiolini, M. 1998. Chemokines and leukocyte traffic. *Nature* 392:565-568.

36. Luster, A. D. 1998. Chemokines--chemotactic cytokines that mediate inflammation. *N.Engl.J.Med.* 338:436-445.

37. D'Ambrosio, D., M. Mariani, P. Panina-Bordignon, and F. Sinigaglia. 2001. Chemokines and their receptors guiding T lymphocyte recruitment in lung inflammation. *Am.J.Respir.Crit Care Med.* 164:1266-1275.

38. Roach, D. R., A. G. Bean, C. Demangel, M. P. France, H. Briscoe, and W. J. Britton. 2002. TNF regulates chemokine induction essential for cell recruitment, granuloma formation, and clearance of mycobacterial infection. *J.Immunol.* 168:4620-4627.

39. Sallusto, F., D. Lenig, C. R. Mackay, and A. Lanzavecchia. 1998. Flexible programs of chemokine receptor expression on human polarized T helper 1 and 2 lymphocytes. *J.Exp.Med.* 187:875-883.

40. Loetscher, M., B. Gerber, P. Loetscher, S. A. Jones, L. Piali, I. Clark-Lewis, M. Baggiolini, and B. Moser. 1996. Chemokine receptor specific for IP10 and mig: structure, function, and expression in activated T-lymphocytes. *J.Exp.Med.* 184:963-969.

41. Dixon, A. E., J. B. Mandac, D. K. Madtes, P. J. Martin, and J. G. Clark. 2000. Chemokine expression in Th1 cell-induced lung injury: prominence of IFN-gamma-inducible chemokines. *Am.J.Physiol Lung Cell Mol.Physiol* 279:L592-L599.

42. Hildebrandt, G. C., L. A. Corrion, K. M. Olkiewicz, B. Lu, K. Lowler, U. A. Duffner, B. B. Moore, W. A. Kuziel, C. Liu, and K. R. Cooke. 2004. Blockade of CXCR3 receptor:ligand interactions reduces leukocyte recruitment to the lung and the severity of experimental idiopathic pneumonia syndrome. *J.Immunol.* 173:2050-2059.

43. Baker, M. S., X. Chen, A. R. Rotramel, J. J. Nelson, B. Lu, C. Gerard, Y. Kanwar, and D. B. Kaufman. 2003. Genetic deletion of chemokine receptor CXCR3 or antibody blockade of its ligand IP-10 modulates posttransplantation graft-site lymphocytic infiltrates and prolongs functional graft survival in pancreatic islet allograft recipients. *Surgery* 134:126-133.

44. Agostini, C., F. Calabrese, F. Rea, M. Facco, A. Tosoni, M. Loy, G. Binotto, M. Valente, L. Trentin, and G. Semenzato. 2001. CXCR3 and its ligand CXCL10 are expressed by inflammatory cells infiltrating lung allografts and mediate chemotaxis of T cells at sites of rejection. *Am.J.Pathol.* 158:1703-1711.

45. Jiang, D., J. Liang, J. Hodge, B. Lu, Z. Zhu, S. Yu, J. Fan, Y. Gao, Z. Yin, R. Homer, C. Gerard, and P. W. Noble. 2004. Regulation of pulmonary fibrosis by chemokine receptor CXCR3. *J.Clin.Invest* 114:291-299.

46. Seiler, P., P. Aichele, S. Bandermann, A. E. Hauser, B. Lu, N. P. Gerard, C. Gerard, S. Ehlers, H. J. Mollenkopf, and S. H. Kaufmann. 2003. Early granuloma formation after aerosol Mycobacterium tuberculosis infection is regulated by neutrophils via CXCR3-signaling chemokines. *Eur.J.Immunol.* 33:2676-2686.

47. Shi, S., C. Nathan, D. Schnappinger, J. Drenkow, M. Fuortes, E. Block, A. Ding, T. R. Gingeras, G. Schoolnik, S. Akira, K. Takeda, and S. Ehrt. 2003. MyD88 primes

macrophages for full-scale activation by interferon-gamma yet mediates few responses to Mycobacterium tuberculosis. *J.Exp.Med.* 198:987-997.

48. Lande, R., E. Giacomini, T. Grassi, M. E. Remoli, E. Iona, M. Miettinen, I. Julkunen, and E. M. Coccia. 2003. IFN-alpha beta released by Mycobacterium tuberculosis-infected human dendritic cells induces the expression of CXCL10: selective recruitment of NK and activated T cells. *J.Immunol.* 170:1174-1182.

49. Lambrecht, B. N., J. B. Prins, and H. C. Hoogsteden. 2001. Lung dendritic cells and host immunity to infection. *Eur.Respir.J.* 18:692-704.

50. Nicod, L. P., L. Cochand, and D. Dreher. 2000. Antigen presentation in the lung: dendritic cells and macrophages. *Sarcoidosis.Vasc.Diffuse.Lung Dis.* 17:246-255.

51. Banchereau, J., F. Briere, C. Caux, J. Davoust, S. Lebecque, Y. J. Liu, B. Pulendran, and K. Palucka. 2000. Immunobiology of dendritic cells. *Annu.Rev.Immunol.* 18:767-811.

52. Bhatt, K., S. P. Hickman, and P. Salgame. 2004. Cutting edge: A new approach to modeling early lung immunity in murine tuberculosis. *J.Immunol.* 172:2748-2751.

53. Tailleux, L., O. Schwartz, J. L. Herrmann, E. Pivert, M. Jackson, A. Amara, L. Legres, D. Dreher, L. P. Nicod, J. C. Gluckman, P. H. Lagrange, B. Gicquel, and O. Neyrolles. 2003. DC-SIGN is the major Mycobacterium tuberculosis receptor on human dendritic cells. *J.Exp.Med.* 197:121-127.

54. Iyonaga, K., K. M. McCarthy, and E. E. Schneeberger. 2002. Dendritic cells and the regulation of a granulomatous immune response in the lung. *Am.J.Respir.Cell Mol.Biol.* 26:671-679.

55. Tsuchiya, T., K. Chida, T. Suda, E. E. Schneeberger, and H. Nakamura. 2002. Dendritic cell involvement in pulmonary granuloma formation elicited by bacillus calmette-guerin in rats. *Am.J.Respir.Crit Care Med.* 165:1640-1646.

56. Uehira, K., R. Amakawa, T. Ito, K. Tajima, S. Naitoh, Y. Ozaki, T. Shimizu, K. Yamaguchi, Y. Uemura, H. Kitajima, S. Yonezu, and S. Fukuhara. 2002. Dendritic cells are decreased in blood and accumulated in granuloma in tuberculosis. *Clin.Immunol.* 105:296-303.

57. Sallusto, F., P. Schaerli, P. Loetscher, C. Schaniel, D. Lenig, C. R. Mackay, S. Qin, and A. Lanzavecchia. 1998. Rapid and coordinated switch in chemokine receptor expression during dendritic cell maturation. *Eur.J.Immunol.* 28:2760-2769.

58. Krupa, W. M., M. Dewan, M. S. Jeon, P. J. Kurtin, B. R. Younge, J. J. Goronzy, and C. M. Weyand. 2002. Trapping of misdirected dendritic cells in the granulomatous lesions of giant cell arteritis. *Am.J.Pathol.* 161:1815-1823.

59. Walsh, G. P., E. V. Tan, E. C. dela Cruz, R. M. Abalos, L. G. Villahermosa, L. J. Young, R. V. Cellona, J. B. Nazareno, and M. A. Horwitz. 1996. The Philippine cynomolgus

monkey (Macaca fasicularis) provides a new nonhuman primate model of tuberculosis that resembles human disease. *Nat.Med.* 2:430-436.

60. Fuller, C. L., J. L. Flynn, and T. A. Reinhart. 2003. In situ study of abundant expression of proinflammatory chemokines and cytokines in pulmonary granulomas that develop in cynomolgus macaques experimentally infected with Mycobacterium tuberculosis. *Infect.Immun.* 71:7023-7034.

61. Taha, R. A., T. C. Kotsimbos, Y. L. Song, D. Menzies, and Q. Hamid. 1997. IFN-gamma and IL-12 are increased in active compared with inactive tuberculosis. *Am.J.Respir.Crit Care Med.* 155:1135-1139.

62. Qiu, B., K. A. Frait, F. Reich, E. Komuniecki, and S. W. Chensue. 2001. Chemokine expression dynamics in mycobacterial (type-1) and schistosomal (type-2) antigen-elicited pulmonary granuloma formation. *Am.J.Pathol.* 158:1503-1515.

63. Robinson, D. S., S. Ying, I. K. Taylor, A. Wangoo, D. M. Mitchell, A. B. Kay, Q. Hamid, and R. J. Shaw. 1994. Evidence for a Th1-like bronchoalveolar T-cell subset and predominance of interferon-gamma gene activation in pulmonary tuberculosis. *Am.J.Respir.Crit Care Med.* 149:989-993.

64. Fenhalls, G., A. Wong, J. Bezuidenhout, P. van Helden, P. Bardin, and P. T. Lukey. 2000. In situ production of gamma interferon, interleukin-4, and tumor necrosis factor alpha mRNA in human lung tuberculous granulomas. *Infect.Immun.* 68:2827-2836.

65. Fenhalls, G., A. Wong, J. Bezuidenhout, P. van Helden, P. Bardin, and P. T. Lukey. 2000. In situ production of gamma interferon, interleukin-4, and tumor necrosis factor alpha mRNA in human lung tuberculous granulomas. *Infect.Immun.* 68:2827-2836.

66. D'Ambrosio, D., M. Mariani, P. Panina-Bordignon, and F. Sinigaglia. 2001. Chemokines and their receptors guiding T lymphocyte recruitment in lung inflammation. *Am.J.Respir.Crit Care Med.* 164:1266-1275.

67. Qiu, B., K. A. Frait, F. Reich, E. Komuniecki, and S. W. Chensue. 2001. Chemokine expression dynamics in mycobacterial (type-1) and schistosomal (type-2) antigen-elicited pulmonary granuloma formation. *Am.J.Pathol.* 158:1503-1515.

68. Reinhart, T. A., B. A. Fallert, M. E. Pfeifer, S. Sanghavi, S. Capuano, III, P. Rajakumar, M. Murphey-Corb, R. Day, C. L. Fuller, and T. M. Schaefer. 2002. Increased expression of the inflammatory chemokine CXC chemokine ligand 9/monokine induced by interferon-gamma in lymphoid tissues of rhesus macaques during simian immunodeficiency virus infection and acquired immunodeficiency syndrome. *Blood* 99:3119-3128.

69. Langermans, J. A., P. Andersen, D. van Soolingen, R. A. Vervenne, P. A. Frost, L. T. van der, L. A. van Pinxteren, H. J. van den, S. Kroon, I. Peekel, S. Florquin, and A. W. Thomas. 2001. Divergent effect of bacillus Calmette-Guerin (BCG) vaccination on Mycobacterium tuberculosis infection in highly related macaque species: implications for

primate models in tuberculosis vaccine research. *Proc.Natl.Acad.Sci.U.S.A* 98:11497-11502.

70. Capuano, S., III, D. A. Croix, S. Pawar, A. Zinovik, A. Myers, P. L. Lin, S. Bissel, C. Fuhrman, E. Klein, and J. L. Flynn. 2003. Experimental *Mycobacterium tuberculosis* infection of cynomolgus macaques closely resembles the various manifestations of human *M. tuberculosis* infection. *Infect.Immun.*

71. Fallert, B. A. and T. A. Reinhart. 2002. Improved detection of simian immunodeficiency virus RNA by in situ hybridization in fixed tissue sections: combined effects of temperatures for tissue fixation and probe hybridization. *J.Virol.Methods* 99:23-32.

72. Choi, Y. K., B. A. Fallert, M. A. Murphey-Corb, and T. A. Reinhart. 2003. Simian immunodeficiency virus dramatically alters expression of homeostatic chemokines and dendritic cell markers during infection in vivo. *Blood* 101:1684-1691.

73. Basu, S., T. M. Schaefer, M. Ghosh, C. L. Fuller, and T. A. Reinhart. 2002. Molecular cloning and sequencing of 25 different rhesus macaque chemokine cDNAS reveals evolutionary conservation among C, CC, CXC, and CX3C families of chemokines. *Cytokine* 18:140-148.

74. Patel, S., M. Yates, and N. A. Saunders. 1997. PCR-enzyme-linked immunosorbent assay and partial rRNA gene sequencing: a rational approach to identifying mycobacteria. *J.Clin.Microbiol.* 35:2375-2380.

75. Cooper, A. M., D. K. Dalton, T. A. Stewart, J. P. Griffin, D. G. Russell, and I. M. Orme. 1993. Disseminated tuberculosis in interferon gamma gene-disrupted mice. *J.Exp.Med.* 178:2243-2247.

76. Flynn, J. L., J. Chan, K. J. Triebold, D. K. Dalton, T. A. Stewart, and B. R. Bloom. 1993. An essential role for interferon gamma in resistance to Mycobacterium tuberculosis infection. *J.Exp.Med.* 178:2249-2254.

77. Jouanguy, E., F. Altare, S. Lamhamedi, P. Revy, J. F. Emile, M. Newport, M. Levin, S. Blanche, E. Seboun, A. Fischer, and J. L. Casanova. 1996. Interferon-gamma-receptor deficiency in an infant with fatal bacille Calmette-Guerin infection. *N.Engl.J.Med.* 335:1956-1961.

78. Newport, M. J., C. M. Huxley, S. Huston, C. M. Hawrylowicz, B. A. Oostra, R. Williamson, and M. Levin. 1996. A mutation in the interferon-gamma-receptor gene and susceptibility to mycobacterial infection. *N.Engl.J.Med.* 335:1941-1949.

79. Bean, A. G., D. R. Roach, H. Briscoe, M. P. France, H. Korner, J. D. Sedgwick, and W. J. Britton. 1999. Structural deficiencies in granuloma formation in TNF gene-targeted mice underlie the heightened susceptibility to aerosol Mycobacterium tuberculosis infection, which is not compensated for by lymphotoxin. *J.Immunol.* 162:3504-3511.

80. Bergeron, A., M. Bonay, M. Kambouchner, D. Lecossier, M. Riquet, P. Soler, A. Hance, and A. Tazi. 1997. Cytokine patterns in tuberculous and sarcoid granulomas: correlations with histopathologic features of the granulomatous response. *J.Immunol.* 159:3034-3043.

81. Chensue, S. W., K. S. Warmington, J. H. Ruth, P. Lincoln, and S. L. Kunkel. 1995. Cytokine function during mycobacterial and schistosomal antigen-induced pulmonary granuloma formation. Local and regional participation of IFN-gamma, IL-10, and TNF. *J.Immunol.* 154:5969-5976.

82. Sertl, K., T. Takemura, E. Tschachler, V. J. Ferrans, M. A. Kaliner, and E. M. Shevach. 1986. Dendritic cells with antigen-presenting capability reside in airway epithelium, lung parenchyma, and visceral pleura. *J.Exp.Med.* 163:436-451.

83. Van Haarst, J. M., H. C. Hoogsteden, H. J. De Wit, G. T. Verhoeven, C. E. Havenith, and H. A. Drexhage. 1994. Dendritic cells and their precursors isolated from human bronchoalveolar lavage: immunocytologic and functional properties. *Am.J.Respir.Cell Mol.Biol.* 11:344-350.

84. Abe, Y., M. Nakamura, Y. Oshika, H. Hatanaka, T. Tokunaga, Y. Ohkubo, T. Hashizume, K. Suzuki, and T. Fujino. 2001. Serum levels of vascular endothelial growth factor and cavity formation in active pulmonary tuberculosis. *Respiration* 68:496-500.

85. Demangel, C., A. G. Bean, E. Martin, C. G. Feng, A. T. Kamath, and W. J. Britton. 1999. Protection against aerosol Mycobacterium tuberculosis infection using Mycobacterium bovis Bacillus Calmette Guerin-infected dendritic cells. *Eur.J.Immunol.* 29:1972-1979.

86. Giacomini, E., E. Iona, L. Ferroni, M. Miettinen, L. Fattorini, G. Orefici, I. Julkunen, and E. M. Coccia. 2001. Infection of human macrophages and dendritic cells with Mycobacterium tuberculosis induces a differential cytokine gene expression that modulates T cell response. *J.Immunol.* 166:7033-7041.

87. Algood, H. M., P. L. Lin, D. Yankura, A. Jones, J. Chan, and J. L. Flynn. 2004. TNF influences chemokine expression of macrophages in vitro and that of CD11b+ cells in vivo during Mycobacterium tuberculosis infection. *J.Immunol.* 172:6846-6857.

88. Kurashima, K., N. Mukaida, M. Fujimura, M. Yasui, Y. Nakazumi, T. Matsuda, and K. Matsushima. 1997. Elevated chemokine levels in bronchoalveolar lavage fluid of tuberculosis patients. *Am.J.Respir.Crit Care Med.* 155:1474-1477.

89. Sadek, M. I., E. Sada, Z. Toossi, S. K. Schwander, and E. A. Rich. 1998. Chemokines induced by infection of mononuclear phagocytes with mycobacteria and present in lung alveoli during active pulmonary tuberculosis. *Am.J.Respir.Cell Mol.Biol.* 19:513-521.

90. Chensue, S. W., K. S. Warmington, E. J. Allenspach, B. Lu, C. Gerard, S. L. Kunkel, and N. W. Lukacs. 1999. Differential expression and cross-regulatory function of RANTES during mycobacterial (type 1) and schistosomal (type 2) antigen-elicited granulomatous inflammation. *J.Immunol.* 163:165-173.

91. Ragno, S., M. Romano, S. Howell, D. J. Pappin, P. J. Jenner, and M. J. Colston. 2001. Changes in gene expression in macrophages infected with Mycobacterium tuberculosis: a combined transcriptomic and proteomic approach. *Immunology* 104:99-108.

92. Saukkonen, J. J., B. Bazydlo, M. Thomas, R. M. Strieter, J. Keane, and H. Kornfeld. 2002. Beta-chemokines are induced by Mycobacterium tuberculosis and inhibit its growth. *Infect.Immun.* 70:1684-1693.

93. Bonecchi, R., G. Bianchi, P. P. Bordignon, D. D'Ambrosio, R. Lang, A. Borsatti, S. Sozzani, P. Allavena, P. A. Gray, A. Mantovani, and F. Sinigaglia. 1998. Differential expression of chemokine receptors and chemotactic responsiveness of type 1 T helper cells (Th1s) and Th2s. *J.Exp.Med.* 187:129-134.

94. Sozzani, S., P. Allavena, G. D'Amico, W. Luini, G. Bianchi, M. Kataura, T. Imai, O. Yoshie, R. Bonecchi, and A. Mantovani. 1998. Differential regulation of chemokine receptors during dendritic cell maturation: a model for their trafficking properties. *J.Immunol.* 161:1083-1086.

95. Romagnani, P., F. Annunziato, E. Lazzeri, L. Cosmi, C. Beltrame, L. Lasagni, G. Galli, M. Francalanci, R. Manetti, F. Marra, V. Vanini, E. Maggi, and S. Romagnani. 2001. Interferon-inducible protein 10, monokine induced by interferon gamma, and interferon-inducible T-cell alpha chemoattractant are produced by thymic epithelial cells and attract T-cell receptor (TCR) alphabeta+ CD8+ single-positive T cells, TCRgammadelta+ T cells, and natural killer-type cells in human thymus. *Blood* 97:601-607.

96. Park, M. K., D. Amichay, P. Love, E. Wick, F. Liao, A. Grinberg, R. L. Rabin, H. H. Zhang, S. Gebeyehu, T. M. Wright, A. Iwasaki, Y. Weng, J. A. DeMartino, K. L. Elkins, and J. M. Farber. 2002. The CXC chemokine murine monokine induced by IFN-gamma (CXC chemokine ligand 9) is made by APCs, targets lymphocytes including activated B cells, and supports antibody responses to a bacterial pathogen in vivo. *J.Immunol.* 169:1433-1443.

97. Sauty, A., R. A. Colvin, L. Wagner, S. Rochat, F. Spertini, and A. D. Luster. 2001. CXCR3 internalization following T cell-endothelial cell contact: preferential role of IFN-inducible T cell alpha chemoattractant (CXCL11). *J.Immunol.* 167:7084-7093.

98. Rhoades, E. R., A. M. Cooper, and I. M. Orme. 1995. Chemokine response in mice infected with Mycobacterium tuberculosis. *Infect.Immun.* 63:3871-3877.

99. Qiu, B., K. A. Frait, F. Reich, E. Komuniecki, and S. W. Chensue. 2001. Chemokine expression dynamics in mycobacterial (type-1) and schistosomal (type-2) antigen-elicited pulmonary granuloma formation. *Am.J.Pathol.* 158:1503-1515.

100. Fenhalls, G., A. Wong, J. Bezuidenhout, P. van Helden, P. Bardin, and P. T. Lukey. 2000. In situ production of gamma interferon, interleukin-4, and tumor necrosis factor alpha mRNA in human lung tuberculous granulomas. *Infect.Immun.* 68:2827-2836.

101. Barnes, P. F., S. Lu, J. S. Abrams, E. Wang, M. Yamamura, and R. L. Modlin. 1993. Cytokine production at the site of disease in human tuberculosis. *Infect.Immun.* 61:3482-3489.

102. Fenhalls, G., A. Wong, J. Bezuidenhout, P. van Helden, P. Bardin, and P. T. Lukey. 2000. In situ production of gamma interferon, interleukin-4, and tumor necrosis factor alpha mRNA in human lung tuberculous granulomas. *Infect.Immun.* 68:2827-2836.

103. Fenhalls, G., A. Wong, J. Bezuidenhout, P. van Helden, P. Bardin, and P. T. Lukey. 2000. In situ production of gamma interferon, interleukin-4, and tumor necrosis factor alpha mRNA in human lung tuberculous granulomas. *Infect.Immun.* 68:2827-2836.

104. Gangur, V., F. E. Simons, and K. T. Hayglass. 1998. Human IP-10 selectively promotes dominance of polyclonally activated and environmental antigen-driven IFN-gamma over IL-4 responses. *FASEB J.* 12:705-713.

105. Means, T. K., S. Wang, E. Lien, A. Yoshimura, D. T. Golenbock, and M. J. Fenton. 1999. Human toll-like receptors mediate cellular activation by Mycobacterium tuberculosis. *J.Immunol.* 163:3920-3927.

106. Underhill, D. M., A. Ozinsky, K. D. Smith, and A. Aderem. 1999. Toll-like receptor-2 mediates mycobacteria-induced proinflammatory signaling in macrophages. *Proc.Natl.Acad.Sci.U.S.A* 96:14459-14463.

107. van Crevel, R., T. H. Ottenhoff, and J. W. van der Meer. 2002. Innate immunity to Mycobacterium tuberculosis. *Clin.Microbiol.Rev.* 15:294-309.

108. Foxman, E. F., J. J. Campbell, and E. C. Butcher. 1997. Multistep navigation and the combinatorial control of leukocyte chemotaxis. *J.Cell Biol.* 139:1349-1360.

109. Van Damme, J., S. Struyf, A. Wuyts, E. Van Coillie, P. Menten, D. Schols, S. Sozzani, M. De, I, and P. Proost. 1999. The role of CD26/DPP IV in chemokine processing. *Chem.Immunol.* 72:42-56.

110. Proost, P., E. Schutyser, P. Menten, S. Struyf, A. Wuyts, G. Opdenakker, M. Detheux, M. Parmentier, C. Durinx, A. M. Lambeir, J. Neyts, S. Liekens, P. C. Maudgal, A. Billiau, and J. Van Damme. 2001. Amino-terminal truncation of CXCR3 agonists impairs receptor signaling and lymphocyte chemotaxis, while preserving antiangiogenic properties. *Blood* 98:3554-3561.

111. Fukunaga, H., T. Murakami, T. Gondo, K. Sugi, and T. Ishihara. 2002. Sensitivity of Acid-Fast Staining for Mycobacterium tuberculosis in Formalin-fixed Tissue. *Am.J.Respir.Crit Care Med.* 166:994-997.

112. Alberts B, Bray D, Lewis J, Raff M, Roberts K, and Watson J D. 1989. Control of gene expression. In *Molecular biology of the cell*. Garland Publishing, Inc., New York, p. 595.

113. Belasco, J. G., G. Nilsson, A. von Gabain, and S. N. Cohen. 1986. The stability of E. coli gene transcripts is dependent on determinants localized to specific mRNA segments. *Cell* 46:245-251.

114. von Gabain, A., J. G. Belasco, J. L. Schottel, A. C. Chang, and S. N. Cohen. 1983. Decay of mRNA in Escherichia coli: investigation of the fate of specific segments of transcripts. *Proc.Natl.Acad.Sci.U.S.A* 80:653-657.

115. Fenhalls, G., L. Stevens-Muller, R. Warren, N. Carroll, J. Bezuidenhout, P. van Helden, and P. Bardin. 2002. Localisation of mycobacterial DNA and mRNA in human tuberculous granulomas. *J.Microbiol.Methods* 51:197-208.

116. Fenhalls, G., L. Stevens, L. Moses, J. Bezuidenhout, J. C. Betts, P. P. Helden, P. T. Lukey, and K. Duncan. 2002. In situ detection of Mycobacterium tuberculosis transcripts in human lung granulomas reveals differential gene expression in necrotic lesions. *Infect.Immun.* 70:6330-6338.

117. Tufariello, J. M., J. Chan, and J. L. Flynn. 2003. Latent tuberculosis: mechanisms of host and bacillus that contribute to persistent infection. *Lancet Infect.Dis.* 3:578-590.

118. Flynn, J. L. and J. Chan. 2001. Immunology of tuberculosis. *Annu.Rev.Immunol.* 19:93-129.

119. Steinman, R. M. 1991. The dendritic cell system and its role in immunogenicity. *Annu.Rev.Immunol.* 9:271-296.

120. Holt, P. G. 2000. Antigen presentation in the lung. *Am.J.Respir.Crit Care Med.* 162:S151-S156.

121. Kaisho, T. and S. Akira. 2001. Dendritic-cell function in Toll-like receptor- and MyD88-knockout mice. *Trends Immunol.* 22:78-83.

122. Trevejo, J. M., M. W. Marino, N. Philpott, R. Josien, E. C. Richards, K. B. Elkon, and E. Falck-Pedersen. 2001. TNF-alpha -dependent maturation of local dendritic cells is critical for activating the adaptive immune response to virus infection. *Proc.Natl.Acad.Sci.U.S.A* 98:12162-12167.

123. Masten, B. J., G. K. Olson, D. F. Kusewitt, and M. F. Lipscomb. 2004. Flt3 ligand preferentially increases the number of functionally active myeloid dendritic cells in the lungs of mice. *J.Immunol.* 172:4077-4083.

124. Alaniz, R. C., S. Sandall, E. K. Thomas, and C. B. Wilson. 2004. Increased dendritic cell numbers impair protective immunity to intracellular bacteria despite augmenting antigen-specific CD8+ T lymphocyte responses. *J.Immunol.* 172:3725-3735.

125. Comeau, M. R., Van der Vuurst de Vries AR, C. R. Maliszewski, and L. Galibert. 2002. CD123bright plasmacytoid predendritic cells: progenitors undergoing cell fate conversion? *J.Immunol.* 169:75-83.

126. Moretti, S., F. Lanza, M. Dabusti, A. Tieghi, D. Campioni, M. Dominici, and G. L. Castoldi. 2001. CD123 (interleukin 3 receptor alpha chain). *J.Biol.Regul.Homeost.Agents* 15:98-100.

127. Appelmelk, B. J., D. van, I, S. J. van Vliet, C. M. Vandenbroucke-Grauls, T. B. Geijtenbeek, and Y. van Kooyk. 2003. Cutting edge: carbohydrate profiling identifies new pathogens that interact with dendritic cell-specific ICAM-3-grabbing nonintegrin on dendritic cells. *J.Immunol.* 170:1635-1639.

128. Geijtenbeek, T. B. and Y. van Kooyk. 2003. Pathogens target DC-SIGN to influence their fate DC-SIGN functions as a pathogen receptor with broad specificity. *APMIS* 111:698-714.

129. Maeda, N., J. Nigou, J. L. Herrmann, M. Jackson, A. Amara, P. H. Lagrange, G. Puzo, B. Gicquel, and O. Neyrolles. 2003. The cell surface receptor DC-SIGN discriminates between Mycobacterium species through selective recognition of the mannose caps on lipoarabinomannan. *J.Biol.Chem.* 278:5513-5516.

130. Saint-Vis, B., J. Vincent, S. Vandenabeele, B. Vanbervliet, J. J. Pin, S. Ait-Yahia, S. Patel, M. G. Mattei, J. Banchereau, S. Zurawski, J. Davoust, C. Caux, and S. Lebecque. 1998. A novel lysosome-associated membrane glycoprotein, DC-LAMP, induced upon DC maturation, is transiently expressed in MHC class II compartment. *Immunity.* 9:325-336.

131. Freeman, G. J., A. J. Long, Y. Iwai, K. Bourque, T. Chernova, H. Nishimura, L. J. Fitz, N. Malenkovich, T. Okazaki, M. C. Byrne, H. F. Horton, L. Fouser, L. Carter, V. Ling, M. R. Bowman, B. M. Carreno, M. Collins, C. R. Wood, and T. Honjo. 2000. Engagement of the PD-1 immunoinhibitory receptor by a novel B7 family member leads to negative regulation of lymphocyte activation. *J.Exp.Med.* 192:1027-1034.

132. Tseng, S. Y., M. Otsuji, K. Gorski, X. Huang, J. E. Slansky, S. I. Pai, A. Shalabi, T. Shin, D. M. Pardoll, and H. Tsuchiya. 2001. B7-DC, a new dendritic cell molecule with potent costimulatory properties for T cells. *J.Exp.Med.* 193:839-846.

133. Lagranderie, M., M. A. Nahori, A. M. Balazuc, H. Kiefer-Biasizzo, Lapa e Silva JR, G. Milon, G. Marchal, and B. B. Vargaftig. 2003. Dendritic cells recruited to the lung shortly after intranasal delivery of Mycobacterium bovis BCG drive the primary immune response towards a type 1 cytokine production. *Immunology* 108:352-364.

134. Choi, H. S., P. R. Rai, H. W. Chu, C. Cool, and E. D. Chan. 2002. Analysis of nitric oxide synthase and nitrotyrosine expression in human pulmonary tuberculosis. *Am.J.Respir.Crit Care Med.* 166:178-186.

135. Godfrey, T. E., S. H. Kim, M. Chavira, D. W. Ruff, R. S. Warren, J. W. Gray, and R. H. Jensen. 2000. Quantitative mRNA expression analysis from formalin-fixed, paraffin-embedded tissues using 5' nuclease quantitative reverse transcription-polymerase chain reaction. *J.Mol.Diagn.* 2:84-91.

136. Maeda, K., M. Matsuda, H. Suzuki, and H. A. Saitoh. 2002. Immunohistochemical recognition of human follicular dendritic cells (FDCs) in routinely processed paraffin sections. *J.Histochem.Cytochem.* 50:1475-1486.

137. Mosialos, G., M. Birkenbach, S. Ayehunie, F. Matsumura, G. S. Pinkus, E. Kieff, and E. Langhoff. 1996. Circulating human dendritic cells differentially express high levels of a 55-kd actin-bundling protein. *Am.J.Pathol.* 148:593-600.

138. Pinkus, G. S., J. L. Pinkus, E. Langhoff, F. Matsumura, S. Yamashiro, G. Mosialos, and J. W. Said. 1997. Fascin, a sensitive new marker for Reed-Sternberg cells of hodgkin's disease. Evidence for a dendritic or B cell derivation? *Am.J.Pathol.* 150:543-562.

139. Fuller, C. L., Y. K. Choi, B. A. Fallert, S. Capuano, III, P. Rajakumar, M. Murphey-Corb, and T. A. Reinhart. 2002. Restricted SIV replication in rhesus macaque lung tissues during the acute phase of infection. *Am.J.Pathol.* 161:969-978.

140. Akasaki, K., N. Nakamura, N. Tsukui, S. Yokota, S. Murata, R. Katoh, A. Michihara, H. Tsuji, E. T. Marques, Jr., and J. T. August. 2004. Human dendritic cell lysosome-associated membrane protein expressed in lung type II pneumocytes. *Arch.Biochem.Biophys.* 425:147-157.

141. Salaun, B., B. Saint-Vis, N. Pacheco, Y. Pacheco, A. Riesler, S. Isaac, C. Leroux, V. Clair-Moninot, J. J. Pin, J. Griffith, I. Treilleux, S. Goddard, J. Davoust, M. Kleijmeer, and S. Lebecque. 2004. CD208/dendritic cell-lysosomal associated membrane protein is a marker of normal and transformed type II pneumocytes. *Am.J.Pathol.* 164:861-871.

142. Voorhout, W. F., T. Veenendaal, H. P. Haagsman, T. E. Weaver, J. A. Whitsett, L. M. van Golde, and H. J. Geuze. 1992. Intracellular processing of pulmonary surfactant protein B in an endosomal/lysosomal compartment. *Am.J.Physiol* 263:L479-L486.

143. Suda, T., K. McCarthy, Q. Vu, J. McCormack, and E. E. Schneeberger. 1998. Dendritic cell precursors are enriched in the vascular compartment of the lung. *Am.J.Respir.Cell Mol.Biol.* 19:728-737.

144. Caux, C., S. Ait-Yahia, K. Chemin, O. de Bouteiller, M. C. Dieu-Nosjean, B. Homey, C. Massacrier, B. Vanbervliet, A. Zlotnik, and A. Vicari. 2000. Dendritic cell biology and regulation of dendritic cell trafficking by chemokines. *Springer Semin.Immunopathol.* 22:345-369.

145. Caux, C., B. Vanbervliet, C. Massacrier, S. Ait-Yahia, C. Vaure, K. Chemin, Dieu-Nosjean And MC, and A. Vicari. 2002. Regulation of dendritic cell recruitment by chemokines. *Transplantation* 73:S7-11.

146. Randolph, G. J. 2001. Dendritic cell migration to lymph nodes: cytokines, chemokines, and lipid mediators. *Semin.Immunol.* 13:267-274.

147. Legge, K. L. and T. J. Braciale. 2003. Accelerated migration of respiratory dendritic cells to the regional lymph nodes is limited to the early phase of pulmonary infection. *Immunity.* 18:265-277.

148. Ladel, C. H., C. Blum, A. Dreher, K. Reifenberg, M. Kopf, and S. H. Kaufmann. 1997. Lethal tuberculosis in interleukin-6-deficient mutant mice. *Infect.Immun.* 65:4843-4849.

149. VanHeyningen, T. K., H. L. Collins, and D. G. Russell. 1997. IL-6 produced by macrophages infected with Mycobacterium species suppresses T cell responses. *J.Immunol.* 158:330-337.

150. Saunders, B. M., A. A. Frank, I. M. Orme, and A. M. Cooper. 2000. Interleukin-6 induces early gamma interferon production in the infected lung but is not required for generation of specific immunity to Mycobacterium tuberculosis infection. *Infect.Immun.* 68:3322-3326.

151. Nagabhushanam, V., A. Solache, L. M. Ting, C. J. Escaron, J. Y. Zhang, and J. D. Ernst. 2003. Innate inhibition of adaptive immunity: Mycobacterium tuberculosis-induced IL-6 inhibits macrophage responses to IFN-gamma. *J.Immunol.* 171:4750-4757.

152. Hartgers, F. C., J. L. Vissers, M. W. Looman, C. van Zoelen, C. Huffine, C. G. Figdor, and G. J. Adema. 2000. DC-STAMP, a novel multimembrane-spanning molecule preferentially expressed by dendritic cells. *Eur.J.Immunol.* 30:3585-3590.

153. Staege, H., A. Brauchlin, G. Schoedon, and A. Schaffner. 2001. Two novel genes FIND and LIND differentially expressed in deactivated and Listeria-infected human macrophages. *Immunogenetics* 53:105-113.

154. Farber, J. M. 1990. A macrophage mRNA selectively induced by gamma-interferon encodes a member of the platelet factor 4 family of cytokines. *Proc.Natl.Acad.Sci.U.S.A* 87:5238-5242.

155. Farber, J. M. 1993. HuMig: a new human member of the chemokine family of cytokines. *Biochem.Biophys.Res.Commun.* 192:223-230.

156. Bros, M., X. L. Ross, A. Pautz, A. B. Reske-Kunz, and R. Ross. 2003. The human fascin gene promoter is highly active in mature dendritic cells due to a stage-specific enhancer. *J.Immunol.* 171:1825-1834.

157. Ross, R., H. Jonuleit, M. Bros, X. L. Ross, S. Yamashiro, F. Matsumura, A. H. Enk, J. Knop, and A. B. Reske-Kunz. 2000. Expression of the actin-bundling protein fascin in cultured human dendritic cells correlates with dendritic morphology and cell differentiation. *J.Invest Dermatol.* 115:658-663.

158. Ross, R., X. L. Ross, J. Schwing, T. Langin, and A. B. Reske-Kunz. 1998. The actin-bundling protein fascin is involved in the formation of dendritic processes in maturing epidermal Langerhans cells. *J.Immunol.* 160:3776-3782.

159. Banyer, J. L., N. H. Hamilton, I. A. Ramshaw, and A. J. Ramsay. 2000. Cytokines in innate and adaptive immunity. *Rev.Immunogenet.* 2:359-373.

160. Bonecchi, R., S. Sozzani, J. T. Stine, W. Luini, G. D'Amico, P. Allavena, D. Chantry, and A. Mantovani. 1998. Divergent effects of interleukin-4 and interferon-gamma on macrophage-derived chemokine production: an amplification circuit of polarized T helper 2 responses. *Blood* 92:2668-2671.

161. Kalinski, P., H. H. Smits, J. H. Schuitemaker, P. L. Vieira, M. van Eijk, E. C. de Jong, E. A. Wierenga, and M. L. Kapsenberg. 2000. IL-4 is a mediator of IL-12p70 induction by human Th2 cells: reversal of polarized Th2 phenotype by dendritic cells. *J.Immunol.* 165:1877-1881.

162. Banyer, J. L., D. C. Halliday, S. A. Thomson, and N. H. Hamilton. 2003. Combinations of IFN-gamma and IL-4 induce distinct profiles of dendritic cell-associated immunoregulatory properties. *Genes Immun.* 4:427-440.

163. Gilman, A. G. 1987. G proteins: transducers of receptor-generated signals. *Annu.Rev.Biochem.* 56:615-649.

164. Marino, S., S. Pawar, C. L. Fuller, T. A. Reinhart, J. L. Flynn, and D. E. Kirschner. 2004. Dendritic Cell Trafficking and Antigen Presentation in the Human Immune Response to Mycobacterium tuberculosis. *J.Immunol.* 173:494-506.

165. Sarris, A. H., H. E. Broxmeyer, U. Wirthmueller, N. Karasavvas, S. Cooper, L. Lu, J. Krueger, and J. V. Ravetch. 1993. Human interferon-inducible protein 10: expression and purification of recombinant protein demonstrate inhibition of early human hematopoietic progenitors. *J.Exp.Med.* 178:1127-1132.

166. Addison, C. L., D. A. Arenberg, S. B. Morris, Y. Y. Xue, M. D. Burdick, M. S. Mulligan, M. D. Iannettoni, and R. M. Strieter. 2000. The CXC chemokine, monokine induced by interferon-gamma, inhibits non-small cell lung carcinoma tumor growth and metastasis. *Hum.Gene Ther.* 11:247-261.

167. Sgadari, C., J. M. Farber, A. L. Angiolillo, F. Liao, J. Teruya-Feldstein, P. R. Burd, L. Yao, G. Gupta, C. Kanegane, and G. Tosato. 1997. Mig, the monokine induced by interferon-gamma, promotes tumor necrosis in vivo. *Blood* 89:2635-2643.

168. Sgadari, C., A. L. Angiolillo, B. W. Cherney, S. E. Pike, J. M. Farber, L. G. Koniaris, P. Vanguri, P. R. Burd, N. Sheikh, G. Gupta, J. Teruya-Feldstein, and G. Tosato. 1996. Interferon-inducible protein-10 identified as a mediator of tumor necrosis in vivo. *Proc.Natl.Acad.Sci.U.S.A* 93:13791-13796.

169. Piali, L., C. Weber, G. LaRosa, C. R. Mackay, T. A. Springer, I. Clark-Lewis, and B. Moser. 1998. The chemokine receptor CXCR3 mediates rapid and shear-resistant adhesion-induction of effector T lymphocytes by the chemokines IP10 and Mig. *Eur.J.Immunol.* 28:961-972.

170. Taub, D. D., A. R. Lloyd, K. Conlon, J. M. Wang, J. R. Ortaldo, A. Harada, K. Matsushima, D. J. Kelvin, and J. J. Oppenheim. 1993. Recombinant human interferon-inducible protein 10 is a chemoattractant for human monocytes and T lymphocytes and promotes T cell adhesion to endothelial cells. *J.Exp.Med.* 177:1809-1814.

171. Strieter, R. M., P. J. Polverini, D. A. Arenberg, and S. L. Kunkel. 1995. The role of CXC chemokines as regulators of angiogenesis. *Shock* 4:155-160.

172. Angiolillo, A. L., C. Sgadari, D. D. Taub, F. Liao, J. M. Farber, S. Maheshwari, H. K. Kleinman, G. H. Reaman, and G. Tosato. 1995. Human interferon-inducible protein 10 is a potent inhibitor of angiogenesis in vivo. *J.Exp.Med.* 182:155-162.

173. Alatas, F., O. Alatas, M. Metintas, A. Ozarslan, S. Erginel, and H. Yildirim. 2004. Vascular endothelial growth factor levels in active pulmonary tuberculosis. *Chest* 125:2156-2159.

174. Jin, H. Y., K. S. Lee, S. M. Jin, and Y. C. Lee. 2004. Vascular endothelial growth factor correlates with matrix metalloproteinase-9 in the pleural effusion. *Respir.Med.* 98:115-122.

175. Cole, A. M., T. Ganz, A. M. Liese, M. D. Burdick, L. Liu, and R. M. Strieter. 2001. Cutting edge: IFN-inducible ELR- CXC chemokines display defensin-like antimicrobial activity. *J.Immunol.* 167:623-627.

176. Loetscher, P., A. Pellegrino, J. H. Gong, I. Mattioli, M. Loetscher, G. Bardi, M. Baggiolini, and I. Clark-Lewis. 2001. The ligands of CXC chemokine receptor 3, I-TAC, Mig, and IP10, are natural antagonists for CCR3. *J.Biol.Chem.* 276:2986-2991.

177. Petkovic, V., C. Moghini, S. Paoletti, M. Uguccioni, and B. Gerber. 2004. I-TAC/CXCL11 is a natural antagonist for CCR5. *J.Leukoc.Biol.*

178. Cole, K. E., C. A. Strick, T. J. Paradis, K. T. Ogborne, M. Loetscher, R. P. Gladue, W. Lin, J. G. Boyd, B. Moser, D. E. Wood, B. G. Sahagan, and K. Neote. 1998. Interferon-inducible T cell alpha chemoattractant (I-TAC): a novel non-ELR CXC chemokine with potent activity on activated T cells through selective high affinity binding to CXCR3. *J.Exp.Med.* 187:2009-2021.

179. Cox, M. A., C. H. Jenh, W. Gonsiorek, J. Fine, S. K. Narula, P. J. Zavodny, and R. W. Hipkin. 2001. Human interferon-inducible 10-kDa protein and human interferon-inducible T cell alpha chemoattractant are allotopic ligands for human CXCR3: differential binding to receptor states. *Mol.Pharmacol.* 59:707-715.

180. Colvin, R. A., G. S. Campanella, J. Sun, and A. D. Luster. 2004. Intracellular Domains of CXCR3 That Mediate CXCL9, CXCL10, and CXCL11 Function. *J.Biol.Chem.* 279:30219-30227.

181. Liao, F., R. L. Rabin, J. R. Yannelli, L. G. Koniaris, P. Vanguri, and J. M. Farber. 1995. Human Mig chemokine: biochemical and functional characterization. *J.Exp.Med.* 182:1301-1314.

182. Farber, J. M. 1997. Mig and IP-10: CXC chemokines that target lymphocytes. *J.Leukoc.Biol.* 61:246-257.

183. Romagnani, P., F. Annunziato, E. Lazzeri, L. Cosmi, C. Beltrame, L. Lasagni, G. Galli, M. Francalanci, R. Manetti, F. Marra, V. Vanini, E. Maggi, and S. Romagnani. 2001. Interferon-inducible protein 10, monokine induced by interferon gamma, and interferon-inducible T-cell alpha chemoattractant are produced by thymic epithelial cells and attract T-cell receptor (TCR) alphabeta+ CD8+ single-positive T cells, TCRgammadelta+ T cells, and natural killer-type cells in human thymus. *Blood* 97:601-607.

184. Ludwig, A., F. Schiemann, R. Mentlein, B. Lindner, and E. Brandt. 2002. Dipeptidyl peptidase IV (CD26) on T cells cleaves the CXC chemokine CXCL11 (I-TAC) and abolishes the stimulating but not the desensitizing potential of the chemokine. *J.Leukoc.Biol.* 72:183-191.

185. Van den Steen, P. E., S. J. Husson, P. Proost, J. Van Damme, and G. Opdenakker. 2003. Carboxyterminal cleavage of the chemokines MIG and IP-10 by gelatinase B and neutrophil collagenase. *Biochem.Biophys.Res.Commun.* 310:889-896.

186. Campanella, G. S., E. M. Lee, J. Sun, and A. D. Luster. 2003. CXCR3 and heparin binding sites of the chemokine IP-10 (CXCL10). *J.Biol.Chem.* 278:17066-17074.

187. Clark-Lewis, I., I. Mattioli, J. H. Gong, and P. Loetscher. 2003. Structure-function relationship between the human chemokine receptor CXCR3 and its ligands. *J.Biol.Chem.* 278:289-295.

188. Scott, P. 1993. Selective differentiation of CD4+ T helper cell subsets. *Curr.Opin.Immunol.* 5:391-397.

189. Ahuja, S. S., R. L. Reddick, N. Sato, E. Montalbo, V. Kostecki, W. Zhao, M. J. Dolan, P. C. Melby, and S. K. Ahuja. 1999. Dendritic cell (DC)-based anti-infective strategies: DCs engineered to secrete IL-12 are a potent vaccine in a murine model of an intracellular infection. *J.Immunol.* 163:3890-3897.

190. Martino, A., A. Sacchi, N. Sanarico, F. Spadaro, C. Ramoni, A. Ciaramella, L. P. Pucillo, V. Colizzi, and S. Vendetti. 2004. Dendritic cells derived from BCG-infected precursors induce Th2-like immune response. *J.Leukoc.Biol.*

191. Sanceau, J., D. D. Boyd, M. Seiki, and B. Bauvois. 2002. Interferons inhibit tumor necrosis factor-alpha-mediated matrix metalloproteinase-9 activation via interferon regulatory factor-1 binding competition with NF-kappa B. *J.Biol.Chem.* 277:35766-35775.

192. Latchman, Y., C. R. Wood, T. Chernova, D. Chaudhary, M. Borde, I. Chernova, Y. Iwai, A. J. Long, J. A. Brown, R. Nunes, E. A. Greenfield, K. Bourque, V. A. Boussiotis, L. L. Carter, B. M. Carreno, N. Malenkovich, H. Nishimura, T. Okazaki, T. Honjo, A. H. Sharpe, and G. J. Freeman. 2001. PD-L2 is a second ligand for PD-1 and inhibits T cell activation. *Nat.Immunol.* 2:261-268.

193. Nguyen, L. T., S. Radhakrishnan, B. Ciric, K. Tamada, T. Shin, D. M. Pardoll, L. Chen, M. Rodriguez, and L. R. Pease. 2002. Cross-linking the B7 family molecule B7-DC directly activates immune functions of dendritic cells. *J.Exp.Med.* 196:1393-1398.

194. Brown, J. A., D. M. Dorfman, F. R. Ma, E. L. Sullivan, O. Munoz, C. R. Wood, E. A. Greenfield, and G. J. Freeman. 2003. Blockade of programmed death-1 ligands on dendritic cells enhances T cell activation and cytokine production. *J.Immunol.* 170:1257-1266.

195. Zhong, X., C. Bai, W. Gao, T. B. Strom, and T. L. Rothstein. 2004. Suppression of expression and function of negative immune regulator PD-1 by certain pattern recognition and cytokine receptor signals associated with immune system danger. *Int.Immunol.* 16:1181-1188.

196. Chemnitz, J. M., R. V. Parry, K. E. Nichols, C. H. June, and J. L. Riley. 2004. SHP-1 and SHP-2 Associate with Immunoreceptor Tyrosine-Based Switch Motif of Programmed Death 1 upon Primary Human T Cell Stimulation, but Only Receptor Ligation Prevents T Cell Activation. *J.Immunol.* 173:945-954.

197. Quinn, F. D., K. A. Birkness, and P. J. King. 2002. Alpha-crystallin as a potential marker of *Mycobacterium tuberculosis* latency. *ASM News* 68:612-617.

198. Drake, W. P., Z. Pei, D. T. Pride, R. D. Collins, T. L. Cover, and M. J. Blaser. 2002. Molecular analysis of sarcoidosis tissues for mycobacterium species DNA. *Emerg.Infect.Dis.* 8:1334-1341.

199. Chensue, S. W., K. S. Warmington, J. H. Ruth, P. S. Sanghi, P. Lincoln, and S. L. Kunkel. 1996. Role of monocyte chemoattractant protein-1 (MCP-1) in Th1 (mycobacterial) and Th2 (schistosomal) antigen-induced granuloma formation: relationship to local inflammation, Th cell expression, and IL-12 production. *J.Immunol.* 157:4602-4608.

200. Chiu, B. C. and S. W. Chensue. 2002. Chemokine responses in schistosomal antigen-elicited granuloma formation. *Parasite Immunol.* 24:285-294.

201. Gu, L., S. Tseng, R. M. Horner, C. Tam, M. Loda, and B. J. Rollins. 2000. Control of TH2 polarization by the chemokine monocyte chemoattractant protein-1. *Nature* 404:407-411.

202. Warmington, K. S., L. Boring, J. H. Ruth, J. Sonstein, C. M. Hogaboam, J. L. Curtis, S. L. Kunkel, I. R. Charo, and S. W. Chensue. 1999. Effect of C-C chemokine receptor 2 (CCR2) knockout on type-2 (schistosomal antigen-elicited) pulmonary granuloma

formation: analysis of cellular recruitment and cytokine responses. *Am.J.Pathol.* 154:1407-1416.

203. Sugawara, I., H. Yamada, S. Mizuno, and Y. Iwakura. 2000. IL-4 is required for defense against mycobacterial infection. *Microbiol.Immunol.* 44:971-979.

204. North, R. J. 1998. Mice incapable of making IL-4 or IL-10 display normal resistance to infection with Mycobacterium tuberculosis. *Clin.Exp.Immunol.* 113:55-58.

205. Seah, G. T. and G. A. Rook. 2001. Il-4 influences apoptosis of mycobacterium-reactive lymphocytes in the presence of TNF-alpha. *J.Immunol.* 167:1230-1237.

206. Butler, N. S., M. M. Monick, T. O. Yarovinsky, L. S. Powers, and G. W. Hunninghake. 2002. Altered IL-4 mRNA stability correlates with Th1 and Th2 bias and susceptibility to hypersensitivity pneumonitis in two inbred strains of mice. *J.Immunol.* 169:3700-3709.

207. Umland, S. P., S. Razac, H. Shah, D. K. Nahrebne, R. W. Egan, and M. M. Billah. 1998. Interleukin-5 mRNA stability in human T cells is regulated differently than interleukin-2, interleukin-3, interleukin-4, granulocyte/macrophage colony-stimulating factor, and interferon-gamma. *Am.J.Respir.Cell Mol.Biol.* 18:631-642.

208. Fenhalls, G., L. Stevens, J. Bezuidenhout, G. E. Amphlett, K. Duncan, P. Bardin, and P. T. Lukey. 2002. Distribution of IFN-gamma, IL-4 and TNF-alpha protein and CD8 T cells producing IL-12p40 mRNA in human lung tuberculous granulomas. *Immunology* 105:325-335.

209. Fenhalls, G., G. R. Squires, L. Stevens-Muller, J. Bezuidenhout, G. Amphlett, K. Duncan, and P. T. Lukey. 2002. Associations between Toll-like Receptors and IL-4 in the Lungs of Patients with Tuberculosis. *Am.J.Respir.Cell Mol.Biol.*

210. Kronenberg, M. and L. Gapin. 2002. The unconventional lifestyle of NKT cells. *Nat.Rev.Immunol.* 2:557-568.

211. Sugawara, I., H. Yamada, S. Mizuno, C. Y. Li, T. Nakayama, and M. Taniguchi. 2002. Mycobacterial infection in natural killer T cell knockout mice. *Tuberculosis.(Edinb.)* 82:97-104.

212. Kawakami, K., Y. Kinjo, K. Uezu, S. Yara, K. Miyagi, Y. Koguchi, T. Nakayama, M. Taniguchi, and A. Saito. 2002. Minimal contribution of Valpha14 natural killer T cells to Th1 response and host resistance against mycobacterial infection in mice. *Microbiol.Immunol.* 46:207-210.

213. Gansert, J. L., V. Kiessler, M. Engele, F. Wittke, M. Rollinghoff, A. M. Krensky, S. A. Porcelli, R. L. Modlin, and S. Stenger. 2003. Human NKT cells express granulysin and exhibit antimycobacterial activity. *J.Immunol.* 170:3154-3161.

214. Johnston, B., C. H. Kim, D. Soler, M. Emoto, and E. C. Butcher. 2003. Differential chemokine responses and homing patterns of murine TCR alpha beta NKT cell subsets. *J.Immunol.* 171:2960-2969.

215. Thomas, S. Y., R. Hou, J. E. Boyson, T. K. Means, C. Hess, D. P. Olson, J. L. Strominger, M. B. Brenner, J. E. Gumperz, S. B. Wilson, and A. D. Luster. 2003. CD1d-restricted NKT cells express a chemokine receptor profile indicative of Th1-type inflammatory homing cells. *J.Immunol.* 171:2571-2580.

216. Orme, I. M., A. D. Roberts, J. P. Griffin, and J. S. Abrams. 1993. Cytokine secretion by CD4 T lymphocytes acquired in response to Mycobacterium tuberculosis infection. *J.Immunol.* 151:518-525.

217. Ehlers, S. 2003. [Pathomorphogenesis of tubercular histologic changes: mechanisms of granuloma formation, maintenance and necrosis]. *Internist (Berl)* 44:1363-1373.

218. Mohan, V. P., C. A. Scanga, K. Yu, H. M. Scott, K. E. Tanaka, E. Tsang, M. M. Tsai, J. L. Flynn, and J. Chan. 2001. Effects of tumor necrosis factor alpha on host immune response in chronic persistent tuberculosis: possible role for limiting pathology. *Infect.Immun.* 69:1847-1855.

219. Bell, I., C. Ashman, J. Maughan, E. Hooker, F. Cook, and T. A. Reinhart. 1998. Association of simian immunodeficiency virus Nef with the T-cell receptor (TCR) zeta chain leads to TCR down-modulation. *J.Gen.Virol.* 79 (Pt 11):2717-2727.